

**Studies towards the selective inhibition of β -alanine
pathways in *Mycobacterium tuberculosis***

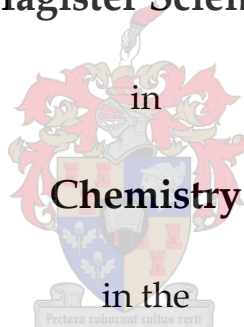
by

Lizbé Koekemoer

Thesis

presented in partial fulfilment of the
requirements for the degree

Magister Scientiae



Faculty of Science

University of Stellenbosch

Supervisor: Dr. E. Strauss

Co-supervisor: Dr. M. A. Jardine

April 2006

Declaration:

I, the undersigned, hereby declare that the work contained in this thesis is my own original work and that I have not previously in its entirety or in part submitted it at any university for a degree.

Signature

Date.....



Summary:

The focus of this study was the pathways for β -alanine production in *Mycobacterium tuberculosis* (Mtb), the causative agent of tuberculosis. The major pathway for β -alanine production is the decarboxylation of L-aspartate by L-aspartate- α -decarboxylase (PanD). This enzyme is not essential for the survival for Mtb which implies that an alternative pathway for β -alanine production must exist. We postulated that such a secondary pathway may be based on the oxidation of various polyamines by a polyamine oxidase to give the β -alanine precursor 3-aminopropanal, and therefore set out to find data in support of this hypothesis.

Based on sequence homology to the FAD-dependent *Saccharomyces cerevisiae* polyamine oxidase Fms1, Mtb AofH was identified as a likely candidate. The soluble expression and purification of AofH proved troublesome and led to the investigation of various techniques to increase protein yield. These methods include fusion to various tags, co-expression with the protein chaperones, addition of scarce codon tRNA's to the translation mixture and protein refolding. AofH was eventually purified as fusions to the Nus and MBP proteins and its activity determined by analysis of the enzymatic reactions by TLC, reverse phase HPLC, ESI-MS and LC-MS. TLC analysis indicated that 3-aminopropanol formed as a product during polyamine oxidation, but this could not be confirmed by any of the more sensitive analytical techniques. We set out to confirm the presence of the FAD cofactor in the enzyme by various methods and concluded that the AofH fusions did not contain FAD. Efforts to refold the protein in the presence of FAD also failed. From this study it is clear that the biochemical confirmation of the presumed activity of AofH will remain elusive until the enzyme can be purified in its active form, i.e. with FAD bound. A genetic test for activity based on functional complementation studies of *Escherichia coli* Δ panD strains proved inconclusive since no difference in growth rate was found between cell transformed with the *aofH* gene and the negative control.

We continued our studies of β -alanine biosynthesis by attempting the design of mechanism-based inhibitors for the PanD enzyme. Various structural analogues were identified and tested by qualitative and quantitative methods. Our results show that β -substituted aspartate analogues may be good potential inhibitors of Mtb's PanD protein and can thus be used in rational drug design.

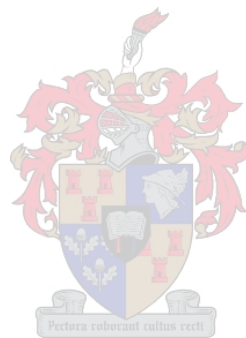
Opsomming:

In hierdie studie het ons gefokus op die biologiese padweë vir die vervaardiging van β -alanien in *Mycobacterium tuberculosis* (Mtb), die organisme wat tuberkulose veroorsaak. Die hoofpadweg behels die dekarboksilering van L-aspartaat deur L-aspartaat dekarboksilase (PanD). Siende dat hierdie ensiem nie noodsaaklik is vir die oorlewing van die organisme nie, is die gevolgtrekking gemaak dat daar 'n alternatiewe padweg vir die produksie van β -alanien moet bestaan. Ons hipotese was dat hierdie alternatiewe padweg die oksidasie van verskeie poliamiene deur 'n poliamien oksidase ensiem is om die β -alanien voorloper 3-aminopropanaal te vorm. Die eerste deel van hierdie studie fokus op die bevinding van resultate ter ondersteuning van hierdie hipotese.

Gebaseer op DNA volgorde vergelykings met die poliamien oksidase Fms1 van die gis *Saccharomyces cerevisiae*, is die Mtb ensiem AofH as 'n moontlike kandidaat geïdentifiseer. Probleme is ondervind met die oplosbare uitdrukking en suiwering van hierdie ensiem. Om die oplosbaarheidsprobleem te oorbrug, is verskeie proteïen merkers aan AofH geheg. Metodes om die opbrengs te vermeerder is ook ondersoek, insluitende die toevoeging tRNA's van skaars kodons en die proteïene wat tydens die vouproses help fasiliteer. AofH is na vele probeerslae gesuiwer as 'n fusieproteïen saam met die proteïene Nus en MBP, waarna die aktiwiteit daarvan geanaliseer is deur gebruik te maak van dunlaag chromatografie, omgekeerde fase HPLC, ESI-MS en LC-MS. Volgens die dunlaag chromatografie analise vorm 3-aminopropanol as 'n produk gedurende die oksidasie van die poliamiene. Hierdie waarneming kon egter nie bevestig word met enige van die meer sensitiewe analitiese tegnieke nie. Toetse om die teenwoordigheid van FAD te bevestig, het gewys dat die kofaktor nie gebind het aan die ensiem nie. Aan hand hiervan kan die onaktiwiteit van AofH verklaar word.

Ons studie van β -alanien biosintese is voortgesit deur te konsentreer op die ontwerp van 'n meganisties-gebaseerde inhibitor van die PanD ensiem. Vir hierdie doeleindes is verskeie strukturele analoë van L-aspartaat geïdentifiseer en getoets deur middel van kwalitatiewe en kwantitatiewe tegnieke. Ons resultate wys dat β -gesubstitueerde aspartaatanaloë heel moontlik goeie inhibitors van die Mtb PanD ensiem mag wees en dus gebruik kan word in die rasionale ontwerp van medisyne.

The financial assistance of the National Research Foundation (NRF) towards this research is hereby acknowledged. Opinions expressed and conclusions arrived at, are those of the author and are not necessarily to be attributed to the NRF.



Aan Ouma
(17-12-1926 tot 2-12-2005)

Die enigste Spreuke 31 vrou wat ek ken.



In Christ alone

I place my trust

And find my glory in the power of the cross

In every victory

Let it be said of me

My source of strength

My source of hope

Is Christ alone



Acknowledgements

My supervisor Dr. Erick Strauss. When you told me at the start of the project that we might experience some problems with solubility, I didn't quite get what you meant. Unfortunately now I do. Thank you for the last two years, for all the help, guidance and "good job"-s , even when we both knew that the results were not that spectacular. Contrary to what you may believe, I am going to miss the lab.

To my co-supervisor Dr Anwar Jardine. Thank you for all the help with the HPLC and all the ideas of how to make the analysis work.

To my fellow lab rats: Leisl; for teaching me all the molecular biology stuff that I forgot after undergrad. Jandr ; for all the songs and doing most of my NMR analysis for me. Marianne; you have walked this road with me from first year. Sorry to leave you behind now and blessings with your doctorate.

To my family. Thank you for all the love and support and understanding throughout the years.

To my friends. Liska and Gretha for sharing everything with me, from feeling-sorry-for-ourselves fits to the greatest travel adventures. Casper; I would always think of you when I eat fish. Bertie and Jessica; for your faithful friendship through this whole study process. The rest of the dinner club; I would keep on looking for new recipes for mushrooms. Carin; thank you for always being honest, even in difficult situations.

To my cell and church, Shofar Christian church. Thank you for being my home and my family and always bringing me back in touch with reality.

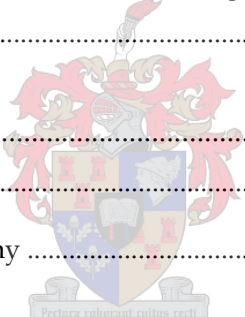
The financial assistance of the National Research Foundation (NRF) and the Medical Research Council (MRC) towards this research.

All honour to my Abba Father. During the last two years I have been stubborn and unrelenting, but thank you for always picking me up and giving me hope again for the future that You have promised me.

Table of contents

Summary:	iii
Opsomming:	iv
Acknowledgements	viii
Table of contents	ix
Abbreviations	xiv
Chapter 1.....	1
1.1 Introduction	1
1.2 Background.....	1
1.3 Pantothenate mediated virulence of Mtb	2
1.4 Pantothenate biosynthesis - An overview	3
1.4.1 <i>Biosynthetic pathway</i>	3
1.4.2 <i>The enzymes involved</i>	4
1.4.2.1 <i>Ketopantoate hydroxymethyltransferase (PanB)</i>	4
1.4.2.2 <i>Ketopantoate reductase (PanE)</i>	5
1.4.2.3 <i>l-Aspartate-α-decarboxylase (PanD)</i>	6
1.4.2.4 <i>Pantothenate synthetase (PanC)</i>	8
1.5 Essentiality of the pantothenate biosynthesis genes.....	9
1.6 Alternative sources of β -alanine	10
1.6.1 <i>Degradation of uracil</i>	10
1.6.2 <i>Degradation of polyamines</i>	11
1.6.3 <i>Propionate degradation</i>	12
1.6.4 <i>Cyanide metabolism</i>	13
1.7 Degradation of polyamines in <i>S. cerevisiae</i>	13
1.7.1 <i>Polyamine oxidase: Fms1</i>	13
1.7.1.1 <i>Background</i>	13
1.7.1.2 <i>Characteristics</i>	14
1.7.2 <i>Aldehyde dehydrogenases: Ald2 and Ald3</i>	14
1.7.2.1 <i>Background</i>	14
1.7.2.2 <i>Characteristics</i>	15
1.8 Identification of AofH	15
1.9 Conclusion	17

1.10 Aims of this thesis.....	17
1.11 References	17
Chapter 2.....	21
2.1 Introduction	21
2.1.1 Cloning and initial expression trials.....	21
2.1.2 Attempts at solubility.....	21
2.1.3 Expression of AofH fusions	24
2.2 Attempts at native expression and purification	24
2.2.1 GST-tag.....	25
2.2.2 His-GST	27
2.2.3 His-MBP-tag.....	31
2.2.4 His-Nus-tag.....	32
2.2.5 His Lumio™-tag.....	33
2.2.6 His-Patch Thioredoxin	34
2.2.7 Conclusion on fusion tags	34
2.3 Increasing solubility and translation efficiency	34
2.3.1 Scarce codons.....	35
2.3.2 Chaperone plasmids.....	35
2.4 Other expression methods	39
2.4.1 Expression from yeast.....	39
2.5 Protein refolding	39
2.5.1 Method 1: Artificial chaperone chemical-assisted method.....	40
2.5.2 Method 2: Dilution into non-denaturing buffer	40
2.6 Conclusion	41
2.7 Experimental.....	41
2.7.1 DNA amplification	42
2.7.2 Restriction Digestions.....	42
2.7.3 Construction of plasmids.....	43
2.7.3.1 Method 1 - Ligation and screening	43
2.7.3.2 Method 2 - Gateway™ LR reaction	43
2.7.3.3 The constructed plasmids.....	44
2.7.3.3.1 pENTR4N-aofH.....	44
2.7.3.3.2 pET28a-aofH	45
2.7.3.3.3 pEXP15-aofH.....	45
2.7.3.3.4 pEXP566-aofH.....	45
2.7.3.3.5 pEXP544-aofH.....	45
2.7.3.3.6 pET160-EXP-aofH.....	45
2.7.3.3.7 pET160-GST-EXP-aofH.....	45

2.7.3.3.8	<i>pBAD-EXP49-aofH</i>	45
2.7.3.3.9	<i>pYES-EXP52-aofH</i>	46
2.7.4	<i>Overexpression and purification methodology:</i>	46
2.7.4.1	<i>Expression trails</i>	46
2.7.4.2	<i>Large scale expression</i>	47
2.7.4.3	<i>Purification of expression trials to analyze soluble and insoluble proteins</i>	47
2.7.4.4	<i>Purification of protein obtained in large scale expressions</i>	47
2.7.4.5	<i>Analysis on 12% SDS PAGE gels</i>	48
2.7.4.6	<i>Determination of protein concentration</i>	48
2.7.5	<i>Overexpression and purification used in this study.</i>	49
2.7.5.1	<i>His-GST</i>	49
2.7.5.2	<i>MBP-tag</i>	50
2.7.5.3	<i>Nus-tag</i>	50
2.7.5.4	<i>Lumio™-tag</i>	50
2.7.5.5	<i>His-Patch Thioredoxin</i>	51
2.7.5.6	<i>Scarce codons</i>	51
2.7.5.7	<i>Chaperone plasmids</i>	51
2.7.5.8	<i>Alternative expression methods for GST-tag fusions (7)</i>	51
2.7.5.9	<i>Protein Refolding</i>	52
2.7.5.9.1	<i>Method 1: Artificial chaperone chemical-assisted method</i>	52
2.7.5.9.2	<i>Method 2: Dilution into non-denaturing buffer</i>	53
2.8	<i>References</i>	53
		
Chapter 3	56
3.1	<i>Introduction</i>	56
3.2	<i>Thin Layer Chromatography</i>	59
3.3	<i>Reverse phase HPLC</i>	62
3.3.1	<i>Analysis of all the amines</i>	63
3.3.1.1	<i>Dansylated products</i>	63
3.3.1.2	<i>NBD-Cl</i>	63
3.3.2	<i>Analysis of the 3-carbon products</i>	64
3.3.2.1	<i>o-Phthaldialdehyde and β-mercaptoethanol</i>	64
3.3.2.2	<i>Fluram</i>	66
3.3.3	<i>Conclusion on HPLC</i>	66
3.4	<i>ESI-MS and LC-MS analysis</i>	67
3.5	<i>Functional complementation studies</i>	70
3.5.1	<i>In E. coli</i>	70
3.5.1.1	<i>Plate assays</i>	70
3.5.1.2	<i>In Solution</i>	72
3.5.2	<i>In S. cerevisiae</i>	74
3.5.3	<i>Conclusion on complementation</i>	74

3.6 Test for monoamine oxidase activity	74
3.7 Assay for the presence of H ₂ O ₂	75
3.7.1 Horseradish peroxidase assay	75
3.7.2 Fluorescent assay	77
3.8 FAD Scans	79
3.9 Conclusion	81
3.10 Experimental.....	82
3.10.1 Cloning, overexpression and purification of Fms1	82
3.10.2 TLC.....	82
3.10.3 Synthesis of standards	83
3.10.4 HPLC.....	83
3.10.4.1 Dansylated products	83
3.10.4.2 NBD-Cl.....	83
3.10.4.3 o-Phthaldialdehyde and β-mercaptoethanol	84
3.10.4.4 Fluram.....	84
3.10.5 ESI-MS and LC-MS analysis.....	85
3.10.6 Functional complementation studies.....	85
3.10.6.1 In <i>E. coli</i> DV-strains.....	85
3.10.6.2 In JW0127	85
3.10.7 Test for monoamine oxidase activity	86
3.10.8 Assays for FAD activity	86
3.10.8.1 HRP.....	86
3.10.8.2 Fluorescent assay	86
3.10.8.3 FAD scans.....	86
3.11 References	87
Chapter 4.....	89
4.1 Introduction	89
4.2 Inhibitors	92
4.2.1 Inhibition of pyruvoyl formation.....	92
4.2.2 Structural- and mechanism- based inhibitors	93
4.3 Overview of inhibitors for <i>E. coli</i> PanD	94
4.4 Design of an inhibitor	95
4.4.1 Synthesis of an inhibitor	97
4.4.1.1 Overview	97
4.5 Testing of substrates and inhibitors	99

4.5.1 Overview of existing assay methods.....	99
4.5.2 Testing with HPLC.....	100
4.5.3 Developing assays for steady-state kinetics.....	101
4.5.3.1 Assays for PanC activity.....	103
4.5.3.2 Assay with AMP.....	103
4.5.3.3 Assay using pantothenic acid	104
4.5.3.4 Assay using pyrophosphate.....	104
4.5.3.5 Steady-state kinetics for PanD.....	105
4.6 Conclusion	107
4.7 Experimental.....	108
4.7.1 DNA amplification, cloning, expression and purification	108
4.7.2 Synthesis of β -fluoroaspartate	109
4.7.2.1 Synthesis of oxazoline ring	109
4.7.2.2 Ring opening with aqueous HCl.....	109
4.7.2.3 Ring opening with dry HCl	110
4.7.2.4 Protection with BOC-group.....	110
4.7.3 HPLC.....	110
4.7.4 Steady-state kinetics	110
4.7.4.1 Preparation of <i>d</i> -pantoic acid	111
4.7.4.2 Coupled assay with myokinase, PK and LDH	111
4.7.4.3 Assay coupled to CoaA.....	111
4.7.4.4 Assay with the Sigma Pyrophosphate kit.....	111
4.7.4.5 Coupled Mtb PanD and PanC reaction.....	111
4.8 References	112
Chapter 5.....	115
5.1 Solubility of AofH.....	115
5.2 AofH activity	115
5.3 Synthesis of PanD inhibitors	116
5.4 Assay methods	117
5.5 Conclusion	117
5.6 References	118



Abbreviations

ACN	acetonitrile
Adk	adenylate kinase, myokinase
ADP	adenine diphosphate
α -KIVA	α -ketoisovalerate
AMP	adenine monophosphate
Ap ^R	ampicillin resistance
ATP	adenine triphosphate
BCG	bacilli Calmette-Guérin
BSA	Bovine serum albumin
CE	crude extract
Cm	chloramphenicol
CoA	coenzyme A
CoaA	pantothenate kinase
CV	column volume
DAST	(Diethylamino) sulphur trifluoride
ddH ₂ O	distilled, Milli Q deionised water
DHAP	dihydroxyacetone phosphate
DNA	deoxyribonucleic acid
Dns-Cl	dansyl-chloride
DTT	Dithiothreitol
<i>E. coli</i>	<i>Escherichia coli</i>
ESI-MS	electron spray mass spectroscopy
EtOH	ethanol
FT	flow through
GAP	D-glyceraldehyde-3-phosphate
GST-tag	glutathione-S-transferase tag
His-tag	6xHistidine tag
HRP	horseradish peroxidase
HP	His-patch
HPLC	high-performance liquid chromatography
IPTG	isopropyl- β -D-thiogalactoside

kDa	kilo Dalton
Kn ^R	kanamycin resistance
LB	Luria-Bertani
LC-MS	liquid chromatography mass spectroscopy
LDH	lactate dehydrogenase
λ_{ex}	excitation wavelength
λ_{em}	emission wavelength
MAO	monoamine oxidase
MBP-tag	maltose binding protein-tag
MeOH	methanol
min	minute(s)
Mr	relative molecular mass
Mtb	<i>Mycobacterium tuberculosis</i>
NADPH	nicotinamide adenine dinucleotide phosphate
NBD-Cl	4-Chloro-7-nitrobenzofurazan
N ¹ -spm	N ¹ -acetyl spermine
N ⁸ -spd	N ⁸ -acetyl spermidine
NMR	nuclear magnetic resonance spectroscopy
Nus-tag	nut utilization substance-tag
PEP	potassium phosphoenolpyruvate
OD ₆₀₀	optical density at 600nm
OPA	<i>o</i> -phthaldialdehyde
OAc	acetate
PEPC	phosphoenolpyruvate carboxylase
PK	pyruvate kinase
PPi	pyrophosphate
RNA	ribonucleic acid
t _R	retention time
tRNA	transfer ribonucleic acid
UV	ultra violet
PanB	ketopantoate hydroxymethyltransferase
PanC	pantothenate synthetase
PanD	L-aspartate- α -decarboxylase

PanE	ketopantoate reductase
PAO	polyamine oxidase
PCR	polymerase chain reaction
PLP	pyridoxal 5'-phosphate
R _F	retardation factor
SAM	S-adenosylmethionine
SCID	Severely compromised immune deficient
SDS-PAGE	sodium dodecyl sulphate-polyacrylamide gel electrophoresis
spd	spermidine
spm	spermine
TB	tuberculosis
Tet	tetracycline
TFA	trifluoroacetic acid
THF	tetrahydrofuran
met-THF	<i>N</i> ⁵ , <i>N</i> ¹⁰ -methylene tetrahydrofolate
TLC	thin layer chromatography
TraSH	transposon site hybridization



Chapter 1

Introduction:

The importance of β -alanine in pantothenate biosynthesis

1.1 Introduction

Tuberculosis (TB) is a disease that primarily affects the respiratory system and is estimated to be the second greatest cause of adult mortality among the infectious diseases. According to the World Health Organization TB is responsible for approximately two million deaths annually and the organization estimates that it infects a third of the world's population. A mere 50 years ago there was no cure for TB and today *Mycobacterium tuberculosis* (Mtb) strains have emerged that are resistant to all major anti-TB drugs. Drug resistance arises mainly in the third world countries due to incorrect or partial treatments given. The immune deficiency state caused by HIV also increases vulnerability to Mtb infections. It has been estimated that 13% of AIDS deaths worldwide are due to TB. Currently treatments for TB include the vaccine Bacille Calmette-Guérin (BCG) and short course chemotherapy, but with the spread of multi-drug resistant Mtb and the HIV co-infections the urgency to identify and develop new drugs still exist (1).

1.2 Background

TB is caused by the Gram-positive bacteria *Mycobacterium tuberculosis*. Since its isolation in 1905 the Mtb strain H37Rv has found extensive application in biomedical research mainly because it has retained its full virulence. The complete genome sequence of this strain has been determined, analyzed and published in 1998 by Cole *et al.* (2) Its genome contains $\pm 4\ 000$ genes and has a high guanine and cytosine content. This is reflected in a bias towards certain amino acids (2).

The problem with Mtb is that it has a natural resistance to many antibiotics that makes it difficult to treat. A large part of this natural resistance can be contributed to the highly hydrophobic cell envelope that acts as a permeability barrier. Mtb has an additional layer besides the normal peptidoglycan cell wall that is rich in unusual lipids, glycolipids and polysaccharides. Another factor that contributes to the natural resistance is that the

genome encodes for many potential resistance determinants. These include the hydrolytic or drug-modifying enzymes such as the β -lactamases and aminoglycoside acetyl transferases. Mtb also have many potential drug-efflux systems such as the ABC-transporters (2).

In addition to Mtb's inherent resistance, the pathogen also has the ability to persist within its host for extended periods of time without ever making the host ill. This is what is known as latent or chronic infections. It is estimated that only 10% of people with an intact immune system infected with Mtb will show any symptoms of the disease in their lifetimes. For the pathogen to persist in its latent state, however, certain genes still need to be expressed and certain metabolic paths need to be maintained. The genes necessary for the latent state survival fall into one of three categories. Their gene products are either part of the respiratory enzymes or of the stress-related and metabolic enzymes or they are proteins involved in fatty acid biosynthesis (3).

1.3 Pantothenate mediated virulence of Mtb

As briefly mentioned above, the biosynthesis and metabolism of fatty acids play an important role in the replication and persistence of Mtb in the latent state. It has also been found that the biosynthesis of pantothenate is essential for the growth of Mtb (4). Pantothenate or Vitamin B₅ is the precursor in the biosynthesis of coenzyme A (CoA) and the acyl carrier proteins. These metabolites have important functions in metabolic pathways like fatty acid metabolism, the tricarboxylic acid cycle and the biosynthesis of polyketides. Pantothenate is supplemented to the diet of higher animals, but bacteria, plants and fungi can biosynthesize it *de novo*. Since the biosynthesis pathway of pantothenate is absent in humans, this pathway is a possible drug target in Mtb.

A study done by Jacobs *et al.* to design new TB vaccines focused on this biosynthetic pathway (5). In this study they created a double deletion mutant of Mtb by deleting the *panC* and *panD* genes, the two genes involved in the *de novo* synthesis of pantothenic acid from L-aspartate. The Δ *panCD* mutant was found to be auxotrophic for pantothenate. Full virulence was restored with the integration of the *panCD* wild type genes back into the Δ *panCD* mutant. The viability of this deletion mutant as vaccine was tested by infecting severely compromised immune deficient (SCID) mice with the strain. The survival rate of these mice where compared to that of control experiments where the mice

were infected with either the virulent H37Rv Mtb strain or with BCG vaccine. Mice infected with the $\Delta panCD$ mutant survived noticeable longer (250 days) than those infected with the BCG vaccine (77 days) and the virulent strain (35 days). It would thus appear that Mtb is dependent on pantothenate for its virulence.

1.4 Pantothenate biosynthesis - An overview

1.4.1 Biosynthetic pathway

(*R*)-Pantothenate (**1.1**) (pantothenic acid, Vitamin B₅) is the condensation product of β -alanine (**1.2**) and (*R*)-pantoic acid (**1.3**). This reaction is catalyzed by pantothenate synthetase (PanC) and is adenine triphosphate (ATP) dependent. (Refer to Figure 1.1)

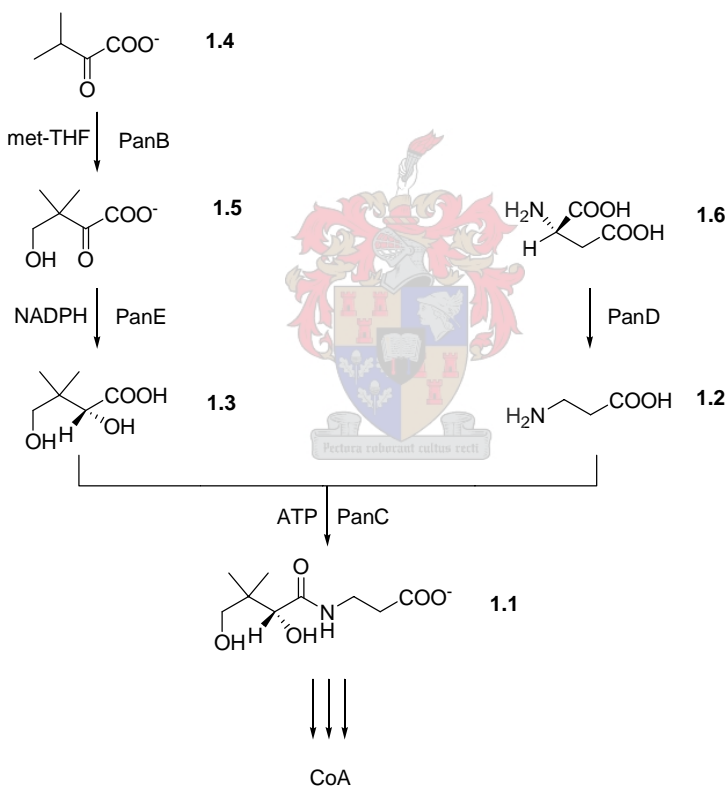


Figure 1.1: The biosynthetic pathway for the production of (*R*)-pantothenate (**1.1**) from its precursors β -alanine (**1.2**) and (*R*)-pantoic acid (**1.3**). β -alanine is obtained by the decarboxylation of L-aspartate (**1.6**) and (*R*)-pantoic acid via a two step process in which the precursor α -ketoisovalerate (**1.4**) is hydroxymethylated to α -ketopantoate (**1.5**) and subsequently reduced.

(*R*)-Pantoic acid is formed in two catalytic steps from its precursor, α -ketoisovalerate (**1.4**). This compound is also an intermediate in valine and leucine biosynthesis. The first step is

catalyzed by ketopantoate hydroxymethyltransferase (PanB) and involves the hydroxymethylation of **1.4** to form α -ketopantoate (**1.5**). The product is reduced to pantoic acid by ketopantoate reductase (PanE) in the presence of nicotinamide adenine dinucleotide phosphate (NADPH). The second precursor of pantothenate, β -alanine (**1.2**), is formed by the decarboxylation of L-aspartate (**1.6**) by the enzyme L-aspartate- α -decarboxylase (PanD) (6).

1.4.2 The enzymes involved

1.4.2.1 Ketopantoate hydroxymethyltransferase (PanB)

Although the condensation of α -ketoisovalerate (**1.4**) with formaldehyde to form α -ketopantoate (**1.5**) was already demonstrated chemically in 1942, the enzyme with the corresponding activity was only identified in 1957 (7).

PanB has been overexpressed and purified from *E. coli* as a hexameric protein consisting of 28kDa subunits (6). Its analogue in Mtb (designated Rv2225) has also been cloned, overexpressed and purified to near homogeneity as the native protein and as a 6x histidine (His-tag) fusion (7, 8). The crystal structure of the Mtb PanD was solved to 2.8Å using gadolinium soaked crystals. The subunit complexes Mg^{2+} to form a decameric structure with pentameric rings. These rings are held together by C-terminal α -helices that switch around between promoters in opposite pentamers. This helix swapping was not observed in the structures solved for the PanD-crystals of *E. coli* or *N. meningitides* (7).

As far as the catalytic mechanism of PanB is concerned, the exact route is still unclear. It is known that PanB is dependent on N^5, N^{10} -methylene tetrahydrofolate (met-THF) and that a divalent metal ion is required for substrate enolization. All the proposed mechanisms (refer to Figure 1.2) start of with the coordination of **1.4** to Mg^{2+} . The coordination to the divalent metal ion is presumed to lower the pK_a of the β -proton of **1.4** which favors the abstraction thereof for enolate formation. Sugatino *et al.* suggested that nucleophilic attack occurs via the enolate on the methylene group of the met-THF and that results in the breaking of the bond between N^5 and the cofactor (Figure 1.2, route a). The hydrolysis of the newly formed C-N bond leads to the formation of **1.5** (8). The second proposed mechanism starts of with ring opening of met-THF followed by deprotonation of Glu¹⁸¹, nucleophilic attack by **1.4** and hydrolysis (Figure 1.2, route b). The third mechanism (Figure 1.2, route c) involves the formation of formaldehyde by the hydrolysis of met-THF (7). Of all the mechanisms, this one is the most unlikely since it is

known that the reaction proceeds via the inversion of stereochemistry at C-3 of **1.4** (6). A free formaldehyde group would allow attack from both sides of the stereomeric centre and a racemate would form.

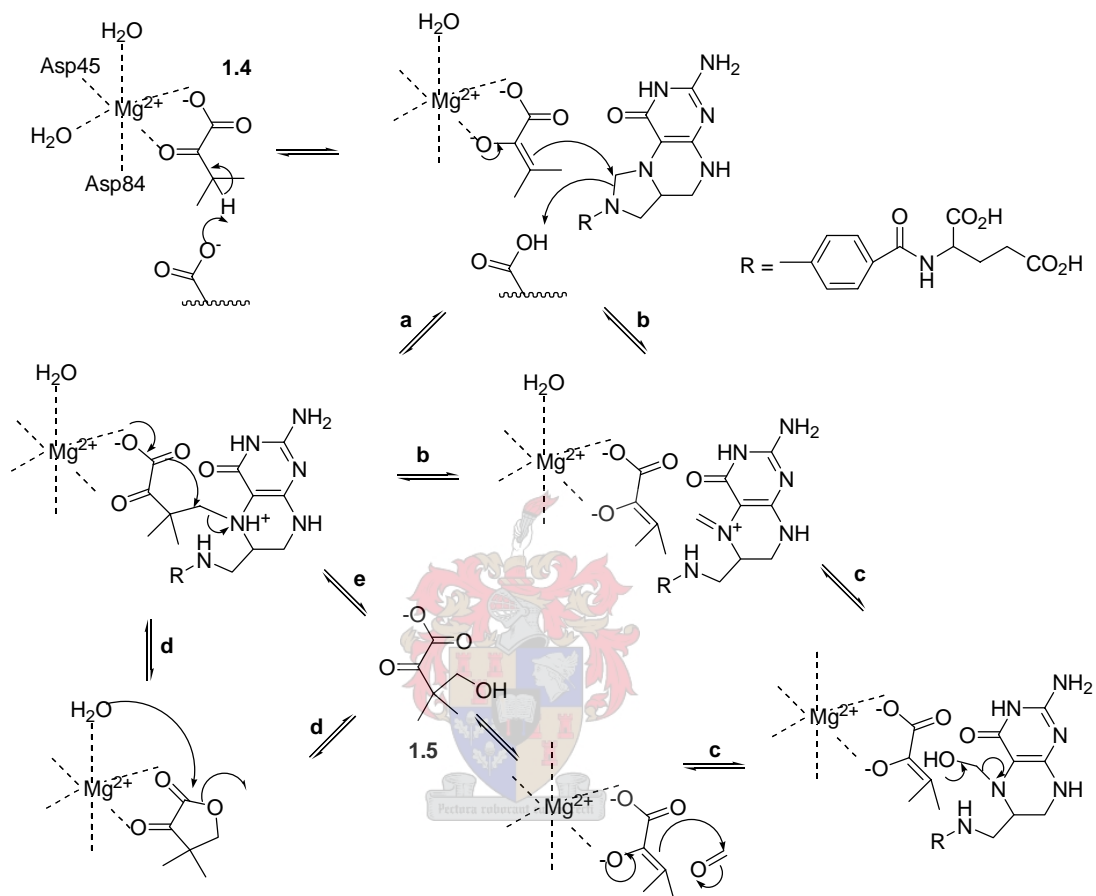


Figure 1.2: The 3 catalytic mechanisms proposed for PanB. Routes **a**, **b** and **c** indicate the three postulated mechanisms for nucleophilic attack on met-THF. Routes **d** and **e** are the two mechanisms for hydrolysis.

As for the hydrolysis two possible routes are postulated. The first method involves intramolecular attack of the C-3 oxygen to the carbonyl carbon to form ketopantolactone followed by hydrolysis (Figure 1.2, route **d**). The second method involves nucleophilic attack by one of the H_2O molecules that was coordinated to Mg^{2+} (Figure 1.2, route **e**).

1.4.2.2 Ketopantoate reductase (PanE)

There are more than 80 known sequences for putative ketopantoate reductases. These homologues share very little sequence conservation with only nine conserved residues.

Three of these residues are glycines (Gly⁷, Gly⁹ and Gly¹²) that form part of the GXGXXG nucleotide binding motif. This motif binds flavin and structurally forms part of the Rossmann-fold (7).

PanE (also known as ApbA) has been cloned, overexpressed and characterized as a monomer of 34kDa in *E. coli* (6). The *Stenotrophomonas maltophilia* PanE on the other hand is a multimeric protein consisting of a 30.5kDa subunits and multimeres of 87, 115, 140 and 160kDa. The size of the multimeres depends on the purification method used (7). Mtb PanE (Rv2573) is labeled as a gene that causes slow growth of the pathogen when mutated (9). A search for this gene on the Tuberculist database (10) identified it as a conserved hypothetical protein with no known function. No other information was obtained thus far.

Two different reaction mechanisms have been proposed for this reduction. The only differences between them are the residues that donate the proton to the keto acid and the residues that stabilize the γ -hydroxyl group by H-bonding. In both mechanisms the *si*-face hydrogen of NADPH attacks the carbonyl group of α -ketopantoate (**1.5**) (refer to Figure 1.3). The resulting alkoxide is protonated by either Lys¹⁷⁵ (1st mechanism) or Glu²⁵⁶ (2nd mechanism) to form **1.3** (7).

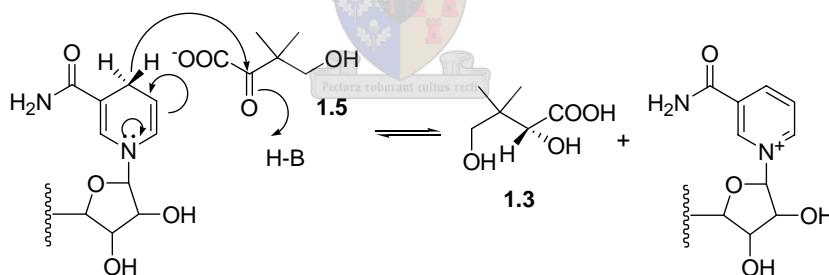


Figure 1.3: The basis mechanism of ketopantoate reductase (PanE) where α -ketopantoate (**1.5**) is reduced to pantoic acid (**1.3**) in the presence on NADH.

1.4.2.3 *L*-Aspartate- α -decarboxylase (*PanD*)

Shive and Mascow (7) discovered the role of *L*-aspartate in pantothenate biosynthesis in 1946. They found that bacterial cellular growth was inhibited by β -hydroxyaspartate, but was stimulated when asparagine, pantothenate and aspartate were added to the growth media. They took the experiment one step further and also found inhibition of cellular growth when a structural analogue of *L*-aspartate, cysteic acid, was added. This growth

rate was restored when additional supplements of β -alanine and pantothenate were added to the growth media. They concluded that β -alanine must be formed from L-aspartate.

PanD forms part of a small class of pyruvoyl-dependent decarboxylases. These enzymes undergo post-translation modification to form the catalytically active pyruvoyl group. Other enzymes in this class include the histidine decarboxylases, arginine decarboxylases, S-adenosylmethionine (SAM) decarboxylases and the phosphatidylserine decarboxylases (7). The tetrameric Mtb PanD is translated into an inactive pro-enzyme, called the π -protein (15,95kDa). Activation of the enzyme occurs with the cleavage of the bond between Gly²⁴ and Ser²⁵. The two subunits that form are labeled as the α -subunit (13.22kDa) that contains the pyruvoyl group at its N-terminal and the β -subunit (2.74kDa) with a carboxyl group at its C-terminal. The covalently bound pyruvoyl group of PanD- α is the essential factor for catalysis (11).

In the catalytic reaction (refer to Figure 1.4) the pyruvoyl group binds L-aspartate (1.6) to form a protonated imine (also known as a Schiff-base). This binding interaction activates the L-aspartate for decarboxylation. The hydrolysis of the Schiff-base leads to the release of β -alanine (1.2) and the enzyme (6).

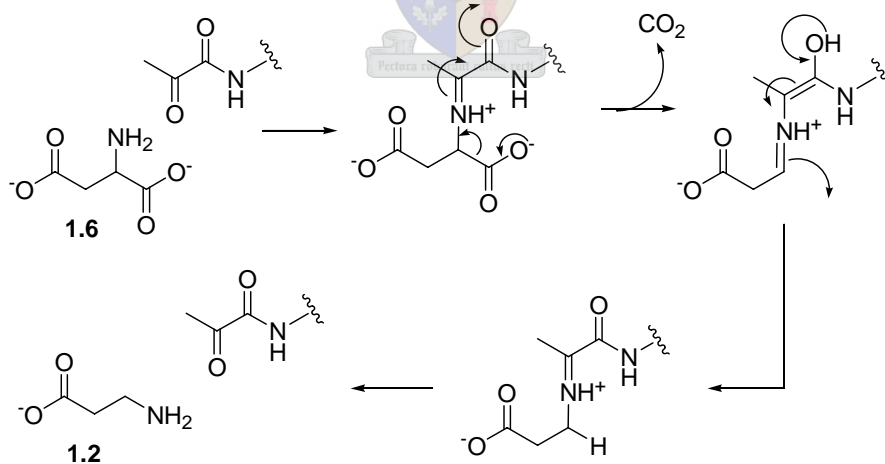


Figure 1.4: Catalytic mechanism of aspartate-1-decarboxylase (PanD). β -alanine (1.2) is formed by the decarboxylation of L-aspartate (1.6).

The PanD's from *E. coli*, Mtb and *Helicobacter pylori* were purified to near homogeneity as His-tag fusions. The tetrameric enzyme consists of 10.8kDa subunits in *E. coli* (6) and

15.95kDa subunits in Mtb (11). The crystal structures of these homologues were also solved and will be discussed in Chapter 4.

1.4.2.4 Pantothenate synthetase (PanC)

PanC was identified as early as 1952 in cell extracts of *E. coli*. Since then the *E. coli* enzyme has been purified to near homogeneity and identified as an 18kDa homotetramer (6). The Mtb homologue, a larger enzyme of 33kDa, has also been overexpressed and purified as a His-tag fusion (4).

Unlike PanE the primary structure of PanC is relatively highly conserved with over 30 amino acids that are identical in most of the homologues. The crystal structures of the *E. coli*, Mtb and *Thermus thermophilus* homologues have been solved (7, 12). According to the three dimensional structures of the Mtb and *E. coli* proteins, PanC belongs to the cytidylyl transferase family of proteins (13, 14). The protein has a well defined *N*-terminal Rossmann fold that contains the active cavity and a *C*-terminal domain that acts as a hinged lid for this cavity. Extensive work has been done to characterize the active site of the Mtb protein (7, 13, 14).

PanC is an ATP dependent ligase. The formation of the amide bond between pantoate (**1.3**) and β -alanine (**1.2**) is a two step process (Figure 1.5).

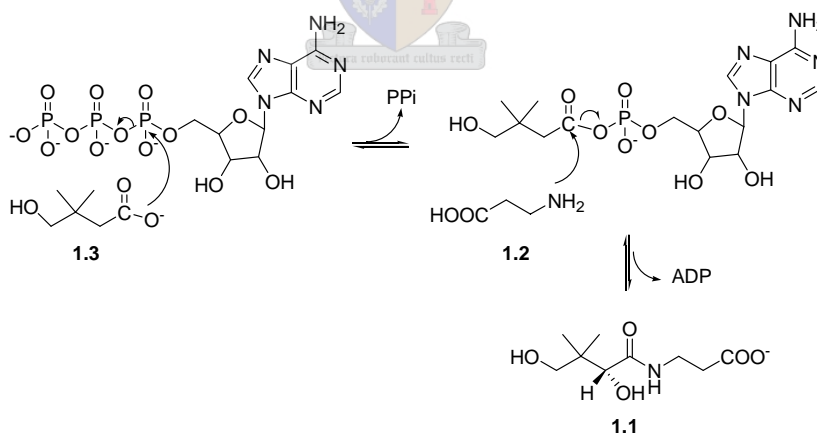
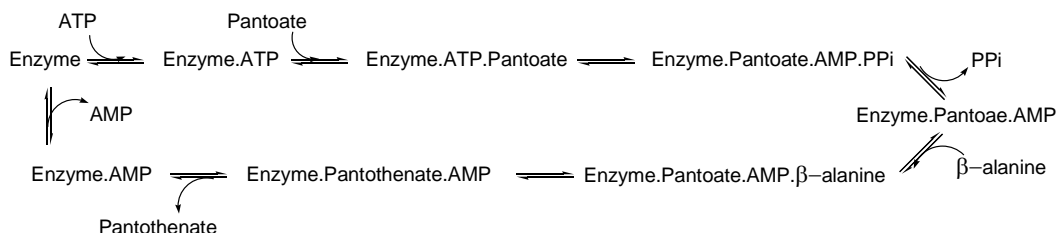


Figure 1.5: The catalytic mechanism of pantothenate synthetase (PanC). An amide bond forms between pantoate (**1.3**) and β -alanine (**1.2**) in the presence of ATP to form pantothenic acid (**1.1**).

In the first step **1.3** and ATP forms pantoate adenylate with the release of pyrophosphate. The second step is a nucleophilic attack by **1.2** on the intermediate to form pantothenate and AMP (15). The presence of the pantoate adenylate intermediate has been confirmed by

^{31}P -NMR and with positional isotope exchange reaction within ^{18}O -labeled ATP in the presence of D-pantoate (15).

The reaction proceeds via a Bi Uni Uni Bi Ping Pong mechanism (Scheme 1.1). This involves the initial binding of ATP followed by the binding of pantoate. In the proceeding step pyrophosphate is released, followed by the binding of β -alanine and the release of pantothenate. AMP is the last to be released. This reaction is dependent on Mg^{2+} and has a pH optimum of 10. Although Mg^{2+} is thought to be essential for the synthetase reaction, Mn^{2+} was also able to stimulate activity in Mtb (7).



Scheme 1.1: Schematic representation of the Bi Uni Uni Bi Ping Pong mechanism as used in the pantothenate synthetase reaction (7).

1.5 Essentiality of the pantothenate biosynthesis genes

The same study that observed that Mtb displays pantothenate dependant virulence found that the $\Delta panCD$ mutant could persist in the host organism for over 8 months (5). The organism has to obtain pantothenate from somewhere to survive, since it has been shown that fatty acid metabolism is one of the essential processes for survival in the latent state. Jacobs *et al.* postulated that an unidentified permease could be present to transport adequate amounts of pantothenic acid into the cells for survival, but not to restore virulence. They go further to state that such pantothenate permeases have been described in *Plasmodium falciparum* and *E. coli*. One problem though is that the intracellular life style of Mtb makes it difficult for it to obtain any essential nutrients from its host (5).

In an important study Rubin *et al.* aimed to identify the genes essential for survival in Mtb. This study included already characterized pathways as well as genes with unknown functions. To determine essentiality, genes were systematically knocked out by transposon site mutagenesis, a method using Himar1-based transposon deliverance by a

transducing bacteriophage and transposon site hybridization (TraSH). Interestingly, Rubin found that *panC* is essential for the survival of Mtb, but *panD* is not (9).

Since pantothenate biosynthesis is essential in Mtb, the organism must be able to obtain β -alanine from an alternative source or via another route. One of the sources postulated is a pantothenate salvage pathway that uses a permease, but until date no enzyme with this function has been identified in Mtb (5). The second solution is that an alternative metabolic pathway must exist and this is what we set out to identify in this study.

1.6 Alternative sources of β -alanine

Apart from the PanD-catalyzed decarboxylation of L-aspartate there are four other pathways postulated to produce β -alanine. These pathways include the catabolism of uracil, the degradation of polyamines, propionate degradation and cyanide metabolism in some plants. Even with 5 different pathways to choose from, only the decarboxylation of L-aspartate and polyamine degradation are thought to be involved in the synthesis of β -alanine for pantothenate production. The catabolism of pyrimidine may well contribute, but then only in a few species while propionate degradation and cyanide metabolism occur only in organisms that either do not synthesize pantothenate or where the pathways are presumed not to contribute significantly to the cellular pool of β -alanine (7). The four alternative routes are reviewed briefly.

1.6.1 Degradation of uracil

This pathway is present in the yeast *Saccharomyces kluyeri*, in mammals who use it for the biosynthesis of anserine and carnosine (mammals do not biosynthesize pantothenate *de novo*) and in other eukaryotes like *Drosophila melanogaster* in which β -alanine is a component of the cuticle (7).

The degradation of uracil (**1.7**) is initiated by its hydrogenation at the double bond to form 5,6-dihydouracil (**1.8**) by dihydrouracil dehydrogenase, followed by hydrolytic ring opening to form β -ureidopropionate (**1.9**). β -alanine (**1.2**) is formed by the deamination and decarboxylation of **1.9** (Figure 1.6). The reduction reaction is catalyzed by dihydrouracil dehydrogenase in the presence of either reduced nicotinamide adenine dinucleotide (NADH₂) or reduced nicotinamide adenine dinucleotide phosphate (NADPH₂) (16, 17).

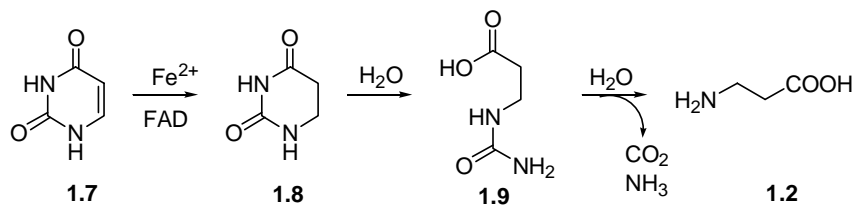


Figure 1.6: The degradation of uracil (1.7) to β-ureidopropionate (1.9) to β-alanine (1.2).

The degradation of uracil to β-alanine does not occur in baker's yeast, *S. cerevisiae* (18), and this pathway is also reported to be absent in bacteria (7). There is some controversy on this point, since it has been reported that there are certain *E. coli*-mutants that do indeed get their β-alanine from this pathway (19). The reports by Slotnick *et al.* however discount uracil as the β-alanine source, but clearly states the use of dihydrouracil as growth factor (20, 21). It has been shown that β-ureidopropionate and 5,6-dihydrouracil provide sufficient nutrition to maintain static stocks in auxotrophic *E. coli* strains but this pathway cannot support growth unless an excess of these metabolites is fed into the system (7). Studies done by Cronan *et al.* also discarded dihydrouracil as a growth factor. They concluded that the decarboxylation of L-aspartate is definitely the major route for β-alanine production (22). This is confirmed by the fact that bacteria normally first oxidizes uracil to barbiturate. The hydrolytic ring opening of barbiturate leads to the formation of malonate and urea and not β-alanine (16). In conclusion, if this pathway is present in *Mtb*, it will probably not provide sufficient amounts of β-alanine in the absence of the decarboxylation of L-aspartate to account for the steady state survival of the organism (7).

1.6.2 Degradation of polyamines

Polyamines are polybasic hydrocarbons of which the most well known are spermine, spermidine, putrescine and cadaverine. These compounds interact with the acidic cell components DNA, RNA, nucleotides and proteins. Many reactions with the polyamines have been characterized *in vivo*, which include the synthesis of DNA, RNA, proteins, stabilization of tRNA and increasing translation efficiency and fidelity under conditions of reduced Mg²⁺ concentrations (23, 24). Polyamines also have applications in fundamentally important processes including wound healing, tissue growth and tissue differentiation.

Degradation of the polyamines occurs in the presence of the amine oxidases to form a variety of smaller amine containing compounds (19). To form β -alanine a polyamine is first oxidized to 3-aminopropanal (**1.10**) in the presence of O_2 (Figure 1.7). This is followed by further oxidation to form the carboxylic acid, β -alanine (**1.2**). This reaction is catalyzed by the aldehyde dehydrogenases (25). The oxidation reaction is flavin-dependent and the gene sequence of the oxidation enzyme has sequence homology to the enzymes in the flavin dependent amine oxidizes enzyme family.

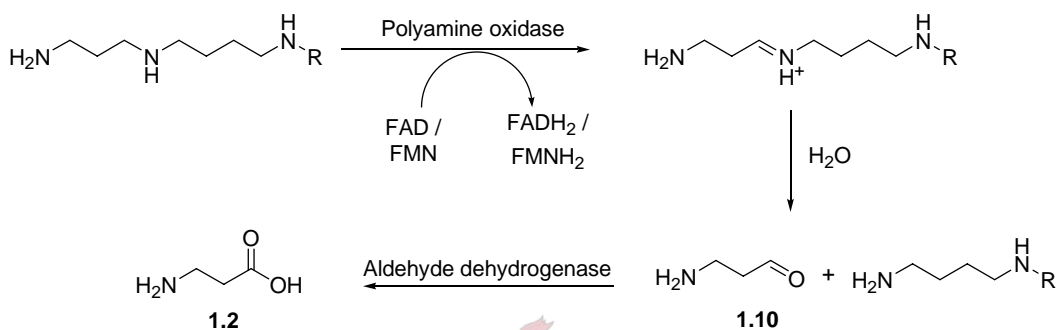


Figure 1.7: The oxidation of a polyamine to β -alanine.

This pathway is already well documented in the baker's yeast, *S. cerevisiae*. This is also the pathway we identified and attempted to characterize in Mtb.

1.6.3 Propionate degradation

As already mentioned this pathway is not regarded as a source of β -alanine for pantothenate biosynthesis. Propionyl-CoA (**1.11**) is dehydrogenated to acryloyl-CoA (**1.12**) that in turn is hydrolyzed to form β -hydroxypropionyl-CoA (**1.13**) (refer to Figure 1.8). This product is hydrolyzed to β -hydroxypropionate (**1.14**). The oxidation of **1.14** and the transamination of the resulting malonate semialdehyde (**1.15**) leads to the formation of β -alanine (**1.2**) (7).

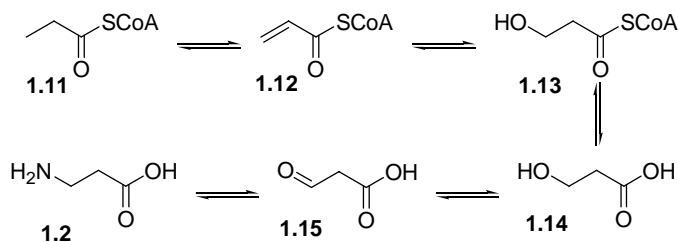


Figure 1.8: Biosynthesis of β -alanine via propionate degradation

1.6.4 Cyanide metabolism

This three step degradation reaction has not been characterized in any organism to date and is also presumed not to be the primary source of β -alanine in any organism. As can be seen in Figure 1.9, the reaction is initiated by the interaction of cysteine (**1.15**) with a free cyanide ion to form β -cyanoalanine (**1.16**). This product is hydrolyzed to asparagine or decarboxylated to form 3-aminopropionitrile (**1.17**). Hydrolysis of **1.17** forms β -alanine (**1.2**).

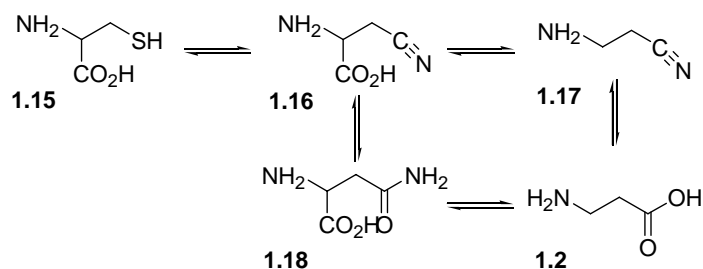


Figure 1.9: Hypothetical biosynthesis of β -alanine via cyanide metabolism

1.7 Degradation of polyamines in *S. cerevisiae*

The degradation of polyamines in the yeast *S. cerevisiae* occurs in two steps. In the first step the polyamine is oxidized by the polyamine oxidase Fms1 which was identified by White *et al.* (19) and purified to near homogeneity and characterized by Landry *et al.* (24). The aldehyde dehydrogenases required for the oxidation of the aldehyde to β -alanine is Ald2 and/or Ald3 (26). A brief overview of these enzymes follows.

1.7.1 Polyamine oxidase: *Fms1*

1.7.1.1 Background

It was originally reported that *S. cerevisiae* needed exogenous pantothenic acid for growth. Later it was found that it only needs a β -alanine supplement. This implied that *S. cerevisiae* has all the enzymes necessary for *de novo* biosynthesis of pantothenate except for a PanD homolog. Consistent with this homologs have been identified for all the enzymes in the pantothenic acid biosynthetic pathway except for PanD. The gene ECM31, thought to be involved in cell wall maintenance, has homology to *panB*. YIL145c is a *panC* orthologue that has been shown to be functional in *E. coli* and the putative YHR063c has structural homology to *panE*. To find a source for β -alanine White *et al.* studied the

putative polyamine oxidase Fms1. Functional screens done with Fms1 indicated that this enzyme was rate limiting in β -alanine and pantothenic acid biosynthesis and that overexpression of the gene lead to β -alanine excretion into the growth media. The role of Fms1 in β -alanine production from the polyamines was confirmed when it was found that all the enzymes in the polyamine biosynthesis pathway are necessary for β -alanine production (19).

1.7.1.2 Characteristics

Fms1 is a protein of 508 amino acids with sequence homology to polyamine oxidase of *Candida albicans*, human monoamine oxidase A and B and the peroxisomal acetylspermidine oxidase Aso1p of *Candida boidinii* (24). It contains the GXGXXG dinucleotide FAD recognition motif and it has been experimentally determined that it binds FAD non-covalently in a molar ratio of 1:1. Substrates for the enzyme include spermine (Spm), *N*¹-acetylspermine (*N*¹-spm), *N*¹-acetylspermidine and to a lesser extend *N*⁸-acetylspermidine (*N*⁸-spd). Of these only the oxidation of spermine yields β -alanine as a final product (24).

1.7.2 Aldehyde dehydrogenases: Ald2 and Ald3 (26)

1.7.2.1 Background

The complete yeast genome encodes for 7 different members of the aldehyde dehydrogenase family and any one of them could hypothetically be involved in β -alanine production. Two of these, ALD2 and ALD3, encode closely related cytosolic enzymes that are induced in response to stress or on ethanol media. ALD4 encodes the major K⁺-dependent mitochondrial enzyme and ALD5 encodes the minor one. ALD5 is also induced on ethanol. The Mg²⁺ mitochondrial enzyme is encoded by ALD6. Of the two remaining sequences MSC7/YHR039c encodes a protein with sequence homology to an aldehyde dehydrogenase that affects meiotic sister-chromatid recombination and YMR110c is a hypothetical protein. Even though multiple gene sequences exist, only acetaldehyde has been identified as a physiological substrate and only Ald4p and Ald6p are involved in oxidizing this substrate to acetate. Ald2p, Ald3p and Ald5p are not involved in this process. Ald5p also has been postulated to have an undefined role in heme biosynthesis. Furthermore, Ald4p and Ald5p are mitochondrial enzymes as opposed to Ald2p, Ald3p and Ald6p which are cytosolic enzymes. This may make Ald4p and Ald5p unavailable for the oxidation of 3-aminopropanal since is most likely produced

and consumed in the cytosol. Studies with deletion mutants done by White *et al.* revealed that only the double deletion mutant $\Delta ald2\Delta ald3$ showed complete pantothenate auxotrophy. This auxotrophy was lifted by introducing a plasmid that contains either of the two gene sequences. They also showed that although there is a significant degree of amino acid conservation between the aldehyde dehydrogenases, only ALD2 and ALD3 could be implicated in β -alanine biosynthesis.

1.7.2.2 Characteristics

It was shown that ALD2 and ALD3 functions downstream from FMS1 and oxidizes 3-aminopropanal to β -alanine. Although there is 91% amino acid conservation between Ald2p and Ald3p, a degree of functional specialization does exist. A mutant strain without the *ALD2* gene is partially defective for pantothenate biosynthesis. This leads to the conclusion that Ald2p is responsible for the majority of β -alanine production. By placing the *ALD2*-mutant under K^+ - or Na^+ -induced osmotic stress, the defect seizes. Since it is known that transcription of Ald3p is osmo-induced (27) a sufficient rate of conversion from 3-aminopropanal to β -alanine *in vivo* should occur with this enzyme.

1.8 Identification of AofH

To identify a possible polyamine oxidase in *Mycobacterium tuberculosis*, a sequence homology search was done of FMS1 against the Mtb genome. The orthologue that aligned the best was designated *aofH* (amine oxidase flavin dependent protein) or Rv3170 (10). According to the Tuberculist database AofH is a putative monoamine oxidase (MAO) that is flavin dependent. An amino acid alignment of *aofH* and *FMS1* in ClustalW shows that *aofH* is 60 amino acids shorter than *FMS1*. Of these amino acids 99 residues match exactly, 88 residues are closely related, a further 60 residues align to a degree and 201 residues show no similarity at all. The enzyme Fms1 was identified as a member of the Glutathione reductase (GR) structural subfamily of the FAD-containing protein family. One of the most conserved sequences of this family is the N-terminally located motif xhxhGxGxxGxxhxxh(x)shxhE where x = any residue and h = any hydrophobic residue (28). This motif normally comprises part of the Rossmann fold. This sequence is conserved in *aofH* along with the GxGxxG FAD binding domain (Figure 1.10). This indicates that AofH may well be part of the GR enzymatic family and confirms the FAD dependence postulate.

1.9 Conclusion

TB is still a very relevant problem in the African Health context today and the need for new drugs and the identification of new drug targets exist. In the search for new drug targets we focused on the biosynthesis of pantothenate since it is an essential process in Mtb pertaining to the virulence of the pathogen. Of the enzymes involved in this process PanD, the enzyme that catalyses the decarboxylation of L-aspartate to β -alanine, was found not to be essential. If this is the case, Mtb must be able to obtain β -alanine by either a permease or another biosynthetic route. Currently there are four alternative pathways known for the production of β -alanine of which the degradation of polyamines seems to be the most likely alternative to obtain this metabolite. This pathway has been well characterized in the yeast *S. cerevisiae* that uses the polyamine oxidase Fms1 and the aldehyde dehydrogenases Ald2 and Ald3. Based on this we set out to identify the alternative pathway for β -alanine production as the degradation of polyamines.

1.10 Aims of this thesis

The main aims of this project are to clone and express AofH solubly and to determine the activity of the enzyme. With the activity known, the substrates of choice can be identified and used in the rational design of mechanism based inhibitors for the enzyme.

The second aim is to study the inhibitory effects of small molecules on the enzyme that supplies the main source of β -alanine to Mtb, L-aspartate- α -decarboxylase (PanD). To do this however methods have to be developed to screen these molecules both quantitative and qualitative. Once this is done we want to design mechanism based inhibitors that are specific for PanD.

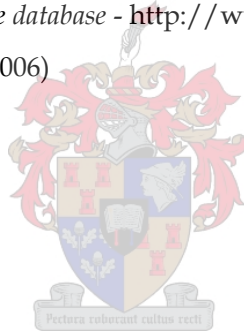
1.11 References

- (1) World Health organisation (WHO) -
<http://www.who.int/tb/dots/dotsplus/faq/en/index.html>
http://www.who.int/vaccine_research/diseases/tb/en/
(Last accessed: 15 October 2005)
- (2) Cole, S. T., Brosch, R., Parkhill, J., Garnier, T., Churcher, C., Harris, D., Gordon, S. V., Eiglmeier, K., Gas, S., Barry, C. E., III, Tekaia, F., Badcock, K., Basham, D., Brown, D.,

- Chillingworth, T., Connor, R., Davies, R., Devlin, K., Feltwell, T., Gentles, S., Hamlin, N., Holroyd, S., Hornsby, T., Jagels, K., Krogh, A., McLean, J., Moule, S., Murphy, L., Oliver, K., Osborne, J., Quail, M. A., Rajandream, M. A., Rogers, J., Rutter, S., Seeger, K., Skelton, J., Squares, R., Squares, S., Sulston, J. E., Taylor, K., Whitehead, S., and Barrell, B. G. (1998) *Deciphering the biology of Mycobacterium tuberculosis from the complete genome sequence*. *Nature* **393**, 537-544.
- (3) Honer zu Bentrup, K., and Russell, D. G. (2001) *Mycobacterial persistence: adaptation to a changing environment*. *Trends in Microbiology* **9**, 597-605.
- (4) Zheng, R., and Blanchard, J. S. (2001) *Steady-State and Pre-Steady-State Kinetic Analysis of Mycobacterium tuberculosis Pantothenate Synthetase*. *Biochemistry* **40**, 12904-12912.
- (5) Sambandamurthy Vasan, K., Wang, X., Chen, B., Russell Robert, G., Derrick, S., Collins Frank, M., Morris Sheldon, L., and Jacobs William, R., Jr. (2002) *A pantothenate auxotroph of Mycobacterium tuberculosis is highly attenuated and protects mice against tuberculosis*. *Nature Medicine* **8**, 1171-4.
- (6) Begley, T. P., Kinsland, C., and Strauss, E. (2001) *The biosynthesis of coenzyme A in bacteria*. *Vitamins and Hormones* **61**, 157-71.
- (7) Webb, M. E., Smith, A. G., and Abell, C. (2004) *Biosynthesis of pantothenate*. *Natural Product Reports* **21**, 695-721.
- (8) Sugantino, M., Zheng, R., Yu, M., and Blanchard John, S. (2003) *Mycobacterium tuberculosis ketopantoate hydroxymethyltransferase: tetrahydrofolate-independent hydroxymethyltransferase and enolization reactions with alpha-keto acids*. *Biochemistry* **42**, 191-9.
- (9) Sassetti, C. M., Boyd, D. H., and Rubin, E. J. (2003) *Genes required for mycobacterial growth defined by high density mutagenesis*. *Molecular Microbiology* **48**, 77-84.
- (10) Tuberculist -TubercuList World-Wide Web Server -
<http://genolist.pasteur.fr/TubercuList/> (Last accessed: 4 January 2006)
- (11) Chopra, S., Pai, H., and Ranganathan, A. (2002) *Expression, purification, and biochemical characterization of Mycobacterium tuberculosis aspartate decarboxylase, PanD*. *Protein Expression and Purification* **25**, 533-540.

- (12) Wang, S., and Eisenberg, D. (2003) *Crystal structures of a pantothenate synthetase from M. tuberculosis and its complexes with substrates and a reaction intermediate*. Protein Science **12**, 1097-1108.
- (13) von Delft, F., Lewendon, A., Dhanaraj, V., Blundell, T. L., Abell, C., and Smith, A. G. (2001) *The crystal structure of E. coli pantothenate synthetase confirms it as a member of the cytidyltransferase superfamily*. Structure **9**, 439-450.
- (14) Zheng, R., Dam, T. K., Brewer, C. F., and Blanchard, J. S. (2004) *Active Site Residues in Mycobacterium tuberculosis Pantothenate Synthetase Required in the Formation and Stabilization of the Adenylate Intermediate*. Biochemistry **43**, 7171-7178.
- (15) Williams, L., Zheng, R., Blanchard, J. S., and Raushel, F. M. (2003) *Positional Isotope Exchange Analysis of the Pantothenate Synthetase Reaction*. Biochemistry **42**, 5108-5113.
- (16) Michal, G. (1999) in *Biochemical Pathways*, John Wiley & Sons Inc.
- (17) Schmuck, C., and Wennemers, H. (2004) *Highlights in Bioorganic Chemistry: Methods and Applications*, Wiley-VCH.
- (18) Gojkovic, Z., Sandrini, M. P., and Piskur, J. (2001) *Eukaryotic beta-alanine synthases are functionally related but have a high degree of structural diversity*. Genetics **158**, 999-1011.
- (19) White, W. H., Gunyuzlu, P. L., and Toyn, J. H. (2001) *Saccharomyces cerevisiae is capable of de novo pantothenic acid biosynthesis involving a novel pathway of b-alanine production from spermine*. Journal of Biological Chemistry **276**, 10794-10800.
- (20) Slotnick, I. J. (1956) *Dihydrouracil as a growth factor for a mutant strain of Escherichia coli*. Journal of Bacteriology **72**, 276-7.
- (21) Slotnick, I. J., and Weinfeld, H. (1957) *Dihydrouracil as a growth factor for mutant strains of Escherichia coli*. Journal of Bacteriology **74**, 122-5.
- (22) Cronan, J. E., Jr. (1980) *b-Alanine synthesis in Escherichia coli*. Journal of Bacteriology **141**, 1291-7.
- (23) Tabor, C. W., and Tabor, H. (1985) *Polyamines in microorganisms*. Microbiological Reviews **49**, 81-99.
- (24) Landry, J., and Sternglanz, R. (2003) *Yeast Fms1 is a FAD-utilizing polyamine oxidase*. Biochemical and Biophysical Research Communications **303**, 771-776.

- (25) Large, P. J. (1992) *Enzymes and pathways of polyamine breakdown in microorganisms*. FEMS Microbiology Reviews **8**, 249-62.
- (26) White, W. H., Skatrud, P. L., Xue, Z., and Toyn, J. H. (2003) *Specialization of function among aldehyde dehydrogenases: the ALD2 and ALD3 genes are required for b-alanine biosynthesis in Saccharomyces cerevisiae*. Genetics **163**, 69-77.
- (27) Navarro-Avino, J. P., Prasad, R., Miralles, V. J., Benito, R. M., and Serrano, R. (1999) *A proposal for nomenclature of aldehyde dehydrogenases in Saccharomyces cerevisiae and characterization of the stress-inducible ALD2 and ALD3 genes*. Yeast **15**, 829-42.
- (28) Huang, Q., Liu, Q., and Hao, Q. (2005) *Crystal Structures of Fms1 and its Complex with Spermine Reveal Substrate Specificity*. Journal of Molecular Biology **348**, 951-959.
- (29) Notredame, C., Higgins, D., and Heringa, J. (2000) *T-Coffee: A novel method for multiple sequence alignments*. Journal of Molecular Biology **302**, 205-217.
- (30) SGD™ -Saccharomyces online database - <http://www.yeastgenome.org/>
(Last accessed: 4 January 2006)



Chapter 2

Cloning, expression and purification of AofH:

A closer look at different solubilization and purification strategies

2.1 Introduction

AofH was identified as a possible polyamine oxidase in *Mycobacterium tuberculosis*. With the gene sequence known, the *aofH*-gene could be amplified from Mtb genomic DNA, ligated into an expression vector and overexpressed. This chapter focuses on the cloning and soluble expression of AofH.

2.1.1 Cloning and initial expression trials

The *aofH* DNA sequence was amplified from genomic DNA of Mtb strain H37Rv with the introduction of an N-terminal NdeI-site and a C-terminal XhoI-site. After restriction digestion with these enzymes, the PCR product was subcloned into pET28a(+). This plasmid is part of the Novagen pET expression system and introduces an N-terminal 6×histidine-tag (His-tag) to the protein. The His-tag facilitates affinity purification of the protein by coordinating to Ni²⁺ (discussed later). The formation of the construct was confirmed by screening and sequencing. Expression trials were used to determine the conditions for the most efficient AofH overexpression. These conditions included the temperature at which the expression was induced with isopropyl-β-D-thiogalactoside (IPTG), time of growth after induction and the concentration of IPTG used. Except when the induction amount of IPTG was varied, all expression trials and large scale expressions were done from an *E. coli* B-strain, either BL21 (DE3) or BL21*(DE3). For the variation of IPTG amounts Tuner (DE3) cell strain were used as it is a *lac* permease deletion mutant that allows uniform entry of IPTG into cells and thus provides strict concentration-dependent control of induction.

2.1.2 Attempts at solubility

To obtain soluble expression of AofH, we initially focused on fusing different tags to the protein and evaluating the degree of expression obtained of the fused protein. To do this new expression plasmids, which contained the new tag and the *aofH* gene sequence, had

to be created. For this we moved towards the Invitrogen Gateway™ system. This system allows the formation of expression clones by adding together an entry plasmid (pENTR), containing the gene sequence, and a destination plasmid (pDEST), containing the tag, with an enzyme mixture dubbed “LR clonase” to form the new expression plasmid (pEXP) that contains both the tag and target sequence. (Refer to Figure 2.1).

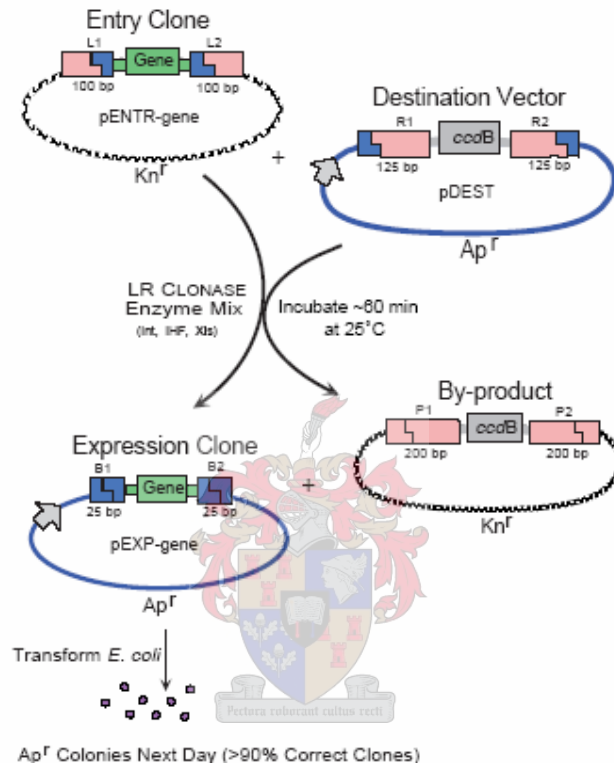


Figure 2.1: The Gateway LR reaction (1). The entry clone (pENTR) combines with the destination clone (pDEST) in the presence of LR clonase to form the expression clone (pEXP). Kn^R = kanamycin resistance and Ap^R = ampicillin resistance. (Reproduced from the GIBCO BRL Gateway™ cloning technology Instruction manual, version A)

The entry plasmid used was pENTR4N. This plasmid was derived from the commercial plasmid pENTR4 in which the NcoI-site has been mutated to an NdeI-site (2). The amplified *aofH* DNA was ligated into pENTR4N using the XhoI and NdeI restriction sites. From there *aofH* was successfully subcloned into pDEST15 (GST-tag), pDEST566 (His-MBP-tag), pDEST544 (His-Nus-tag), pET160-DEST (His-Lumio™-tag), pET160-GST-DEST (His-GST-Lumio™-tag), pBAD-DEST49 (thioredoxin-tag) and pYES-DEST52. A summary of the plasmids and tags used in this study are given in Table 2.1.

Table 2.1: A summary of the plasmid used in this study, the application they were used for and the result obtained.

Plasmid	Fusion tag	Parents	Method of construction	Source of parent	Application	Expressed	Soluble	Purified	Section
pET28a(+)- <i>aofH</i>	6×His	pET28a(+) <i>aofH</i> PCR product	Restriction digests and ligation	Novagen	Expression trials	√	X	X	2.1.1
pENTR4N- <i>aofH</i>	N/A	pENTR4N <i>aofH</i> PCR product	Restriction digests and ligation	Created by Leisl Brand	Entry vector for LR reactions	N/A	N/A	N/A	2.1.2
pEXP15- <i>aofH</i>	GST	pDEST15 pENTR4N- <i>aofH</i>	LR reaction	Invitrogen	Expression trials/ Purification	√	√	X	2.2.1
pEXP566- <i>aofH</i>	6×His-MBP	pDEST566 pENTR4N- <i>aofH</i>	LR reaction	Cynthia Kinsland	Expression trials/ Purification	√	√	√	2.2.3
pEXP544- <i>aofH</i>	6×His-Nus	pDEST544 pENTR4N- <i>aofH</i>	LR reaction	Cynthia Kinsland	Expression trials/ Purification	√	√	√	2.2.4
pET160-EXP- <i>aofH</i>	6×His + Lumio™	pET160-DEST pENTR4N- <i>aofH</i>	LR reaction	Invitrogen	Purification	√	X	X	2.2.5
pET160-EXP GST- <i>aofH</i>	6×His-GST + Lumio™	pET160-GST-DEST pENTR4N- <i>aofH</i>	LR reaction	Created by Leisl Brand	Purification	√	√	X	2.2.2
pBAD-EXP49- <i>aofH</i>	His-Patch thioredoxin	PBAD-DEST49 pENTR4N- <i>aofH</i>	LR reaction	Invitrogen	Purification/ Complementation	√	X	X	2.2.6 3.5.1
pYES-EXP52- <i>aofH</i>	N/A	pYES-DEST52 pENTR4N- <i>aofH</i>	LR reaction	Invitrogen	Expression trials Complementation	X	X	X	2.4.1 3.5.2

2.1.3 Expression of AofH fusions

The rate of cell growth and protein expression is important factors for the expression of foreign proteins from the *E. coli* system. The solubility of the target protein fusions was tested initially by expression trials at 37°C for a set period of time. If soluble expression was not obtained, the following three parameters, all pertaining to rate of cell growth and protein expression, were changed.

1. By transforming the plasmid into the Tuner (DE3) cell strain, the IPTG concentration with which are induced could be changed. In the T7 promoter systems we use, T7 RNA polymerase induces expression of the plasmids containing the target sequence. The IPTG-inducible *lacUV5* promoter controls the expression of T7 RNA polymerase in the host strain. By changing the amount of IPTG used for induction, the expression of T7 RNA polymerase can be controlled and subsequently the rate of protein expression (3). In our experiments we induced with IPTG to final concentration of 1mM, 0.75mM, 0.5mM, 0.2mM, 0.1mM and 0.05mM.
2. Another parameter that controls the rate of expression is the temperature at which induction and expression occurs. The decrease in temperature decreases the rate at which proteins are synthesized and may in some cases enhance solubility (4). All expression trials were at 15°C, 20°C, 25°C, 30°C and 37°C.
3. The third parameter that was varied is the period of incubation after induction. Too short expression times may lead in too little protein being expressed, while too long incubation times may lead to protease degradation of the proteins (5). In addition the overgrowth of the culture may lead to overload of the bacterial synthetic apparatus and promote the formation of inclusion bodies (3). All our experiments were incubated for 2 h, 4h or overnight.

Expression was induced when an optical density at 600nm (OD₆₀₀) of 0.6 was reached (mid-log phase). The expression of the different AofH fusions is discussed in the next section.

2.2 Attempts at native expression and purification

Our original attempt to express AofH was as His-AofH from pET28a(+). Soluble expression was not obtained and this led to the investigation of different fusion tags.

2.2.1 GST-tag

The first tag we tried was the 26kDa glutathione-S-transferase tag (GST) that has its origin from *Schistosoma japonicum*. This tag is found in the commercial vector, pDEST15 (6). Soluble GST-AofH was obtained with induction with 0.5mM IPTG at 37°C and leaving the expression for 3 hours (Figure 2.2).

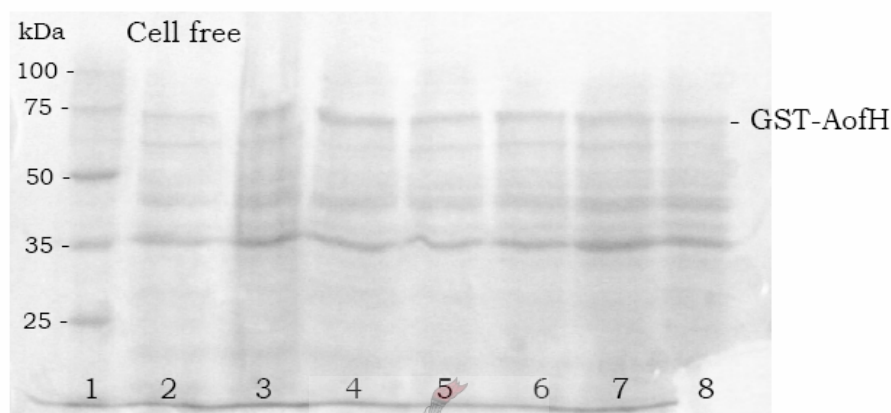


Figure 2.2: Soluble expression of GST-AofH. Lane 1- marker. The following lanes are the soluble protein samples induced with the following final concentration of IPTG and grown for 3h: lane 2 - 1mM, lane 3 - 0.75mM, lane 4 - 0.5mM, lane 5 - 0.2mM, lane 6 - 0.1mM, lane 7 - 0.05mM. Lane 8 -sample induced with 0.5mM IPTG and grown overnight

Purification of the GST-AofH fusion from the bacterial lysate was attempted with affinity chromatography on the ÄKTAprime-system. This system is a compact, automated liquid chromatography system that simplifies the process of purification by affinity chromatography. The GST-tag binds to the glutathione matrix of the 1ml GSTrap FF column. Elution of the tagged protein is obtained by addition of reduced glutathione to the elution buffer.

The first attempt to purify GST-AofH made use of His-tag binding buffer (20mM Tris-HCl; 150mM NaCl; pH 7.3) and the elution buffer recommended by the suppliers (20mM Tris-HCl, 10mM reduced glutathione, pH 8.0). Chromatography was recorded with a UV detector at 280nm to determine when the protein elutes. Two different purification methods were used as discussed below and in both instances no purification was obtained. 12% SDS PAGE analysis of the purification showed that the protein never bound to the column.

In the effort to purify GST-AofH we experimented with different protocols for the purification runs, buffer compositions and even tried a new column. The different runs, buffer changes and detection methods used are summarized in Table 2.2.

Table 2.2: Experimental changes for purification of GST tagged proteins

Change	Self program-med run	Tem-plate run	Manual controlled run	Detect protein	Reason for change
Initial run	√	√		UV detector at 280nm	No protein purified
Add DTT to buffers	√			UV detector at 280nm	Cleave disulfide bonds that may have formed in protein
Change binding buffer to PBS + DTT	√	√		UV detector at 280nm	Exchange the Tris buffer for phosphate buffers.
Slower injection step	√	√		UV detector at 280nm	Increase efficiency of protein binding to column
Shorter wash steps	√			UV detector at 280nm	Reduce changes of losing protein
Elution buffer +40mM reduced glutathione			√	Bradford reagent	Higher elution efficiency due to increase affinity binding of glutathione
Elution buffer + 200mM NaCl			√	Bradford reagent	Increase ionic to increase elution affinity
Elution buffer + 0.1% Triton X-100			√	Bradford reagent	Non-ionic detergent to prevent hydrophobic interactions which may prevent solubility and elution of fusion proteins

The self-programmed run mentioned in Table 2.2 consist of (excluding column equilibration and injection of the protein onto the column) a wash step of 10 column volumes (CV) of binding buffer followed by a wash step with 15 CV of 15% elution buffer (final concentration of 1.5mM reduced glutathione) to remove any non-specifically bound proteins. The protein was eluted with 20 CV of 100% elution buffer. A flow rate of 1ml.min⁻¹ is maintained throughout the run. The template run is pre-programmed on the ÄKTAprime-system for purifications of GST fusions. The only difference between the self-programmed run and the template run is that the wash step with 15% elution buffer was omitted from the template run. The manual run was controlled from the user interface

based on the observations made from the UV chromatogram being recorded during the run.

The changes in buffer composition were made according to the trouble-shooting guide in the Amersham GST Instruction manual (6). One of the methods suggested to increase binding efficiency of the protein to the column is to add dithiothreitol (DTT) to the lysate mixture before lysis. DTT, a reagent that cleaves disulfide bonds, was added to both buffers to a final concentration of 10mM and the purification runs repeated, without success. The binding buffer was changed to PBS-buffer (140mM NaCl, 2.7mM KCl, 10mM Na₂HPO₄, 1.8mM KH₂PO₄, 10mM DTT, pH 7.3), which is the buffer recommended by Amersham. Milder sonication conditions were also used to eliminate the change of denaturation of the tagged protein during cell lysis. The injection tempo while the protein sample was loaded on the column was also lowered from 1.0ml.min⁻¹ to 0.5ml.min⁻¹. No protein was purified.

Further attempts to elute the GST-protein from the column included limiting the time and volume of column washing, increasing the concentration of reduced glutathione from 10 to 40mM in the elution buffer and increasing the ionic strength of the elution buffer by adding 200mM NaCl. These purifications were performed manually by changing the parameters on the ÄKTAprime-system and adding Bradford reagent to an aliquot of the fractions that were assumed to contain protein. A non-ionic detergent, Triton X-100, was also added to a final concentration of 0.1% to the elution buffer to counter any non-specific hydrophobic interactions that may prevent solubilization and elution. After careful experimentation with all the different elution buffers and obtaining no results a new column was tested. This was also unsuccessful.

2.2.2 His-GST

Since the problems experienced with the GST-AofH fusion where all purification related, a fusion was created that adds a His-tag in front of the GST-tag. This combination tag is found in pET160-GST-DEST, a plasmid that was created in our lab by Ms. Leisl Brand from the commercial plasmid pET160-DEST, which contains a His-Lumio™ tag. pET160-GST-DEST was created by inserting the GST tag between the His and Lumio™ tags. This affords the real tag to be a fusion between the His, Lumio™ and GST tags, but since only the His-tag is important for purification and the GST-tag for solubility, it is designated His-GST.

As can be seen from the 12% SDS PAGE gel in Figure 2.3 soluble expression of the 76kDa protein was easily obtained at all IPTG concentrations. Large-scale overexpression was induced with a final concentration of 0.1mM IPTG at 37°C and the expression left overnight.

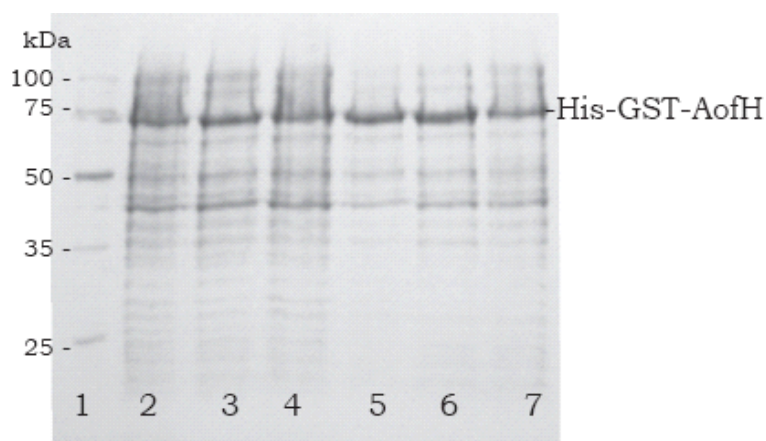


Figure 2.3: The 12% SDS-PAGE gel of the cell free lysate samples to determine the optimum amount of IPTG to obtain soluble His-GST-AofH. All expressions were performed at 37°C and cultures were grown overnight. The samples are as follows: Lane 1- marker, Induced with final concentration IPTG: lane 2 - 1mM, lane 3 - 0.75mM, lane 4 - 0.5mM, lane 5 - 0.2mM, lane 6 - 0.1mM, lane 7 - 0.05mM

Purification of the enzyme by affinity chromatography on a 1ml HiTrap Chelating column with the ÄKTAprime -system failed (data not shown). As in the case of GST-AofH, the protein bands were clearly visible on the 12% SDS PAGE gels in the crude extract and flow through samples. As in the previous cases the protein thus expresses solubly, but does not bind to the column. The purifications were tried by replacing the HiTrap chelating columns with a Sigma Ni²⁺-NTA column. These columns already have Ni²⁺ chelated to the resin. The new column made no a difference.

Since we know His-GST-AofH does express solubly and the problem lies with the binding interaction of the protein to the column, we tested different buffers with different pH values for the purification. The buffer compositions are given in Table 2.3. The enzymes were purified on small scale using the batch purification method and buffer combinations given in Table 2.4. The fractions were analyzed on 12% SDS PAGE gels as shown in Figure 2.4.

Table 2.3: The composition of the different buffers used for the purification of His-GST-AofH.

Identifier	Composition	pH	Binding/ Elution	Source
His-tag binding buffer	20mM Tris-HCl 500mM NaCl 5mM Imidazole	pH 7.9	Binding	Our standard binding buffers
His-tag elution buffer	20mM Tris-HCl 500mM NaCl 50mM Imidazole	pH 7.9	Elution	Our standard elution buffer
PBS	140mM NaCl 2.7mM KCl 10mM Na ₂ HPO ₄ 1.8mM KH ₂ PO ₄	pH 7.3	Binding	(6)
Buffer A	20mM Tris-HCl 100mM NaCl 10mM β -mercaptoethanol	pH 6.7	Binding	Protein refolding (8)
Buffer A elution	20mM Tris-HCl 100mM NaCl 10mM β -mercaptoethanol 600mM imidazole	pH 8.0	Elution	Protein refolding (8)
High Tris	50mM Tris-HCl 20mM KCl 10mM MgCl ₂	pH 7.6	Binding	Had in laboratory
Tris-EDTA	10mM Tris-HCl 1mM EDTA 0.8% MgCl ₂	pH 7.75	Binding	(9)
HEPES	20mM HEPES 300mM NaCl 5mM β -mercaptoethanol	pH 8.0	Binding	(7)
His-select binding buffer	50mM Na ₃ PO ₄ 300mM NaCl 10mM imidazole	pH 8.0	Binding	(10)
His-select elution buffer	50mM Na ₃ PO ₄ 300mM NaCl 250mM imidazole	pH 8.0	Elution	(10)

From these results it seemed that purification was obtained with Tris-buffer with added β -mercaptoethanol and the phosphate buffers. The experiments were scaled up using PBS as binding buffer and the His-tag elution buffer (Tris-buffer, Table 2.3) for purification on the ÄKTA_{prime}-system with the flow rate during injection decreased to 0.1 ml.min⁻¹. The upscaling proved to be unsuccessful.

Table 2.4: Experimental set-up for purifications of His-GST-AofH with different buffers.

Experiment number	Identifier	Binding Buffer	Elution Buffer
1	High Tris	High Tris	His-tag elution buffer
2	Tris + Imidazole	His-tag binding buffer	His-tag elution buffer
3	Tris + EDTA	Tris-EDTA	His-tag elution buffer
4	Tris + β -mercaptoethanol	Buffer A	Buffer A elution
5	Phosphate	PBS	His-select elution buffer
6	Phosphate + imidazole	His-select binding buffer	His-select elution buffer
7	HEPES	HEPES	His-tag elution buffer

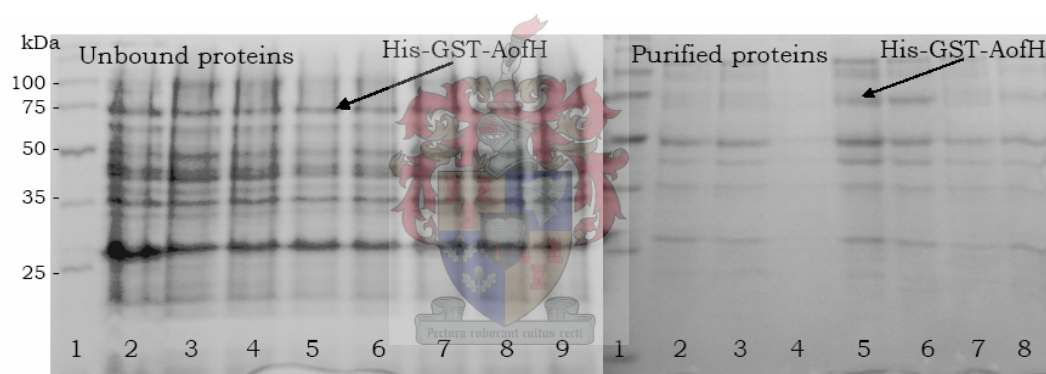


Figure 2.4: SDS PAGE gels of His-GST-AofH purifications with different buffer combinations. The gel on the right is of the proteins that did not bind to the resin (unbound proteins, flow through) and the gel on the left of the purified proteins. Lanes 1 - marker. The rest of the lanes indicate the buffer combinations used as given in Table 2.4: Lanes 2 - 1, lanes 3 - 2, lanes 4 - 3, lanes 5 - 4, lanes 6 - 5, lanes 7 - 6 and lanes 8 - 7.

Since purification was obtained with the batch method, but not on large scale, a manual purification was attempted using the same resin as was used for the batch purifications. The fractions obtained from the manual purification were analyzed on a 12% SDS PAGE gel (Figure 2.5) and a degree of purification was obtained between the flow through (the proteins that did not bind to the column) and the wash peak (non-specifically bound proteins). Furthermore the protein did not express as well as in earlier experiments. SDS PAGE analysis indicated a band at 50kDa, the size of AofH without the GST-tag (His-

GST-AofH = 76kDa). The question arose if this is AofH without a tag, but attempts to purify this band failed and its identity could thus not be confirmed.



Figure 2.5: Gel picture of the manual purifications of His-GST-AofH. Lane1 - marker, lane 2 - flow through (attempt 1), lane 3 - Purified protein (attempt 1), lane 4 - flow through (attempt 2), lane 5 - purified protein (attempt 2), lane 6 - crude extract from the bacterial lysate that contains a protein band the size of AofH. This band could not be identified and is therefore indicated as unknown.

Purification of His-GST-AofH from crude bacterial lysate was attempted with gradient elution in which the concentration of imidazole was increased very gradually. For each new concentration the column was eluted with 2 CV of the elution buffer in steps with imidazole concentrations from 1.73 to 100mM. SDS PAGE analysis indicated that the bands at 76kDa (GST-AofH) and 26kDa (GST) were absent, but the unknown band at 50kDa again appeared.

2.2.3 His-MBP-tag

Maltose binding protein is a 43.277kDa fusion tag that is thought to be a far better fusion partner than GST to increase solubility (4). This tag is fused C-terminally to a His-tag in the pDEST566 vector.

One round of expression trials were performed in BL21* (DE3) at 37°C. According to the SDS PAGE analysis (Figure 2.6) the 93.3kDa fusion expresses solubly, although not very well, at all the IPTG induction concentrations. The cell free (soluble proteins) and whole cell (total cell lysate) SDS PAGE analyses are shown.

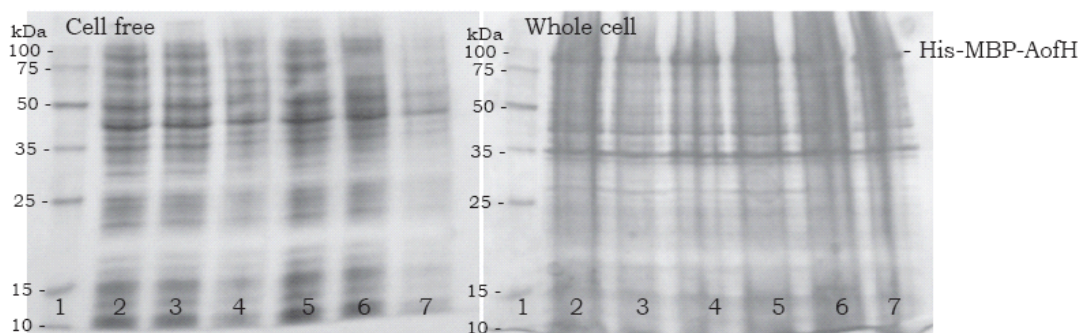


Figure 2.6: The 12% SDS PAGE gel analysis of the expression trials of His-MBP-AofH. The expressions were induced with different concentrations IPTG at 37°C and expressed for 3 hours after induction. The gel on the left is the cell free lysate samples that contains the soluble proteins and the gel on the right the whole cell samples. Lane 1- marker, Induced with final concentration IPTG: lane 2 - 1mM, lane 3 - 0.75mM, lane 4 - 0.5mM, lane 5 - 0.2mM, lane 6 - 0.1mM, lane 7 - 0.05mM

Large-scale expressions were induced with a final concentration of 0.2mM IPTG at 37°C and grown for 3 hours. The protein was easily purified using affinity chromatography on a 1ml HiTrap Chelating column with the ÄKTAprime -system (refer to Figure 2.7).

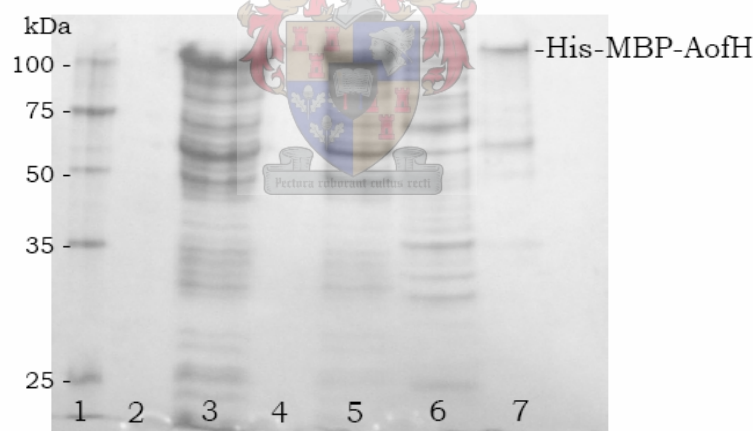


Figure 2.7: The 12% SDS PAGE gel analysis of the large scale expression of His-MBP-AofH. Lane 1- marker, lane 2 - nothing, lane 3 - crude extract (total cell lysate), lane 4 - nothing, lane 5 - flow through (proteins that do not bind to column), lane 6 - wash (non-specifically bound proteins), lane 7 - protein.

2.2.4 His-Nus-tag

The Nut Utilization Substance (Nus) is 54kDa tag. NusA is not only efficient in solubilizing its fusion due to its size, but also because high levels of expression of this

protein occur in *E. coli* (11). This tag has an N-terminally fused His-tag in the pDEST544 vector.

Extensive expression trials were done with the His-Nus-AofH fusion and soluble expression was only obtained when induced with a final concentration of 0.5mM IPTG at 20°C and left to express overnight. The fusion protein was easily purified using affinity chromatography on a 1ml HiTrap Chelating column with the ÄKTAprime -system as can be seen in Figure 2.8.

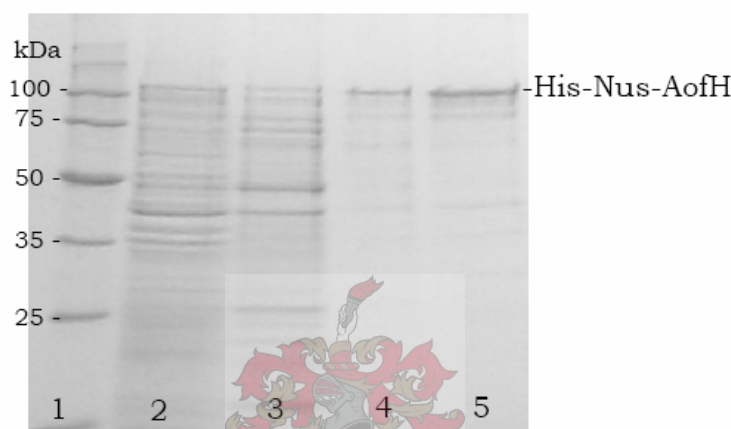


Figure 2.8: The 12% SDS PAGE gel analysis of the large scale expression of His-Nus-AofH. Lane 1- marker, lane 2 - crude extract (total cell lysate), lane 3 -wash (non-specifically bound proteins), lane 4 and 5 - protein.

2.2.5 His Lumio™-tag

Since this tag is extremely small, it was not used to obtain better solubility, but rather to develop a screening method. The Lumio™ green detection system is a fluorescent base screen in which a FIAsh™ (Fluorescein Arsenical Hairpin binding) reagent binds site specifically to the tetracysteine motif Cys-Cys-Xaa-Xaa-Cys-Cys, where Xaa is any amino acid. In pET160-DEST the Lumio™-tag is Cys-Cys-Pro-Gly-Cys-Cys and it binds a biarsenical compound that is non-fluorescent in its unbound form. This specific tag has a proven higher affinity for the biarsenic compound. In addition to the Lumio™-tag the plasmid also incorporates a His-tag N-terminally to the Lumio™-tag for affinity purification (12, 13). The Lumio™ -AofH fusions were expressed in conjunction with the chaperone plasmids (section 3.1) and scarce codon coding plasmids (section 3.2) where the problem exists that some of the chaperone enzymes are the same size as the AofH-

fusion and that their overexpression is much more efficient. When expression was tried with this fusion no soluble protein was obtained.

2.2.6 His-Patch Thioredoxin

Thioredoxin is an 11.7kDa protein that is found in yeast, plants, mammals and bacteria. The protein was originally isolated as a hydrogen donor for ribonuclease reductase in *E. coli* and has already been completely sequenced, crystallized and its structure has been determined. When used as a fusion partner, it has been known to increase translation efficiency and in some cases the solubility of eukaryotic proteins in *E. coli* (14).

pBAD-DEST49, a plasmid we used for functional complementation studies (Chapter 3, section 5.1) contains the His-Patch thioredoxin (HP-thioredoxin) -tag, a slightly modified version of the native thioredoxin protein. This was achieved by replacing the native Glu³² and Glu⁶⁴ residues with histidine residues. When the protein folds the new residues at position 32 and 64 interact with the native histidine residue at position 8 to form a “patch”, from there the name His-patch. This patch has a high affinity for divalent metal ions and could thus be employed in our affinity purification on the ÄKTA_{prime}-system with Ni²⁺ (14).

The AofH fusion was expressed from BL21* (DE3). Unlike the plasmid used so far that has a T7-promoter where expression is induced with the addition of IPTG, pBAD DEST has the *araBAD* promoter (P_{BAD}). Expression is induced with the addition of L-arabinose. No soluble expression was obtained of the 66.7 kDa HP-thioredoxin-*aofH* fusion.

2.2.7 Conclusion on fusion tags

Our study towards the use of different tags to increase solubility of AofH was overall successful. AofH expressed as soluble fusions to the GST-, Nus- and MBP-tags and we managed to purify the Nus- and MBP-tag fusions.

2.3 Increasing solubility and translation efficiency

Although we purified two AofH fusions successfully, we were worried that the large fusion partners may adversely affect the folding and activity of AofH. In an effort to obtain soluble protein without the large fusion partners, we explored co-expression with the molecular chaperones. Another method investigated was to increase the translation

efficiency of AofH by the addition of the tRNAs of the scarce codons to the translation mixture.

2.3.1 Scarce codons

This is a method to increase the translation efficiency of the target protein and hopefully soluble expression of AofH by the supplementation of the tRNAs of the scarce codons to the translation mixture. Scarce codons refer to the codons that are not generally used by *E. coli* for expression of its native proteins. Therefore when recombinant proteins from other organism are overexpressed in *E. coli* that need these scarce codons, problems with protein synthesis may occur. Ten scarce codons were identified in AofH: 7× CGG which encodes arginine, 2× GGA which encodes glycine and 1×CCA which encodes proline. The tRNAs for these codons can be added by expressing from the Rosetta™ cell lines or by co-expression of the plasmids pRARE or pRARE2 (all available from Novagen). pRARE encodes for 6 of these scarce codon tRNAs (AUA, AGG, AGA, CUA, CCA and GGA) and pRARE2 for 7 (the previous 6 + CGG) (15). Co-expression of His-AofH (from pET 160 EXP-aofH) and His-GST-AofH (from pET 160 GST EXP -aofH) with these two plasmids did not increase the solubility of the fusion. (See next section and Figure 2.9)

2.3.2 Chaperone plasmids

One of the many factors that can increase the formation of inclusion bodies is misfolded protein (5). So far we have tried to overcome possible misfolding by fusing AofH to different tags in a hope that when the tags fold correctly AofH would follow suit. Another possible solution is to add proteins during translation that facilitates protein folding. These are known as the molecular chaperone proteins.

The principal molecular chaperones are the heat shock proteins, Hsp70 and Hsp60, where 70 and 60 are the sizes of the proteins in kDa. Hsp70 is known as DnaK in *E. coli*. DnaK functions as part of a chaperone team. Its one co-chaperone is the 40kDa DnaJ (Hsp40). The other one is the nucleotide binding exchange factor, GrpE (16). DnaK and DnaJ was originally identified as being necessary for bacteriophage λ DNA replication, from there their names (17). These proteins are necessary in different shock states. DnaK is necessary in both low and high temperature shock states, while DnaJ is only required at low temperatures. GrpE is required at all temperatures (18). To refold the protein, DnaK binds to the exposed, extended regions of the polypeptide which is rich in hydrophobic

residues, while the polypeptide is still bound to the ribosome. This binding interaction keeps the polypeptide in an unfolded or partially folded configuration until enough of the polypeptide is synthesized for productive folding to take place, thus preventing premature misfolding. Release of Hsp70 is energy dependent and occurs with the hydrolysis of ATP.

The Hsp60 class is also known as chaperonins and the principal ones in *E. coli* are the GroES-GroEL complexes. GroEL folds in a tubular shape of 15nm long and 14nm wide and consists of 2× 60kDa 7-membered rings stacked on top of each of each other. The active site is a 5nm cavity in which ATP dependent protein refolding occurs. The GroES protein is a 10kDa 7-membered ring that forms a cap on the one site of the GroEL tube. This complex chaperones protein folding by binding of the target protein in the central cavity and so preventing folding. The protein is released by ATP hydrolysis and once released it can fold correctly. The complex then moves on along the protein and binds the next exposed area. The proper folding thus takes place in the short intervals during which the protein is released after ATP hydrolysis and before it rebinds (19).

Tig or trigger factor, a 48kDa protein, is one of the chaperones about which little is known. This chaperone is in close association with the ribosome and is involved in protein folding as it emerges from the ribosome. In *E. coli* mutants that lack DnaK, tig is postulated to fulfil the role of this protein (20).

To simplify the use of these different chaperones in protein expression, the HSP Research Institute has developed 5 different types of “chaperone teams” that is sold under the label of Takara Chaperone Plasmid Set (Refer to Table 2.5). These sets were designed to enable efficient expression of molecular chaperones that are known to work in cooperation in the folding process (5).

Table 2.5: The Takara Chaperone Plasmid sets

Plasmid	Chaperones	Promoter	Inducer	Resistant marker
PG-KJE8	dnaK-dnaJ-grpE-groES-groEL	<i>araB</i> Pzt1	L-arabinose Tetracycline	Cloramphenicol (Cm)
pGro7	groES-groEL	<i>araB</i>	L-arabinose	Cm
pKJE7	dnaK-dnaJ-grpE	<i>araB</i>	L-arabinose	Cm
pG-Tf2	groES-groEL-tig	Pzt1	Tetracycline	Cm
pTf16	tig	<i>araB</i>	L-arabinose	Cm

We co-expressed pET160-EXP-*aofH* and pET160-EXP-GST-*aofH* with these chaperone teams. The results of these expression trials are given in Figure 2.9 as the analysis of the lysate on 12% SDS PAGE gels. The marker used is the Invitrogen BenchMark™ Fluorescent Protein Standard.

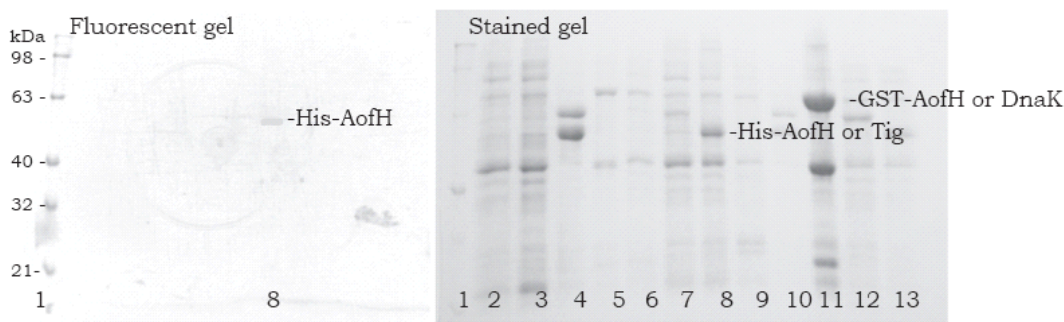


Figure 2.9: 12% SDS PAGE analyses of the coexpressions of AofH fusions with the scarce codon plasmids and the chaperone plasmid set. The gel on the left was visualized by fluorescence and the one on the right stained with Coomassie Brilliant Blue. The following are in each lane: Lane 1 is the marker; Lane 2-8 contain His-AofH + pRARE (lane 2) and pRARE2 (lane3), pG-Tf2 (lane4), pKJE7 (lane5), pG KJE8 (lane6), pGRO7 (lane7) and pTf16 (lane 8). Lane 9-13 contain His-GST-AofH + pRARE (lane 9), pG-Tf2 (lane10), pKJE7 (lane11), pGRO7 (lane12) and pTf16 (lane 13).

Co-expression of pET160-EXP-*aofH* with pTf16 was the only one to yield soluble protein, as there is only one fluorescent band on the fluorescent visualized gel in Figure 2.9. This corresponds to the band at 50kDa band on the stained gel in lane 8. Large-scale expression and purification of the AofH fusion was attempted on the ÄKTA^{prime}-system, without success. The 12% SDS PAGE gels confirmed that overexpression of the proteins had occurred and bands of the right sizes were present in the flow through and non-specifically bound protein wash samples (Figure 2.10, lanes 2-6).

In the stained gel in Figure 2.9 in lane 11 there is a thick band at more or less 76kDa, the size of His-GST-AofH. The band was not visible on the fluorescent gel, but this may be caused by steric interferences of the GST-tag that may interfere with the binding of the FIAsh™ reagent or the protein may be denatured. Large-scale co-expression and purification of this fusion protein with plasmid pKJE7 was attempted. As can be seen in Figure 2.10 in lane 7 the protein expressed well, but we did not manage to purify it with affinity chromatography. Closer inspection revealed that this band, which we identified as His-GST-AofH, may also be one of the chaperones, DnaK.

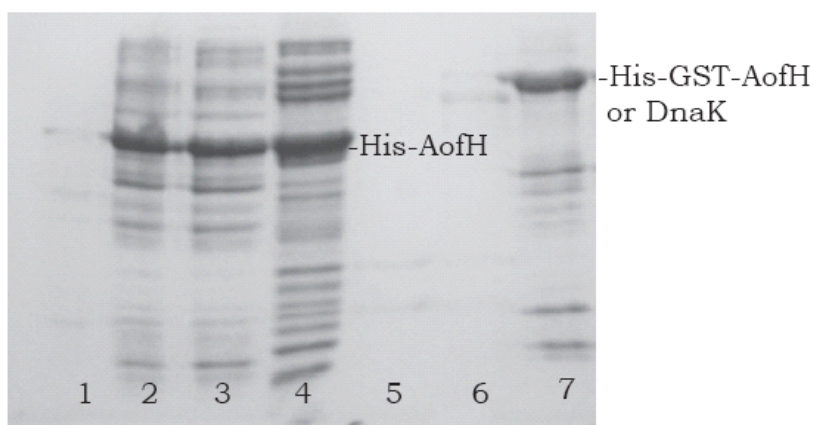


Figure 2.10: The 12% SDS PAGE gel of the purifications attempted of His-AofH and His-GST-AofH obtained with coexpressions with the chaperone plasmids. The lanes contain the following samples: Lane 1-marker, lane 2 - His-AofH crude extract (total cell lysate), lane 3 - His-AofH flow through, lane 4 - His-AofH non-specifically bound protein wash peak, lane 5 - where is the purified protein? lane 6 - purified protein, lane 7 - GST-AofH crude extract which we suspect is the chaperone GroEL.

The purification of His-AofH co-expressed with Tig was tried using different purification conditions. The cells were lysed with Novagen Bugbuster™ Protein Extraction Reagent (a detergent mix that perforates the cell walls of the host without denaturing the proteins it liberates) instead of with sonication. Purification on the ÄKTAprime-system was tried on the Amersham columns and the Sigma Ni²⁺ NTA columns with His-select binding buffer and His-select elution buffer (refer to Table 2.3 for buffer composition). When no purification was obtained under these conditions, gradient elution was attempted by raising the imidazole concentration from 10mM to 46mM over a period of 10 minutes. All the fractions that may contain the purified protein were pooled and concentrated with a SIGMA® IVSS 20 VIVASPIN centrifugal concentrator. This method also proved to be unsuccessful. The conclusion was reached from the SDS PAGE analysis that His-AofH doesn't bind to any of the columns (Figure 2.11). One of the factors that may cause this is N-terminal masking of the His-tag due to the anionic nature of AofH. However, this possibility has not yet been investigated further.

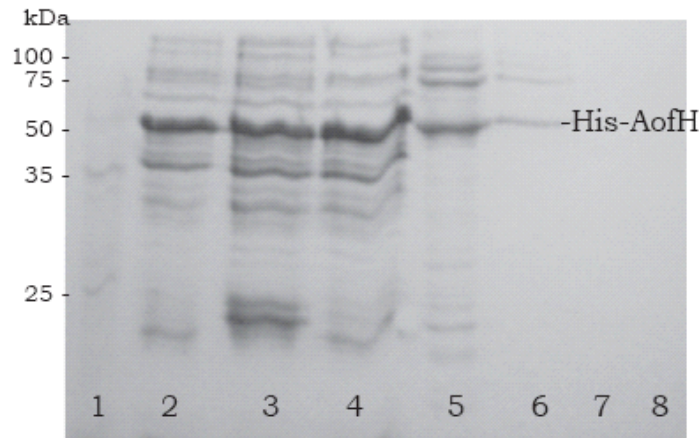


Figure 2.11: Second round of purification of His-AofH co-expressed with Tig. The cells were lysed with Bugbuster™ reagent instead of the normal sonication. The lanes contains the following samples: Lane 1 - marker, lane 2 - crude extract (total cell lysate), lane 3 - flow through of the Sigma Ni²⁺ NTA column, lane 4 - flow through of the Amersham column, lane 5 - wash peak, lane 6 - flow through obtained of the re-injected wash peak, lane 7 - flow through of the concentrator, lane 8 - the concentrated protein.

2.4 Other expression methods

2.4.1 Expression from yeast

Due to the slight expression problems we experienced of native AofH from the *E. coli* system, we also tried expression from a yeast system. We used the *ura⁻* yeast strain Y294 and *aofH* was subcloned into the GATEWAY™ plasmid pYES-DEST52. As in the case of pBAD-DEST49, expression is induced by L-arabinose due to the GAL1 promoter. No expression was detected with SDS PAGE analysis. It only came under our attention much later that yeast expression levels from a plasmid is typically very low and the protein cannot necessarily be visualized with SDS PAGE. In the future Western blot analysis should rather be used.

2.5 Protein refolding

The literature defines insoluble expression as the accumulation of the target protein in insoluble inclusion bodies when expressed from the *E. coli* system. One of the methods described to bridge this problem that hasn't been discussed so far, is protein refolding. Normally the insoluble inclusion bodies are isolated by centrifugation followed by solubilization under denaturing conditions. The protein is then dialyzed or diluted into a

non-denaturing buffer where proper folding occurs to yield a soluble protein. Some of the methods used include single step dialysis/diafiltration, multi-step dialysis, single-step dilution, gel filtration, immobilization assisted refolding and refolding with a detergent and cyclodextrin (21). We tried two different methods to solubilize AofH.

2.5.1 Method 1: Artificial chaperone chemical-assisted method

The first method we tried is the “artificial chaperone chemical-assisted” method. This method is a hybrid between the last two methods mentioned in the previous paragraph and dilution into a non-denaturing buffer. The immobilization assisted refolding method requires that the target protein binds to an insoluble matrix, usually by the use of an affinity tag. The advantages of this system are that aggregation is minimized due to spatial separation of the bound proteins and that the refolded proteins can be eluted at relatively high concentrations. Refolding with detergent and cyclodextrin mimics the role of the chaperonins GroEL-GroES in protein refolding. The detergent prevents aggregation and the cyclodextrin strips away the detergent (21). The refolding of AofH on a column was attempted with minor modifications according to a method described by Oganesyam *et al.* (8)

His-AofH was overexpressed and purification attempted with the ÄKTA_{prime}-system using an Amersham HiTrap chelating column and the peaks obtained analyzed on 12% SDS PAGE gels. Once again the chelating problem was encountered since the protein was present in the crude extract sample and in the flow through, but nowhere else. (Refer to Figure 2.12) To increase the binding efficiency the flow rate from the injection onwards was decreased from 1.0ml.min⁻¹ to 0.1ml.min⁻¹, but this made no difference.

2.5.2 Method 2: Dilution into non-denaturing buffer

The second refolding method attempted was dilution of the ureum treated protein into a large volume of non-denaturing buffer. The refolding was tried according to the method described by Witt *et al.* (22) with minor modifications. The solubilized inclusion bodies were diluted into 50X their volume of renaturing buffer and left at 4°C to refold with mild stirring. After the refolding process was completed, the enzymatic mixture was concentrated and purified on an Amersham 5ml HiPrep™ 16/10 DEAE FF column and gel filtered. The refolded protein was used in assays to determine if FAD was

incorporated during the refolding (see Chapter 3, section 6.3). According to these scans this procedure was also unsuccessful.

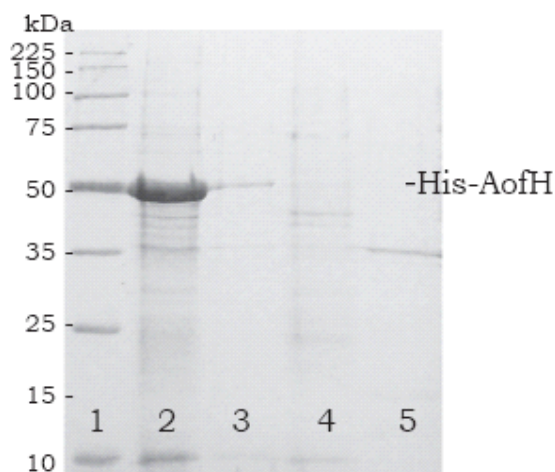


Figure 2.12: Attempts at refolding and purifying His-AofH according to the artificial chaperone chemical-assisted method. The samples in the lanes are as follows: Lane 1 - marker, lane 2 - protein crude extract in denaturing buffer, lane 3 - flow through, lane 4 - non-specifically bound proteins, lane 5 - sample that should contain protein.

2.6 Conclusion

Problems were experienced with the soluble expression and purification of AofH. To overcome this problem various techniques were investigated. One of these methods is the fusion of AofH to various fusion tags, which include the GST-, His-GST-, His-Lumio™-, His-GST-Lumio™-, MBP- and Nus-tags. Soluble protein expression was obtained for all the fusions with the exception of the His-tag. The other methods used to increase solubility and expression were co-expression of the Lumio™-AofH fusions with the chaperone proteins, addition of the scarce codon tRNA's to the translation mixture and protein refolding. Of these methods only His-Lumio™-AofH co-expressed with the trigger factor, Tig, expressed solubly. We purified the Nus- and MBP-tag AofH fusions. These proteins were used in further applications to determine the activity of AofH.

2.7 Experimental

All ÄKTA^{prime} columns except the Ni²⁺ NTA columns were from Amersham Biosciences and purchased from either Amersham or Sigma-Aldrich. The Ni²⁺ NTA columns, FAD

and IPTG were from Sigma-Aldrich. The Novagen Bugbuster™ Protein Extraction Reagent and most of the buffer components were purchased from Merck. The enzymes were purchased from Fermentas, Promega or New England Biolabs. *Mycobacterium tuberculosis* genomic DNA was a gift from Rob Warren from Medical biochemistry at Tygerberg campus, University of Stellenbosch (US). The plasmids pDEST544 and pDEST566 were kind gifts from Dr Cynthia Kinsland from Cornell University, USA.

2.7.1 DNA amplification

The *aofH*-gene was amplified from genomic DNA of Mtb strain H37Rv with the forward primer 5'-CTGTA^{CTTCCAG}CATATGACAAACCCACCGTGG-3' which introduced an NdeI (underlined) restriction enzyme site. The reverse primer was 5'-GAAAGCTGGGTGCTCGAGCTCATAGCAGGGCGG-3' and introduced an XhoI-site (underlined). The primers used were designed according to Gateway™ technology, which includes a universal sequence to introduce the *attB* sites before and after the target sequence. This allows BP-reactions with the pDONR-vectors to yield the necessary entry-vectors to create the expression vectors, although in this case the classic restriction digest and ligations were used to obtain the entry-vectors (discussed later). For amplification AMP-buffer was used with 0.4mM dNTP mix, 1mM forward primer, 1mM reverse primer, 2ng genomic DNA, varied MgSO₄ concentrations, 1.25U *Pfu* and distilled, deionized water (ddH₂O) to a final volume of 25µl. The PCR program had an initial step of 2 min at 95°C followed by denaturation for 15s at 94°C, annealing for 30s at 55°C and a polymerization step of 1min at 68°C. This was repeated for 30 cycles and the program ended with a hold step at 4°C. The reaction mixtures were analyzed by gel electrophoresis on a 1% agarose gel and the bands visualized by staining with SYBR®gold and viewed on a Darkreader. Product bands at 1 347bp were obtained at MgSO₄ concentrations of 2, 3 and 3.5µM, and were purified from the gel with a GFX PCR DNA and Gel band purification kit.

2.7.2 Restriction Digestions

The *aofH* PCR product, pET28a(+) and pENTR4N were digested with NdeI and XhoI. The digestions were carried out at 37°C in Promega buffer D, 0.1mg.ml⁻¹ BSA, 14µl PCR product/plasmid, 20U NdeI, 20U XhoI and ddH₂O to a final volume of 20µl. When the digestion was completed, the mixtures were purified on 1% agarose gels and the bands of the correct size purified from the gel with a GFX PCR DNA and Gel band purification kit.

2.7.3 Construction of plasmids

Two methods were used to construct the plasmids in this study. The first involved the use of restriction digestions (as described above), followed by ligation and screening. In the second method the LR reaction of the GATEWAY™ system was used.

2.7.3.1 Method 1 - Ligation and screening

Equal amounts of the already digested plasmid and PCR product were added together in a final volume of 9µl and incubated at 45°C for 5 min. This was followed by a cooling period on ice for 10min after which T4 ligase buffer and 2U T4 DNA ligase (Promega) were added to give a final volume of 10µl and the mixture incubated at 20°C for 4 hours. The entire reaction mixture was transformed into *DH5a* (or *Mach1*) and plated on Luria Bertani (LB) plates enriched with 30mg.ml⁻¹ kanamycin and incubated overnight at 37°C. Colonies obtained were screened by adding a smear of each colony to 25µl Epilyse solution 1 (30mM Tris-HCl, pH 8.0, 5mM Na₂EDTA, 50mM NaCl, 20% sucrose, 0.047µg.ml⁻¹ lysozyme and 0.047µg.ml⁻¹ RNase) and mixing. After 10µl Epilyse solution 2 (1×TAE, 2% SDS, 5% sucrose and 2mg.ml⁻¹ bromophenol blue) was added, the mixtures were analyzed on 1% agarose gels by comparing the samples to the undigested parent plasmid. DNA-samples that were larger than the original plasmid were subjected to further screening. This involved purification of the target plasmids from overnight cultures by making use of Eppendorf purification kits. For each new plasmid restriction enzyme(s) was identified that yields a unique restriction pattern. The digested plasmids were analyzed on 1% agarose gel. If the desired pattern was obtained, the plasmid was stocked and used in further applications.

2.7.3.2 Method 2 - Gateway™ LR reaction

This system allows the formation of expression clones by adding together an entry plasmid (pENTR) containing the gene sequence and a destination plasmid (pDEST) together with LR clonase. Both plasmids contain defined *att*-sites. During the LR reaction the fragments of DNA between the *att*-sites get exchanged. This allows the formation of an expression vector containing the target DNA sequence. The advantages of this system are that restriction digest are only used in the creation of the entry plasmid and that the plasmids are designed to eliminate false positives. This is obtained by the *ccdB*- suicide gene sequence that are contained within the cassette (the area between the two *att*-sites that are exchanged during the LR reaction) and the ampicillin resistance of the destination

plasmids as opposed to the kanamycin resistance of the entry plasmids. If the exchange reaction failed, the colonies containing destination plasmid would die due to the suicide gene and the entry vector due to the antibiotic selection.

The destination plasmid (pDEST) and an entry plasmid (pENTR) were added together in a ratio of 3:1 with 1µl LR clonase buffer and 1µl LR clonase (final volume: 5µl) and incubated at 25°C. The reactions were terminated by addition of 1µl of Proteinase K and incubation for a further 10min at 37°C. Part of or the entire LR-mixture was transformed into *DH5α* or the *Mach1* cell strain, plated on LB plates enriched with 100mg.l⁻¹ ampicillin and incubated overnight at 37°C. Any colonies found the next day were screened in two different ways. The first round of screening entails streaking each colony on 2 different LB reporter plates, one enriched with 100mg.l⁻¹ ampicillin and the other with 25mg.l⁻¹ chloramphenicol. The colonies that contain the correct construct would grow on the ampicillin enriched plate, but not on those enriched with chloramphenicol. The second round of screening is a digestion with an enzyme that yields a unique digestion pattern. For most of the expression clones this enzyme was BsrGI, a restriction enzyme that digests only within the *att*-sites of the expression clones if the exchange occurred correctly. For the digestions 20U of BsrGI in NEB buffer, BSA and ddH₂O in a final volume of 20µl was used. The digested plasmid was analyzed on 1% agarose gel, stained with SYBR®gold and visualized with the Darkreader. If only two bands were found of which one is more or less the size of the insert, the construct was correct and could be used in further applications.

2.7.3.3 The constructed plasmids

2.7.3.3.1 pENTR4N-aofH

This plasmid was constructed according to method 1 by adding 35fmol of pENTR4N to *aofH* PCR product, both digested with NdeI and XhoI. The ligation mixture was transformed into *DH5α*. The unique cutter enzyme used was PfiMI which has a single restriction site in pENTR4N, but two in pENTR4N-*aofH*. Restriction digestion yields two bands of 2 141bp and 1 494bp. The reaction was done in Fermentas buffer R⁺ (10mM Tris-HCl, pH8.5, 10mM MgCl₂, 100mM KCl, 0.1mg.ml⁻¹ BSA) with 10U of enzyme.

2.7.3.3.2 *pET28a-aofH*

The *aofH* plasmid sequence was cut from pENTR4N-*aofH* using Promega buffer D, BSA, 20U NdeI, 20U XhoI and ddH₂O in a final volume of 20μl. The digestion mixture was separated on a 1% agarose gel, visualized with SYBR®gold on the Darkreader and the correct band purified from the gel with a GFX PCR DNA and Gel band purification kit. 23fmols of each was ligated and transformed into *DH5α*. Overnight cultures were made of the colonies that might contain the right plasmid, the plasmid purified and digested with 20U Bpu1102I in buffer Y⁺/Tango and ddH₂O till 20μl at 37°C for 3.5 hours.

2.7.3.3.3 *pEXP15-aofH*

Ms. Leisl Brand created this plasmid by combining the Gateway plasmid pDEST15 with pENTR4N-*aofH* according to method 2. 40ng of pDEST15 and 30ng of pENTR4N-*aofH* were reacted with LR clonase at 25°C for 2hours and 40 min.

2.7.3.3.4 *pEXP566-aofH*

This plasmid was created as described by method 2 by adding 60ng of pDEST566 to 15ng of pENTR4N-*aofH*. The LR reaction was left at 25°C for 4hours and 45 min before transforming the entire mixture into Top10 *DH5α*.

2.7.3.3.5 *pEXP544-aofH*

48ng pDEST544 was combined with 60ng pENTR4N-*aofH* using method 2.

2.7.3.3.6 *pET160-EXP-aofH*

This plasmid was made by Ms. Leisl Brand. 75ng of pET160-DEST and 30ng of pENTR4N-*aofH* was reacted with LR clonase at 25°C for 2hours and 40 min.

2.7.3.3.7 *pET160-GST-EXP-aofH*

Combine 48ng pET160-GST-DEST with 60ng pENTR4N-*aofH* using the technique described in method 2. Transformation mixtures were transformed into *Mach1*.

2.7.3.3.8 *pBAD-EXP49-aofH*

Using method 2, 75ng pBAD-DEST49 was combined with 30ng pENTR4N-*aofH*. Transformation mixtures were transformed into *Mach1*.

2.7.3.3.9 *pYES-EXP52-aofH*

Once again method 2 was employed. To increase the efficiency of the LR-reaction with pYES-DEST52, 600ng plasmid was first linearized by digesting with 24U of EcoR1 in Promega Buffer H, BSA and ddH₂O at 37°C for 2 hours. The mixture was loaded on a 1% agarose gel, stained with SYBR®gold and visualized on the Darkreader. The linearized plasmid was purified from the gel using the Eppendorf gel band purification kit. 19ng pYES-DEST52 was incubated with 60ng pENTR4N-*aofH* and LR clonase for just short of 24 hours before adding Proteinase K. The transformation mixture was transformed into *Mach1*. Positive results were obtained with the antibiotic screen, but could not be confirmed by restriction digestions with BsrGI. The restriction pattern obtained from the parental plasmid gave bands at 5 607, 1 310, 403 and 302bp while the constructed plasmid have band at 5 607, 1 397 and 302bp. To confirm the construct, restriction digests were done with NdeI and XhoI to cut out the target sequence. NdeI is a single cutter of pYES-DEST52 and the plasmid has no XhoI-site. The digestion was carried out in buffer R⁺ with 20U of NdeI, 20U of XhoI, 7µl of template and ddH₂O to a final volume of 20µl, incubated at 37°C for 3 and half hours and analyzed on 1% agarose gel.

2.7.4 ***Overexpression and purification methodology:***

All the plasmids were first subjected to expression trials to determine the correct parameters for soluble expression of the target protein. When the optimum set of parameters were determined, the tagged protein was overexpressed on large scale and purification attempted.

2.7.4.1 *Expression trails*

The appropriate plasmids were transformed into a suitable *E. coli* strain (BL21 (DE3), BL21*(DE3) or Tuner (DE3)) for expression. For the expression trials 15ml LB media containing the correct antibiotic was inoculated with overnight culture. These were incubated at 37°C and 200rpm (vigorous) shaking until an OD₆₀₀ of more or less 0.6 (mid-log-phase growth) was reached. Each experiment was then induced with a predetermined amount of isopropyl-β-D-thiogalactoside (IPTG). The solubility of the target protein was tested by varying the following parameters at which expression occurs after induction:

1. IPTG concentration (final concentration = 1mM, 0.75mM, 0.5mM, 0.2mM, 0.1mM or 0.05mM)
2. Period of incubation after induction (2h, 4h or overnight)
3. Temperature at which induction occurs (15°C, 20°C, 25°C, 30°C or 37°C)

After the incubation period elapsed, the culture was harvested by centrifugation at 4500rpm for 30min at 4°C. The pellet was stored at -20° C till use.

2.7.4.2 Large scale expression

LB (normally 500ml) containing the correct amount of the specific antibiotic was inoculated with overnight culture of the plasmid containing *E. coli* expression strain. The inoculated media was incubated at 37°C and 200rpm shaking till OD₆₀₀ = 0.6 before induction with IPTG and expression was continued in accordance with the other predetermined parameters. When the time for expression had elapsed, the cells were harvested by centrifugation at 4500rpm for 30min at 4°C and the pellet stored at -20° C till use.

2.7.4.3 Purification of expression trials to analyze soluble and insoluble proteins

The pellets harvested from the 15ml cultures were resuspended in 2ml binding buffer (10mM Tris-HCl, pH 8.0) and 200µl aliquots taken and pelleted again. To evaluate the cell free extracts (i.e. the soluble proteins), the pellets were resuspended in 100µl elution buffer and glass beads added equal to half the volume of the suspended pellet. The mixture was vortexed for 10min to break open the cells and centrifuged at 13 000rpm for 2min to collect the cell debris. A sample of the supernatant was used to analyze the proteins on SDS PAGE gels (as described below). For whole cell samples (to analyze the total protein content of the cell lysate) the original pellet was resuspended in 50µl elution buffer and taken as is for SDS PAGE analyses.

2.7.4.4 Purification of protein obtained in large scale expressions

The pellet was resuspended in a volume of 10× the pellet weight of binding buffer (20mM Tris-HCl, 5mM Imidazole, 500mM NaCl, pH 7.0) and cooled down to below 10°C. Cells were disrupted by sonication and the cell debris was collected by centrifugation at 15 000rpm for 30min at 4°C. To prepare the supernatant for purification it was filtered

using CAMEO 25AS acetate filters with a pore size of 0.45micron after which it was injected into the ÄKTAprime -system.

For purification of the His-tag fusions the following general procedure was followed. The tag-containing protein was loaded on a 1ml Amersham Biosciences HiTrap Chelating HP column that was preloaded with Ni²⁺. After a wash step (15% elution buffer, 85% binding buffer) to remove any non-specific bound proteins from the column, the target protein was eluded by increasing the imidazole, a structural analog of histidine, concentration in the buffer (20mM Tris-HCl, 500mM NaCl, 50mM imidazole, pH 7.9). The elution was monitored by UV at 280nm. After elution all protein samples were desalted (also on the ÄKTAprime-system) using an Amersham Biosciences 5ml HiTrap desalting column and gel filtration buffer (25mM Tris-HCl, 5mM MgCl₂, 5% glycerol, pH 8.0)

2.7.4.5 Analysis on 12% SDS PAGE gels

The proteins were visualized by using 12% SDS PAGE gel electrophoresis. A sample of the appropriate volume was mixed with an equal volume of 2× SDS-PAGE loading buffer (0.125M Tris-HCl, pH 6.8, 4% SDS, 30% glycerol, 1.5% β-mercaptoethanol and 0.02 % bromophenol blue) and boiled at 95°C for 5min after which the samples were loaded on the gel and ran in 1× SDS-PAGE running buffer (0.1% SDS, 0.025M Tris and 0.192M glycine). The standard experiment comprised of at least four samples, the purified protein and as references the crude extract from the bacterial lysate, the flow through (proteins that did not coordinate to the Ni²⁺) and the wash peak (proteins that bound non-specifically to the column). After the run was completed the gel was stained with Coomassie blue stain (45ml MeOH, 40ml ddH₂O, 10ml CH₃COOH and 250mg Coomassie Brilliant Blue) for 30min and destained with destaining solution (45% MeOH, 45% ddH₂O, 10% CH₃COOH) for 2 hours.

2.7.4.6 Determination of protein concentration

The concentration was determined with the Bradford method using bovine serum albumin (BSA) standards. To determine the protein concentration a dye, Coomassie Brilliant Blue, was added to the protein samples. This dye has absorption maxima between 470 and 650nm in its free form, but bound to a protein the absorption maxima shifts to 595nm (23). Bovine serum albumin standards (Biorad) of known concentrations were used to plot a standard curve of absorbance versus concentration using the Thermo Varioskan™ and Skanit software version 2.2.1. This curve was then used to determine the

concentration of the target protein of which the absorbance was measured. For each new protein concentration determination a new standard curve was constructed.

2.7.5 Overexpression and purification used in this study.

2.7.5.1 His-GST

For large scale overexpression 500ml cultures were induced at $OD_{600} = 0.6$ with a final concentration of 0.1mM IPTG at 37°C and left overnight. The harvested cells were disrupted by sonication and the lysate filtered with a 0.45-micron acetate filter. The lysate was purified by affinity chromatography with a 1ml HiTrap Chelating HP column on the ÄKTAprime-system.

When this purification method proved unsuccessful, different buffers were investigated for purification. The compositions of the different buffers are described in Table 2.3 and the combination used given in Table 2.4.

All experiments were based on the small-scale batch method described in the Novagen His-Bind® Kits instruction manual (24). After expression, 0.5g of pellet was resuspended in 2.5ml room temperature Novagen Bugbuster™ Protein Extraction Reagent and incubated at room temperature with mild shaking for 30min. To pellet the cell debris the suspension was centrifuged at 15 000rpm for 30min at 4°C and the protein containing supernatant extracted.

Batch purifications were performed in 1.5ml Eppendorf tubes to which 100µl high density IDA-agarose 6 BCL Ni²⁺ charged resin (Agarose Beads technology) was added to give a bed volume of 50µl. The resin was washed 2× with 100µl sterile ddH₂O and 2× with 100µl of the appropriate binding buffer. The washing was accomplished by adding the liquid, inverting the tubes a few times and then spinning at 8 000rpm for 1min at room temperature. Protein containing supernatant (100µl) was added to the washed Ni²⁺-charged agarose and the mixture was incubated with mild shaking at room temperature for 5min. The agarose was spun down and the eluant removed (flow through sample). The agarose-protein fractions were washed 1× with 100µl binding buffer and 2× with 150µl binding buffer. The protein was eluted with 150µl elution buffer. Aliquots of the flow through, the wash and eluted protein were analyzed on 12% SDS PAGE gels.

For manual purification a column made in a plastic Pasteur pipette and a bed volume of 1ml Ni²⁺ NTA resin was used. The resin was equilibrated by washing 2× with 2 CV sterile

ddH₂O and 2× with 2 CV PBS-buffer. 5ml protein crude extract was loaded on column and washed 3× with 3 CV PBS buffer. To elute any non-specifically bound protein the column was eluted 2× with 3 CV PBS buffer mixed with 15% elution buffer (His-select EB). This was followed by elution 2× with 3 CV 100% elution buffer. 300µl fractions were taken in a microtiter plate and scanned at 280nm.

2.7.5.2 MBP-tag

One round of expression trials were performed in BL21* (DE3) and soluble protein was obtained. For large-scale expression 1litre cultures were induced with a final concentration of 0.2mM IPTG at 37°C and grown for 3hours.

2.7.5.3 Nus-tag

Expression trials were done at 15°C, 20°C, 25°C, 30°C and 37°C for 2h, 4h and overnight in BL21* (DE3) and by varying IPTG concentration in Tuner (DE3). AofH expressed solubly only when induced with a final concentration of 0.5mM IPTG at 20°C and the expression was left overnight.

2.7.5.4 Lumio™-tag

All the expressions with this plasmid were on small scale by growing the plasmid containing BL21*(DE3) cultures in LB media supplemented with 100mg.l⁻¹ ampicillin (selection for pET160-EXP-aofH) and 20 mg.l⁻¹ chloramphenicol (selection for the chaperone and scarce codon plasmids) till an OD₆₀₀ = 0.6. The cultures were induced with a final concentration of 0.5mM IPTG at 37°C and grown for 3 hours at 37°C and 200rpm after which the pellets were harvested by centrifugation at 4500rpm for 30min at 4°C. The pellets were redissolved in lysis solution (50mM potassium phosphate buffer, pH 7.8, 400mM NaCl, 100mM KCl, 10% glycerol, 0.5% Triton X-100, 10mM imidazole) and 15µl aliquots were taken to analyze the protein content of the lysate and to determine which proteins are soluble and insoluble. The aliquot to determine the protein content was analyzed as is while the other sample was pelleted. The supernatant was analyzed for the soluble proteins and the pellet for the insoluble proteins. The pellet was resuspended in 50µl 8M urea and a 15µl aliquot used. To all three samples 5µl 4× Lumio™ Gel sample buffer and 0.2µl Lumio™ Green detection reagent was added before incubating at 70°C for 10min. After cooling down and spinning to collect, 2µl Lumio™ In-Gel Enhancer was

added, the samples mixed and incubated at room temperature for 5 minutes. The samples were analyzed on a 12% SDS-PAGE gel (12, 25).

2.7.5.5 His-Patch Thioredoxin

This AofH fusion was expressed from BL21*(DE3). The cultures were grown at 37°C with 200rpm shaking till an $OD_{600} = 0.6$ after which it was induced with different amounts of L-arabinose (final concentrations: 0.2%, 0.02%, 0.002% 0.0002% and 0.00002%) and grown further at 37°C and 200rpm shaking for another 3 hours. The cells were harvested by centrifugation at 4 500rpm for 30min at 4°C. The pellets were redissolved in Lumio™ lysis solution (as described in section 2.7.5.4) and the supernatant (soluble proteins) analyzed on a 12% SDS PAGE gel.

2.7.5.6 Scarce codons

pRARE or pRARE2 was transformed into competent BL21*(DE3) and plated on LB plates with 20mg.l⁻¹ chloramphenicol. Colonies of both plasmid containing cells were used to make competent cells from. pET160-EXP-*aofH* was transformed into both and pET160-EXP-GST-*aofH* only into the competent cells that contained pRARE. These transformations were plated on LB plates that containing 20mg.l⁻¹ chloramphenicol and 100mg.l⁻¹ ampicillin. We did the expression trials for the pET160-EXP-*aofH* cultures on 15ml scale by growing at 37°C and 200rpm shaking till an $OD_{600} = 0.79$ and inducing with a final concentration of 0.46mM IPTG. The cultures were grown for a further 3 hours at the same conditions. The cells were harvested by centrifugation at 4 500rpm for 30 min at 4°C.

2.7.5.7 Chaperone plasmids

The expressions trials were performed in the same manner as in section 2.7.5.6. The expression of pET160-EXP-*aofH* was done in 1.5ml LB containing 20mg.l⁻¹ chloramphenicol and 100mg.l⁻¹ ampicillin. All the pET160-EXP-GST-*aofH* combinations were expressed using auto-induction media. The cells are harvested by centrifugation at 4 500rpm for 30min at 4°C and the soluble and insoluble proteins were analyzed using the Lumio™ detection method (as described in section 2.7.5.4).

2.7.5.8 Alternative expression methods for GST-tag fusions (7)

Six tubes for small-scale expressions were inoculated. This was grown till an $OD_{600} = 0.68$ (literature: 0.7) at 37°C with shaking at 200rpm. After this the temperature was reduced

till 25°C and grown till an OD₆₀₀ = 1.28 (literature 1.2) and then at 18°C at 200rpm till an OD₆₀₀ = 1.5. The expressions are induced with IPTG (final concentrations: 1, 0.75, 0.5, 0.2, 0.1, 0.05mM) and allowed to grow overnight at 18°C and shaking at 200rpm. The cells were harvested with centrifugation, broken with glass beads and the soluble proteins and whole cell sample analyzed with SDS PAGE gel electrophoresis.

2.7.5.9 Protein Refolding

2.7.5.9.1 Method 1: Artificial chaperone chemical-assisted method

The bacterial cell pellet was lysed with sonication and the inclusion bodies pelleted by centrifugation at 15 000rpm for 30 min. Inclusion bodies were dissolved in denaturing buffer (Table 2.6) and filtered through a 0.45micron CAMEO acetate filter. For the refolding and purification six different buffers were used as described in Table 2.6. The sample was injected into the ÄKTAprime-system on a 1ml Amersham column and washed with denaturing buffer. This was followed by a wash step with 10× CV of detergent buffer and another wash with 10× CV of buffer containing β-cyclodextrin. Before elution the column was washed with wash buffer to remove the β-cyclodextrin. The protein was eluted with elution buffer and the fractions obtained were on a 12% SDS PAGE gel.

Table 2.6: Buffers used for artificial chaperone chemical-assisted AofH refolding

Buffer	Composition	Remark
Buffer A	20mM Tris-HCl 100mM NaCl 10mM β-mercaptoethanol pH 6.7	pH is dependent of pI of target protein. AofH pI was taken form Tuberculist. β-mercaptoethanol is added to cleave possible cysteine bonds
Denaturing buffer	Buffer A 8 M urea	Solubilization of target protein in inclusion bodies
Detergent buffer	Buffer A 0.1% Triton X-100	Detergent minimizes hydrophobic interactions between aliphatic and aromatic residues.
Refolding buffer	Buffer A 5mM β-cyclodextrin 0.05mM FAD (22)	β-cyclodextrin removes the detergent. Since AofH is expected to be a flavin dependent protein, FAD is needed for correct folding.
Wash buffer	20mM Tris-HCl 0.5mM NaCl 10mM β-mercaptoethanol pH 6.7	Removes β-cyclodextrin
Elution buffer	Buffer A 600mM imidazole pH 8	Elute target protein

2.7.5.9.2 Method 2: Dilution into non-denaturing buffer

Protein refolding was done according to the method described by Witt *et al.* (22) with minor modifications. The bacterial cell pellet was lysed with sonication and the inclusion bodies pelleted by centrifugation at 15 000rpm for 30 min. The inclusion bodies were washed once with wash buffer (10mM Tris-HCl, 1mM EDTA, 0.8% NaCl, pH 7.76) excluding and once with wash buffer including 0.1% Triton X-100. After the wash step the inclusion bodies were solubilized in denaturing buffer (8M urea, 50mM DTT) and kept on ice for 60min. The debris was pelleted by centrifugation and the protein concentration of the supernatant determined with the Bradford reagent and BSA protein standards as 4.6 mg.ml⁻¹. The supernatant was diluted 50× in renaturing buffer (20mM Tris-HCl, pH 7.6, 10% (v/v) glycerol and 0.05% FAD) and stirred very slowly at 4°C for 1 week. For the concentration of the protein sample a SIGMA® IVSS 20 VIVASPIN centrifugal concentrators were used and the protein purified on the ÄKTAprime-system with an Amersham 5ml HiPrep™ 16/10 DEAE FF column. The protein was eluted by gradient elution from buffer A (20mM Tris.HCl, pH 7.5) to buffer B (20mM Tris.HCl, pH 7.5, 1M NaCl).

2.8 References

- (1) GIBCO BRL, *Gateway™ cloning technology Instruction manual version A* p4 - http://www.tcd.ie/Genetics/staff/Noel.Murphy/recombinant_dna_ge4021/gatewayman.pdf (last accessed: 11 January 2006)
- (2) Brand, L. A. (2006) MSc thesis p. 143, University of Stellenbosch, Stellenbosch.
- (3) Sambrook, J. F., Russell, D. W., and Editors (2000) *Molecular cloning: A laboratory manual*, third edition.
- (4) Casali, N., and Prestion, A. (2003) *E. coli plasmid vectors: Methods and applications*, Vol. 235.
- (5) Takara - *Chaperone plasmid Set manual Cat # 3340* - <http://www.takara-bio.co.jp/> (Last accessed: 9 January 2006)
- (6) Amersham. (2003) *GSTrap FF, 1ml and 5ml Instructions book* - <http://www.chromatography.amershambiosciences.com/apatrix/upp00919>.

- nsf/(FileDownload)?OpenAgent&docid=38EDC849BD9671FCC1256EB40041802C&file=71502755AC.pdf (Last accessed: 9 January 2006)
- (7) Card, G. L., Peterson, N. A., Smith, C. A., Rupp, B., Schick, B. M., and Baker, E. N. (2005) *The Crystal Structure of Rv1347c, a Putative Antibiotic Resistance Protein from Mycobacterium tuberculosis, Reveals a GCN5-related Fold and Suggests an Alternative Function in Siderophore Biosynthesis*. *Journal of Biological Chemistry* **280**, 13978-13986.
- (8) Oganessian, N., Kim, S.-H., and Kim, R. (2004) *On-column chemical refolding of proteins*. *PharmaGenomics* **4**, 22, 24, 26.
- (9) Chopra, S., Pai, H., and Ranganathan, A. (2002) *Expression, purification, and biochemical characterization of Mycobacterium tuberculosis aspartate decarboxylase, PanD*. *Protein Expression and Purification* **25**, 533-540.
- (10) Sigma Ni NTA instruction manual - <http://www.merckbiosciences.co.uk/docs/docs/PROT/TB273.pdf> (Last accessed: 9 January 2006)
- (11) Harrison, R. G. *Expression of soluble heterologous proteins via fusion with NusA protein*. *inNovations* **11**, 4-7.
- (12) Invitrogen -Lumio™ Green detection kit instruction manual - **Version A** - http://www.invitrogen.com/content/sfs/manuals/lumiogreendetection_man.pdf (Last accessed: 9 January 2006)
- (13) Invitrogen. *Champion™ pET Gateway® Expression Kits with Lumio™ Technology instruction manual. Version A* - http://www.invitrogen.com/content/sfs/manuals/petlumiodest_man.pdf (Last accessed: 9 January 2006)
- (14) Invitrogen *pBAD DEST™ Gateway™ Vector Instruction manual* - http://www.invitrogen.com/content/sfs/manuals/pbaddest49_man.pdf (Last accessed: 9 January 2006)
- (15) Novy, R., Drott, D., Yaeger, K., and Mierendorf, R. (2001) *Overcoming the codon bias of E. coli for enhanced protein expression*. *inNovations* **12**, 1-3.

- (16) Reyes, D. Y., and Yoshikawa, H. (2002) *DnaK chaperone machine and trigger factor are only partially required for normal growth of Bacillus subtilis*. *Bioscience, Biotechnology, and Biochemistry* **66**, 1583-1586.
- (17) Boshoff, A., Nicoll, W. S., Hennessy, F., Ludewig, M., Daniel, S., Modisakeng, K. W., Shonhai, A., McNamara, C., Bradley, G., and Blatch, G. L. (2004) *Molecular chaperones in biology, medicine and protein biotechnology*. *South African Journal of Science* **100**, 665-677.
- (18) Skowyra, D., McKenney, K., and Wickner, S. H. (1995) *Function of molecular chaperones in bacteriophage and plasmid DNA replication*. *Seminars in Virology* **6**, 43-51.
- (19) Garrett, R. H., and Grisham, C. M. (1999) *Protein synthesis and degradation*, in *Biochemistry* 2nd edition pp 192, 1116-1117, Saunders College Publishing.
- (20) Snyder, L., and Champness, W. (2003) *Molecular genetics of bacteria*, 2nd edition ed., ASM press, Washington D.C.
- (21) Novagen (1997) *Protein Refolding Kit 7123-3* - <http://www.merckbiosciences.co.uk/docs/docs/PROT/tb234.pdf> (Last accessed: 9 January 2006)
- (22) Witt, S., Singh, M., and Kalisz, H. M. (1998) *Structural and kinetic properties of nonglycosylated recombinant Penicillium amagasakiense glucose oxidase expressed in Escherichia coli*. *Applied and Environmental Microbiology* **64**, 1405-1411.
- (23) Wilson, K., and Walker, J. (2000) *Practical Biochemistry: Principles and techniques*, 5th edition ed., Cambridge University Press.
- (24) Novagen. (2003) *His-Bind Kits User protocol* - <http://www.merckbiosciences.co.uk/docs/docs/PROT/TB054.pdf> (Last accessed: 9 January 2006)
- (25) Invitrogen Life Technologies (2003) *Lumio™ Green Detection Kit Instruction manual. Version A* - http://www.invitrogen.com/content/sfs/manuals/lumiogreendetection_man.pdf (Last accessed: 9 January 2006)

Chapter 3

Activity of AofH:

Identification of products of the enzymatic reactions and confirmation of the presence of FAD and H₂O₂

3.1 Introduction

With pure AofH in hand (obtained as described in chapter 2) we set out to determine the activity of the protein. Based on sequence homology to the yeast protein Fms1 AofH should be a polyamine oxidase which produces 3-aminopropanal as a product of one of its reactions. The various reactions of Fms1 with different polyamines are summarized in Figure 3.1.

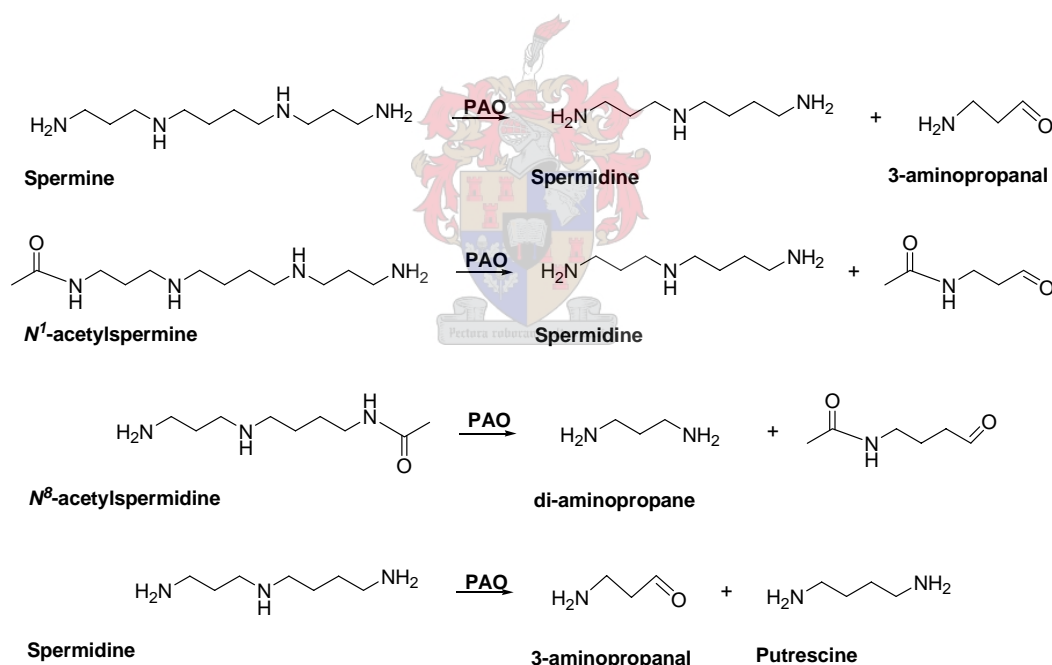


Figure 3.1: PAO reactions based on the reactivity of Fms1. Although spermidine is not a substrate of Fms1 it may still be a substrate of AofH.

Fms1 oxidizes spermine (spm) and N¹-acetylspermine (N¹-spm) to spermidine (spd) and an aldehyde, which is 3-aminopropanal in the case of spm and N-acetyl-3-aminopropanal in the case of N¹-spm. N⁸-acetylspermidine (N⁸-spd), unlike the previous substrates that

are oxidized on the three carbon side of the secondary amine, is oxidized on the four carbon side of the secondary amine. The products obtained from this reaction are diaminopropane and *N*-acetylbutanal. Spermidine is not a substrate of Fms1, but this does not discount it from being a PAO substrate. Should it be oxidized the expected products would be either 3-aminopropanal and putrescine or 3-aminobutanal and diaminopropane.

The products formed with the enzymatic reactions were analyzed with various direct and indirect methods. The first method used was thin layer chromatography (TLC). In this method a small aliquot of the sample ($\approx 5\mu\text{l}$) is applied to a silica plate where it was subsequently resolved by a predetermined eluant. The second method used was reverse phase high performance liquid chromatography (HPLC). In this method the sample was injected onto a non-polar C18 column and separated by a polar mobile phase(s). Samples for analyses were prepared by derivatization of the enzymatic reactions mixtures with fluorescent molecules. This allows for more sensitive detection.

A more direct method of determining the specific products is electrospray mass spectroscopy (ESI-MS) and liquid chromatography mass spectroscopy (LC-MS). In these techniques the molecules are analyzed by mass (1). The major difference between these techniques is that in LC-MS the reaction mixtures are first resolved with HPLC prior to the MS analysis. For analysis the enzymatic mixture had to be diluted to product concentrations of $10\mu\text{g}\cdot\text{ml}^{-1}$ in 50% ACN and ddH₂O. In ESI-MS analysis the enzymatic mixtures were analyzed without further derivatization. However, since the product molecules have masses that are below the detection limit of the MS (need $m/z \geq 100$), the samples for the LC-MS analysis were derivatized with the fluorescent molecule fluram before dilution for the analysis. This derivatization also gives better separation.

Analytical techniques were also used to assay for FAD and H₂O₂. In the Fms1 reaction FAD oxidizes the polyamines, forming reduced FADH₂ in the process. The reduced FADH₂ are oxidized back to FAD by molecular O₂ to form H₂O₂. If we base the activity of our AofH on Fms1, the reaction shown in Figure 3.2 should occur and H₂O₂ should form as a side product.

H₂O₂ can be detected in a number of ways by using coupled enzymatic assays. One of these assays involves oxidation of H₂O₂ to H₂O by the enzyme horseradish peroxidase.

This reaction can be coupled to various other redox reactions and can be observed by a change in colour, change in UV absorbance or fluorescence.

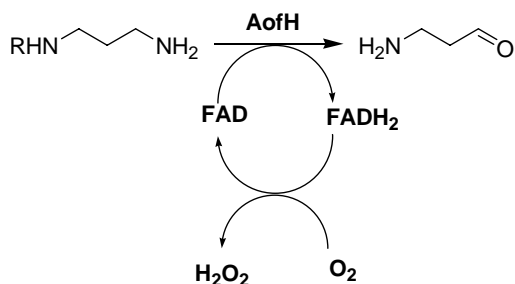


Figure 3.2: The postulated oxidation of polyamines by AofH and FAD to form 3-aminopropanal and FADH₂. FAD is regenerated by the oxidation of FADH₂ by molecular O₂ to H₂O₂.

We used both photometric and fluorometric assays to determine whether H₂O₂ was being formed. In the photometric assay 4-aminoantipyrine is oxidized during the reduction of H₂O₂. This reagent condenses with vanillic acid to form a red quinoneimine dye, which can be monitored by an increase of absorbance at 498nm. In the fluorometric assay non-fluorescent homovanillic acid is oxidized during the reduction of H₂O₂ and condenses with itself to form a highly fluorescent 2,2'-dihydroxy-3,3'-dimethoxybiphenyl-5,5'-diacetic acid. The formation of the fluorescent compound can thus be measured directly.

Apart from the direct analytical methods used to determine the products of the enzymatic reactions, we also used a genetic method in the form of functional complementation studies. This involves the complementation of PanD activity (formation of β-alanine) in a *ΔpanD* strain with a plasmid that contains either *FMS1* or *aofH*.

We also assayed AofH for monoamine oxidase (MAO) activity. Instead of a polyamine, the monoamine benzylamine was used as substrate for the AofH reactions. In a MAO reaction this substrate would be oxidized to benzaldehyde and the formation of this product can be followed spectrophotometrically.

Finally, photometric and fluorometric scans were also performed to determine the FAD content of the purified proteins.

In this chapter these analytical techniques are discussed along with the results obtained from the AofH reactions.

3.2 Thin Layer Chromatography

To identify the products of the AofH enzymatic reaction with the polyamines we used the method described by Sternglanz *et al.* (2) in their study of Fms1. In this procedure the enzymatic reaction mixtures are derivatized with dansyl-chloride (Dns-Cl), a reagent that reacts with primary amines (See Figure 3.3). This reagent is non-fluorescent when in its unbound state, but once it is bound it is highly fluorescent. Aliquots (5 μ l) are spotted on silica plates and subsequently resolved with an eluant consisting of 3:1 cyclohexane:ethyl acetate. The spots are visualized with UV light at 312nm.

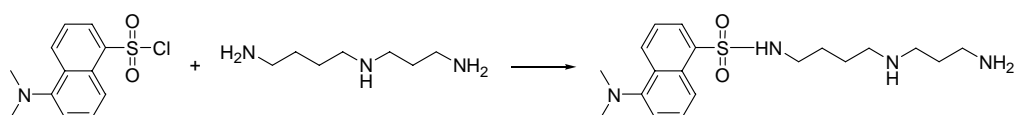


Figure 3.3: Derivatization of spermidine with Dns-Cl to form a fluorescent compound. Dns-Cl is not fluorescent in its unbound form.

The advantages of this method of analysis are that it is relatively quick, easy and cost effective which makes it ideal for initial analysis. It is also easy to change the mobile phase and very little solvent is required. The disadvantage is poor resolution, especially with samples of which the components have a great deal of structural similarity such as the polyamines. We derivatized with Dns-Cl since this fluorescent method is more sensitive than staining with some of the commercial stains for primary amines, such as ninhydrin. Based on the R_F -values obtained we compared the reaction mixtures to stock samples of the substrates and postulated products. However, this limits the identification power and makes the identification of side and unpredicted products difficult. The results obtained here had to be confirmed with other analytical techniques such as HPLC and MS.

To determine the R_F -values of the substrates and expected products of the AofH and Fms1 reactions, stock solutions of the four polyamines (spm, spd, N^1 -spm and N^8 -spd) and of the 3-carbon molecules (β -alanine, 3-aminopropanal, 3-aminopropanol and L-aspartate) were made. These stocks were analyzed on TLC and the results are summarized in Figure 3.4. As can be seen on the figure, 3-aminopropanal, 1-amino-3,3-diethoxypropane and L-aspartate all have high R_F values and run up high on the plate. Spm and spd have slightly lower R_F -values. The alcohol product is situated halfway between the spm/spd spots and the origin while N^1 -spm and N^8 -spd hardly moves from the origin. According to

literature the spots for putrescine and 1,3-diaminopropane are situated between the top two spots on the plate (2). The light spot represents the unreacted Dns-Cl that forms a yellow stain on the plate.

As can be seen from Figure 3.4, it is nearly impossible to distinguish between the spots that have similar R_F -values. For example, spermine and spermidine or 3-aminopropanal and 1,3-diaminopropane are especially hard to distinguish. This makes it difficult to determine whether, for example, the oxidation of spermine occurred and formed spd or not. Despite this shortcoming, we decided to use this technique to get an initial indication of the reactivity of AofH.

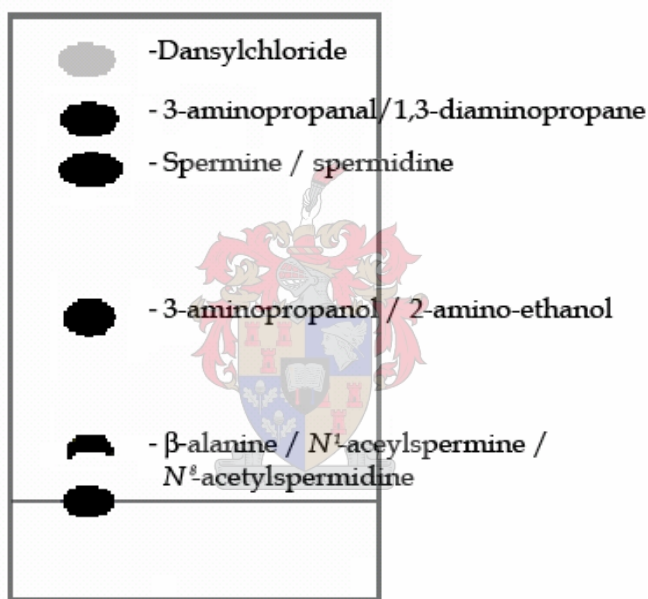


Figure 3.4: Figurative representation of the position of the different compound spot when analyzed on TLC.

We also determined the sensitivity of this technique by measuring the lowest product concentrations that can be visualized as Dns-Cl derivatives. The minimum concentration of spm, spd and N^1 -spm that could be visualized was in the range of 25-100 μ M and for N^8 -spd and the 3-carbon products it was 50 μ M.

The enzymatic reactions of the polyamines with Fms1 were resolved on TLC and used as a standard for the analysis of the AofH reactions (refer to Figure 3.5). The results obtained from the resolved Fms1 enzymatic reactions confirmed that the oxidation of N^1 -spm

occurs by the appearance of the spd spot and the absence of the N^1 -spm spot (lane 9). To a lesser degree a reaction with N^8 -spd could also be confirmed (lane 12). No conclusion could be drawn from the reaction mixtures of spm (lane 3) while spd (lane 6) is not a substrate of Fms1. The reactions with AofH did not compare well to the Fms1 standards.

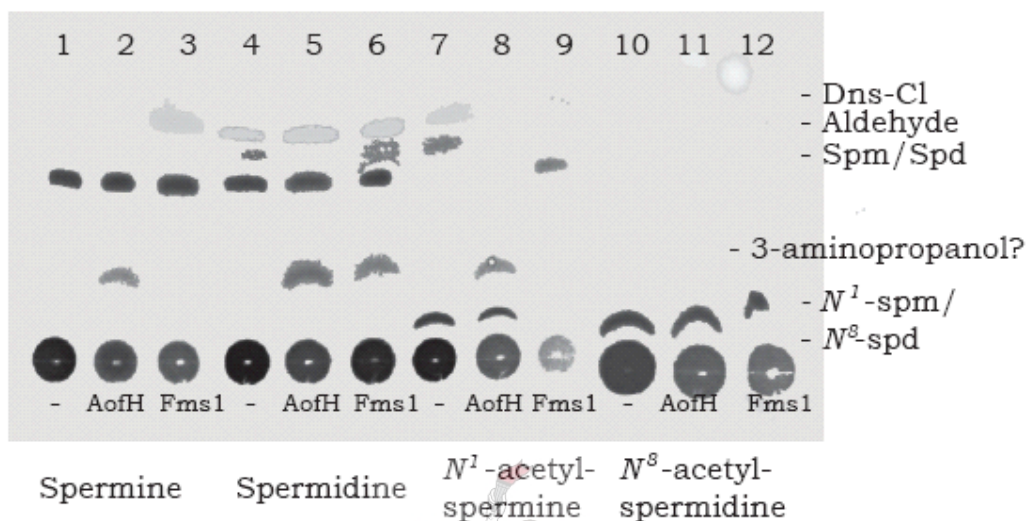


Figure 3.5: Result of the TLC analysis of the AofH and Fms1 enzymatic reactions. Each set of three contains the substrate stock and the analysis of the enzymatic reactions of the substrate with AofH. In some of the reactions a spot is present halfway between the origin and top spm/spd spots. The R_F value of this spot corresponds with that of 3-aminopropanol. The question mark indicates that this compound is not normally a product of polyamine oxidation. This figure was manipulated with Adobe Photoshop to combine different pictures for easier comparison of the different enzymatic reactions, and to optimise contrast.

As in the case of the reaction of Fms1 with spm and spd, it is difficult to determine if the postulated polyamine oxidation reactions occurred of AofH with spm (lane 2) and spd (lane 5). As can be seen in lane 8, the spot for N^1 -spm (lane 8) is still present with no formation of a spd spot; the same can be said of N^8 -spd (lane 11). Although the predicted spots were not present for the AofH reactions, there were spots half way between the origin and the top spm/spd spots for the reactions with spm (lane 2), spd (lane 5) and N^1 -spm (lane 8). This spot was also present for the Fms1 reaction with spd (lane 6). Since these spots are present for all the different substrates, this had to be a fragment common to all the substrates. If we look at the different structures in Figure 3.6 it is clear that they all have the spd backbone. From the TLC analysis we know that this breakdown product is not spd, but has to be a smaller fragment. The only logical fragment consists of 3 carbon atoms and a primary amine group. The only compounds satisfying this

requirement are β -alanine, 3-aminopropanal, 3-aminopropanol and 1,3-diaminopropane. We'll refer to these compounds as the 3-carbon products. The stock samples of the 3-carbon products were analyzed on TLC (refer back to Figure 3.4). The R_F -value of the middle spot corresponded to that of 3-aminopropanol. We set out to confirm this result with other analytical techniques.

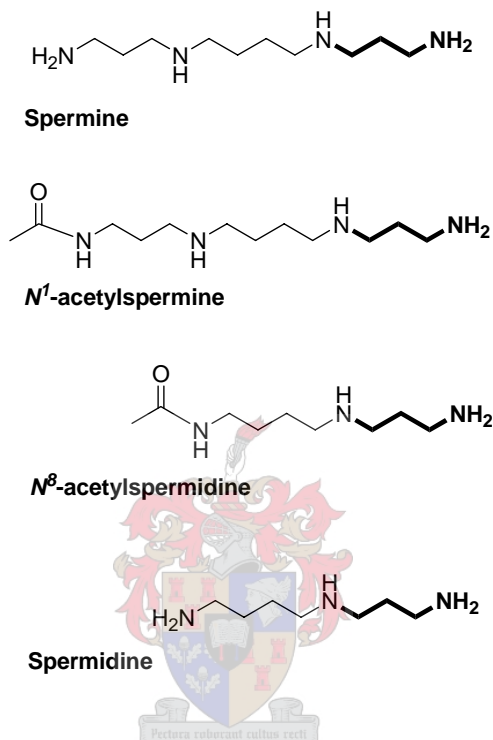


Figure 3.6: The 3-carbon fragment (in bold) that all the substrates have in common.

3.3 Reverse phase HPLC

The limitation with the TLC analysis was that the resolution was insufficient to distinguish between certain compounds. HPLC is more versatile in this regard since the composition of the mobile phases can be changed during a run, thus making more complex separations possible. Changes in the mobile phases can be gradual, as in the case of gradient elution, or sudden, as the case of step programs. The flow rate can also be varied.

Using such an analysis we hoped that the different substrates and 3-carbon products could be resolved and the different compounds of the enzymatic mixtures identified. To increase the sensitivity of the method, the enzymatic reactions were derivatized with

fluorescent molecules for visualization. We experimented with different fluorescent molecules that are discussed individually below. Two of these molecules (Dns-Cl and NBD-Cl) were used for the analysis of all the amines (polyamines and 3-carbon products) while OPA/ β -mercaptoethanol and fluram were only used to analyze the 3-carbon products.

3.3.1 Analysis of all the amines

3.3.1.1 Dansylated products

The first fluorescent molecule used was Dansyl chloride (Dns-Cl). All analyses made use of reverse phase C18 columns. The program and mobile phases initially used were based on the published procedure in the Phenomenex HPLC catalogue (3). This consisted of a step program of 35 minutes where mobile phase A was 65% ACN in ddH₂O and B 93% MeOH in ddH₂O. No separation was obtained and the background was too high, possibly due to the formation of single and double substituted products. Optimization of the derivatization protocol, to eliminate this problem, was not successful.

The samples were also analyzed according to the procedure of Cervelli *et al.* (4). This is another step program over a period of 12min with the mobile phases ddH₂O and acetonitrile (ACN) containing 0.5% trifluoroacetic acid (TFA), but no separation was obtained.

3.3.1.2 NBD-Cl

4-Chloro-7-nitrobenzofurazan (NBD-Cl) is a reagent that reacts with free amines to give a fluorescent substituted product. The reaction scheme of the reagent with 3-aminopropanol is given in Figure 3.7. We used this reagent to see whether chromatograms could be obtained with less background peaks since previous reports have indicated increase success of the analysis of amines with this reagent (5, 6).

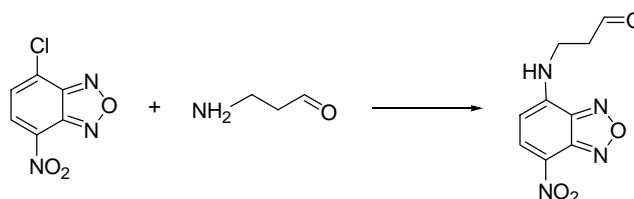


Figure 3.7: Derivatization of 3-aminopropanal with NBD-Cl.

Standards of the different polyamines and 3-carbon products were prepared and analyzed. Initial experiments were carried out with the mobile phases ddH₂O + 0.1% TFA and ACN + 0.1% TFA, but no separation was obtained.

The second set of experiments were based on the method of Toyooka *et al.* (5) which used isocratic elution with the mobile phases 93% methanol (MeOH) and ACN + 0.1% TFA, but again no separation was obtained. However gradient elution with ddH₂O + 0.1% TFA and 100% MeOH gave distinctive retention times (t_R) for the polyamines and 3-carbon standards. (Refer to Table 3.1)

Table 3.1: Retention times of the NBD-Cl derivatives of the polyamines and the three carbon products

Stock	Retention time (min)
Spermine	23,5
Spermidine	22,5 / 24,5
N ¹ -acetyl spermine	24,5
N ⁸ -acetyl spermidine	26,0
β -alanine	32,0
3-amino propanal	Multiple peaks: 25,0 - 35,0
3-amino propanol	32

In the analysis of the enzymatic reactions the background problem reoccurred which made analysis of the chromatograms difficult. Once again this problem was thought to be based on the formation of single and double derivatized products. To circumvent this problem the enzymatic reactions were derivatized with an excess of the NBD-Cl so as to only form the doubly-derivatized compounds. However, in subsequent analyses the high background problem persisted, indicating that derivatization efficiency was not the problem.

3.3.2 Analysis of the 3-carbon products

3.3.2.1 *o*-Phthaldialdehyde and β -mercaptoethanol

o-Phthaldialdehyde (OPA) reacts with primary amines in the presence of the reducing agent β -mercaptoethanol in alkaline medium to form fluorescent compounds (7, 8) as

shown in Figure 3.8. The analyses were based on the method used by Landry *et al.* (2). Gradient elution was used by changing from 100% Buffer A (100mM CH₃COONa) to 100% Buffer B (MeOH + 0.1% TFA) over a period of 30 min.

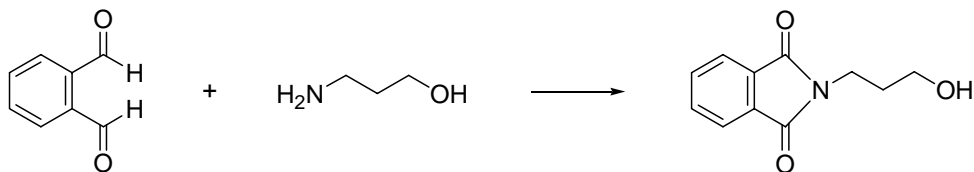


Figure 3.8: Derivatization of 3-aminopropanol with *o*-phthalaldehyde.

In the analysis of the 3-carbon stock solutions, separation of 3 minutes was obtained between the stocks of β -alanine ($t_R = 19.5$ min) and 3-aminopropanol ($t_R = 22.5$ min). (Refer to Figure 3.9)

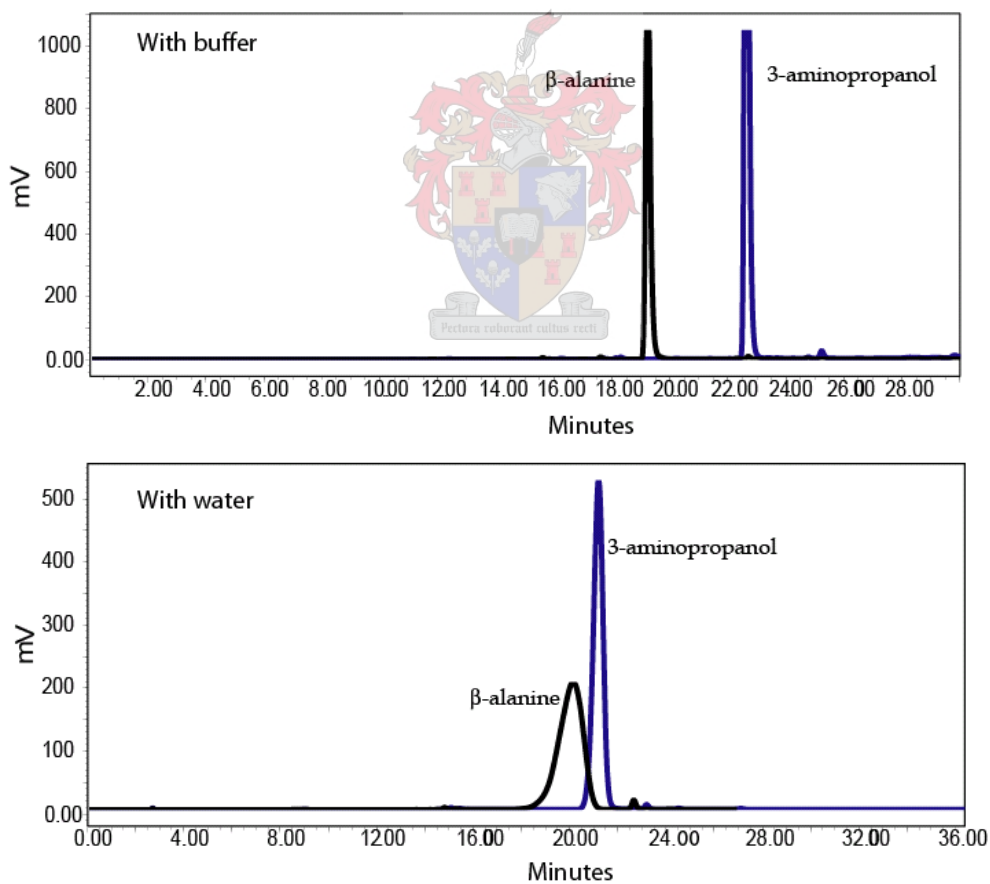


Figure 3.9: Separation of OPA derivatives of β -alanine and 3-aminopropanol. The resolution when one of the mobile phases is CH₃COONa (top) is better than with ddH₂O.

The solvent system, however, gave unreasonably high backpressures on the reverse phase C18 column we used. This problem was subsequently addressed by using ddH₂O as solvent instead of buffer. This resulted in poor resolution. Due to the problem with high backpressure, enzymatic reactions were never analyzed.

3.3.2.2 Fluram

Fluorescamine (fluram) reacts with primary amines to form fluorescent derivatives (refer to Figure 3.10), while the reagent itself and its hydrolysis product are not fluorescent. Derivatization at pH 9 occurs at room temperature with a half-life of a few seconds, while excess reagent is hydrolyzed just as quickly (9).

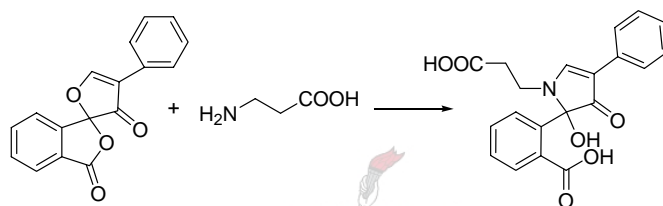


Figure 3.10: Derivatization of β-alanine with fluram

Clear distinctions could be made between peaks corresponding to β-alanine, 3-aminopropanal and 3-aminopropanol (refer to Figure 3.11), but not between the polyamines. Unfortunately, all attempts to analyze the enzymatic reaction were unsuccessful as unreacted polyamine derivatives gave high background signals which made identification of the 3-carbon products impossible.

3.3.3 Conclusion on HPLC

Separation of the polyamines was achieved when derivatized with NBD-Cl. The enzymatic reactions, however, gave too much background for conclusive analysis. Subsequently, we decided to focus on identifying the 3-carbon product of the reaction. Since efficient separation of the compounds derivatized with Dns-Cl or NBD-Cl was not obtained, we also tried OPA/β-mercaptoethanol and fluram. Although the OPA method gave efficient separation, unreasonably high backpressures were obtained. With fluram efficient separation was obtained for the 3-carbon products, but the background caused by the polyamine derivatives in the enzymatic reactions made analysis difficult. We thus decided to analyze the enzymatic reactions with mass spectroscopy.

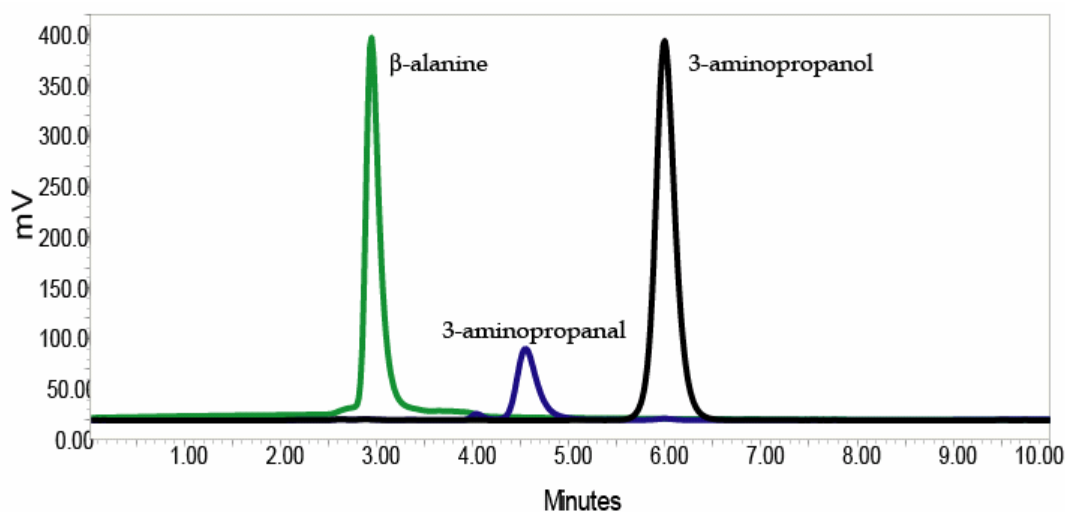


Figure 3.11: Overlaid chromatograms indicating the separation of the 3-carbon products. The products, β -alanine, 3-aminopropanal and 3-aminopropanol, were derivatized with *o*-phthalaldehyde in β -mercaptoethanol and separated on a C18 reverse phase column. Elution was isocratic at $1\text{ml}\cdot\text{min}^{-1}$ flow rate from 100% Buffer A (100mM CH_3COONa) to 100% Buffer B (MeOH + 0.1% TFA) over a period of 30 min.

3.4 ESI-MS and LC-MS analysis

ESI-MS analysis was used to determine products obtained in the enzymatic reactions. Due to the problems with background peaks and insufficient separation, the products obtained could not be confirmed with HPLC.

The reaction mixtures of MBP-AofH and Fms1 with the four polyamine substrates were analyzed with ESI-MS in the ES^+ mode. Product peaks were only observed for the reaction of Fms1 with spermine (refer to Figure 3.12) and *N*¹-acetylspermine (data not shown). In the spectra shown, the spermidine peak at $m/z = 146.1929$ and spermine at $m/z = 203.2$ can be seen on the top spectrum of the Fms1 reaction. The product fragment is absent in the mass spectrum of AofH.

In both the ESI-MS and LC-MS the product peaks for the AofH reactions were absent, while the substrate peaks were prominent. Comparing the ESI-MS spectra of the AofH reactions with those of the Fms1 standards indicate that these enzymes do not share the same function, or that AofH is inactive. No product peaks were present on the LC-MS spectra, which indicate that both the enzymatic reactions did not occur. However, derivatization with fluram was effective.

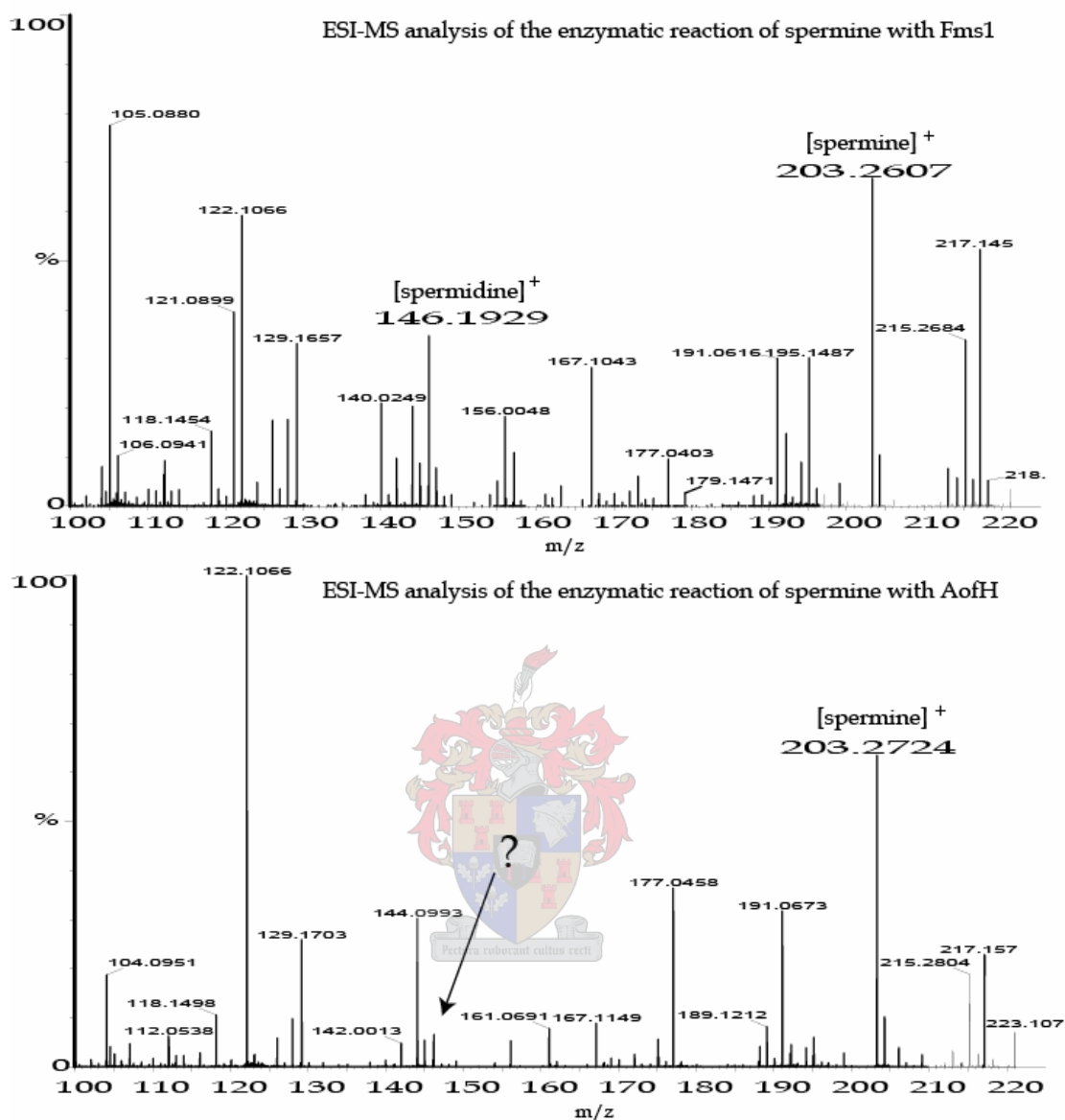
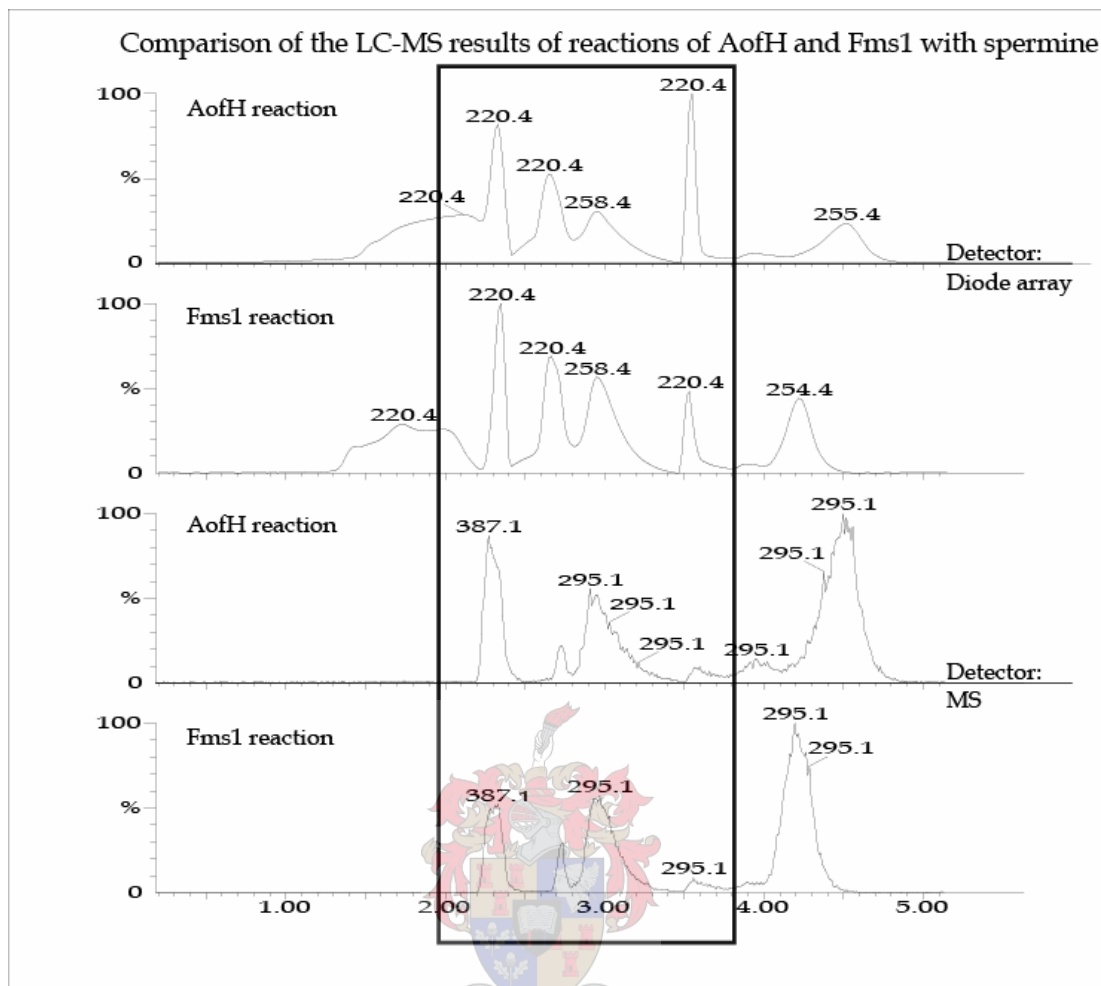


Figure 3.12: ESI-MS spectra (ES⁺ mode) of the enzymatic reactions of Fms1 (top) and AofH (bottoms) with spermine. The peak for the product spermidine is observed in the top spectrum at $m/z = 146.1929$ and for the substrate spermine at $m/z = 203.2$.

Only the enzymatic reactions of spm with MBP-AofH and Fms1 were analyzed with LC-MS. In this round of analysis the reaction mixtures were derivatized with fluram and analyzed in the ES⁻ mode. The results for the reaction were identical, as can be seen from the chromatograms in Figure 3.13. Analysis of the data in the box showed that these peaks all correlate with each other. Unfortunately we observed no product peaks on the mass spectra.



Example of the MS analysis of the peaks

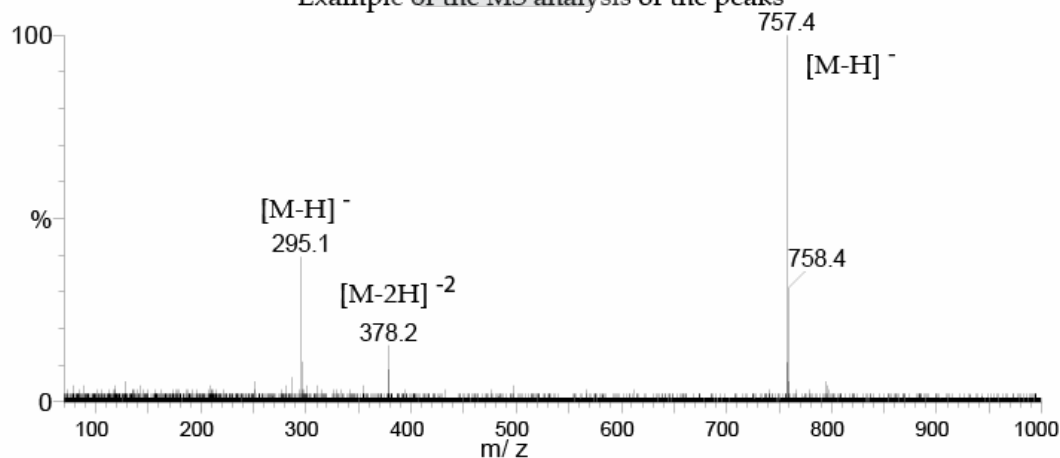
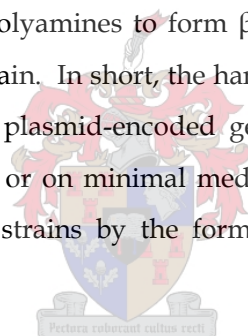


Figure 3.13: ESI-MS analysis (ES⁻ mode) of the enzymatic reaction of AofH and Fms1 with spm. In the top picture the top two chromatograms were recorded with the LC PDA detector and the bottom two with the MS detector. The bottom picture is the typical mass spectrum that was obtained for all substrate containing peaks. The peak at $m/z = 378.2$ is doubly charged spermine-fluram, $m/z = 757.4$ is singly charged spermine-fluram and at $m/z = 295.1$ = hydrolyzed fluram.

Analysis of the spectra obtained with this technique was complicated by the formation of singly and doubly charged molecules. As can be seen in the mass spectrum, the only peaks that could be identified were the singly-charged ($m/z = 757.4$) and doubly-charged ($m/z = 378.2$) spermine-fluram derivative bands and the hydrolyzed fluram peaks ($m/z = 295.1$).

3.5 Functional complementation studies

Since direct analyses of the enzymatic reactions were inconclusive, we set out to use a genetic method to determine the activity of AofH. One of these methods is functional complementation of activity. In functional complementation a deletion strain, lacking a certain metabolic function, is used. In our case the strain lacked the ability to biosynthesize β -alanine via the decarboxylation of L-aspartate. To restore the wild-type phenotype, a plasmid containing a gene sequence whose gene product has a similar function (the oxidation of the polyamines to form β -alanine precursors, for example) is transformed into the deletion strain. In short, the handicap in the function of the deletion strain is complemented by the plasmid-encoded gene (10). The study is initiated by growing the desired colonies in or on minimal media. We thus set out to test whether AofH will complement $\Delta panD$ strains by the formation of the β -alanine precursor 3-aminopropanal from spermine.



3.5.1 In *E. coli*

3.5.1.1 Plate assays

Four $\Delta panD$ strains were identified for complementation studies. They are *E. coli* DV1, *E. coli* DV62, *E. coli* DV79 and JW0127. These strains cannot synthesize β -alanine *de novo*. *E. coli* DV1 is a mutant that cannot grow on pantothenate and requires β -alanine for growth even on rich medium (11). *E. coli* DV62 is a temperature sensitive mutant (12) while *E. coli* DV79 has a pantothenate kinase enzyme that is only 29% as active as the wild type enzyme (13). JW0127 is a $\Delta panD$ that was created in the laboratory of Prof Hirota Mori as part of a concerted effort to replace every gene in the *E. coli* genome with the gene encoding kanamycin resistance (14). The plasmid used for complementation was the Gateway™ pBAD-DEST49 with the *araBAD* promoter which is induced with L-arabinose (which can be added to the minimal media). We decided to use the *araBAD* promoter since it provides tight, dose-dependent regulation of heterologous gene expression based

on the concentration of L-arabinose in the media. The T7 promoters of the pDEST- and pET- vectors allow a degree of leaky expression. The cloning of this plasmid is described in chapter 2, section 2.2.6. A pETBlue-based plasmid with its tetracycline-promoter was also considered as a possibility, but cloning of the genes into these plasmids failed.

For the functional complementation experiments minimal medium plates were used that were supplemented with either β -alanine, L-aspartate, pantothenate or spermine and the appropriate antibiotics. The predicted results are summarized in Table 3.2. pBAD-EXP49-*panD* was the positive control that should grow on all the LB plates. pBAD-EXP49-*gus* served as the negative control and was created from the test plasmid (pGus) that is supplied in all the Invitrogen Gateway™ LR clonase kits. pBAD-EXP49-*aofH* should theoretically grow on the plates supplemented with β -alanine, pantothenate and spermine and not on the plates supplemented with L-aspartate or on minimal media alone. The predicted results are given in Table 3.2.

Table 3.2: Predicted result for complementation in the Δ *panD*-strains. \checkmark indicates expected growth and \times no growth.

Substrate added	pBAD-EXP49- <i>gus</i>	pBAD-EXP49- <i>panD</i>	pBAD-EXP49- <i>aofH</i>
Control	\times	\checkmark	\times
β -alanine	\checkmark	\checkmark	\checkmark
Pantothenate	\checkmark	\checkmark	\checkmark
L-aspartate	\times	\checkmark	\times
Spermine	\times	\checkmark	?

Inconclusive set of results were obtained for the functional complementation of AofH in *E. coli* DV1, *E. coli* DV62 and *E. coli* DV79. As expected, the strains without plasmid grew only on LB plates; however, the strains with plasmid showed no growth discrimination with the different additives. In the experiment shown in Figure 3.14 for the functional complementation experiment in *E. coli* DV79, the strains containing pBAD-EXP49-*panD* and pBAD-EXP49-*aofH* grew on minimal media (E-salts and glycerol) as well as media containing 0.01% spermine. Both plasmid-containing strains were expected to grow on the minimal media plates containing 0.01% spermine, but only pBAD-EXP49-*panD* is expected to grow on just minimal media. No growth was observed for the cultures that contained the negative control plasmid, pBAD-EXP49-*gus*. While the expected results

were obtained in the case of the negative control experiments, the problem is that both the *panD* and *aofH* containing strains grew on both plates. In the case of the *panD* containing strain this is not a problem, since L-aspartate is not an essential metabolite and can be sourced from elsewhere. Spermine however is not essential and it is also reported to be absent in *E. coli*. This indicates that the deletion strains are able to source β -alanine via an unknown route, one of which may be the oxidation of spermidine to 3-aminopropanal. This reaction, however, has not been verified to date.

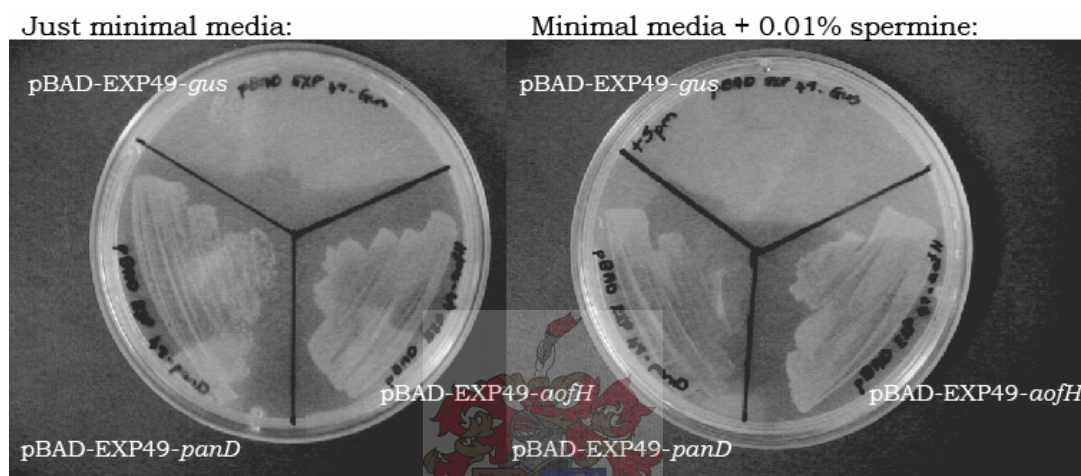


Figure 3.14: Functional complementation in *E. coli* DV 79. Growth was expected for only the pBAD-EXP49-*panD* containing culture on the minimal media plate and for pBAD-EXP49-*panD* and pBAD-EXP49-*aofH* on the 0.01% enriched spermine minimal media plates. The fact that growth occurred of both plasmid containing strains on both plates indicates that these plasmid containing cultures are able to source β -alanine via an unknown route.

The study with JW0127 was also inconclusive. Growth was obtained in all media with all supplements. The only difference was that the strains that contained pBAD-EXP49-*gus* and pBAD-EXP49-*aofH* grew more vigorously on β -alanine and pantothenate supplemented plates than the strain that contained pBAD-EXP49-*panD*. This result was not expected and could not be explained to date.

3.5.1.2 In Solution

Minimal media supplemented with the metabolites described above were inoculated with the JW0127 strain transformed with the different plasmids mentioned above, and subsequently grown at 37°C. The increase in optical density was measured at 600nm over a period of 48 hours. The results obtained are displayed in Figure 3.15. The growth rate

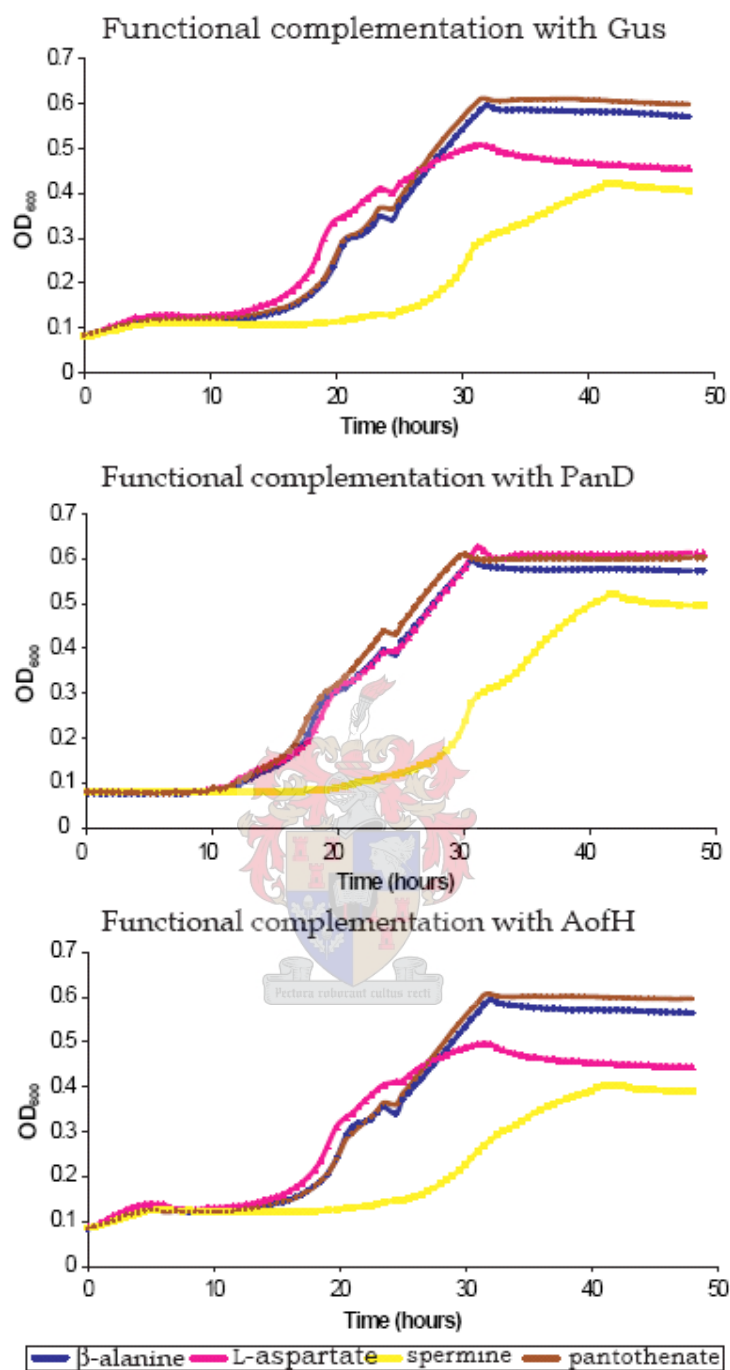


Figure 3.15: Functional complementation of the different plasmids in liquid media from the cell strain JW0127.

for all three plasmids in β -alanine (blue lines) and pantothenate (brown lines) was basically identical, as was expected. With spermine (yellow lines) all three strains have a lag period of 24 hours before growth starts. This lag might be explained due to the

absence of spermine in wild-type *E. coli*. These strains are also affected by a biomass excess after 40h. With L-aspartate (pink line) another interesting result was obtained. Only the *panD* containing strain was not affected by a biomass excess after 24h. The influence that adversely affected the growth of the strains in spermine and L-aspartate enriched media could not be indentified, although there were suggestions that this may be pH related. Moreover, no difference was observed in the growth rates between the cultures containing the negative control strain, pBAD-EXP49-*gus* and pBAD-EXP49-*aofH*. This indicates that the expression of AofH does not alleviate the lack of PanD more than any other protein. These results also suggest that the decarboxylation of L-aspartate by PanD is not the only source of β -alanine in *E. coli*.

3.5.2 In *S. cerevisiae*

Since the complementation in *E. coli* gave inconclusive results, we set out to attempt complementation in the baker's yeast *S. cerevisiae*. The idea was to base the complementation on the work of Liu *et al.* in which $\Delta FMS1$ strains were complemented (15). The $\Delta FMS1$ strain, BY4742 was a gift from the Institute of Wine Biotechnology (IWBT) at Stellenbosch. pYES-EXP52-*aofH* was successfully constructed, but not the positive control plasmid pYES-EXP52-*FMS1*. Although the experiments seemed viable, transformation of the plasmids into the cell line failed.

3.5.3 Conclusion on complementation

The survival of the $\Delta panD$ deletion strains, even in the case of the negative controls (in solution), indicates that the organism can obtain β -alanine via another route than the decarboxylation of L-aspartate. This is surprising since it has been accepted that no other source for β -alanine exists in *E. coli*. No conclusive complementation results were observed. Based on the fact that similar growth rates, although not end bio-masses, were obtained with the negative control and pBAD-EXP49-*aofH* in the complementation studies using the JW0127 strain, genetic methods in *E. coli* were not successful to determine the activity of AofH.

3.6 Test for monoamine oxidase activity

When we first identified AofH as an Fms1 homolog, the enzyme was described on Tuberculist as a "putative polyamine oxidase (PAO)" (16). Somewhere during the course of

the study the description of AofH on the website changed to a “*putative monoamine oxidase (MAO)*”. To test if this was indeed the case, a relatively easy spectroscopic assay was used as described by Tabor *et al.* (17). This assay is based on the difference of the extinction coefficients between benzylamine (substrate of MAO) and benzaldehyde (the product of the monoamine reaction). Benzaldehyde absorbs at 250nm and benzylamine does not. The reaction of benzylamine with MBP-AofH was monitored at 250nm, but no increase in absorption was observed in any of the sets. This led to the conclusion that no benzaldehyde formed and that the cloned AofH does not display MAO activity.

3.7 Assay for the presence of H₂O₂

The results obtained from the TLC analyses of the AofH enzymatic reactions suggested that 3-aminopropanol might be formed as a product of the reaction. This is an unusual result for the PAO's, since the first step of polyamine oxidation leads to formation of an aldehyde (refer back to Figure 3.2). To form an alcohol from the aldehyde requires a reduction step as shown in Figure 3.16.

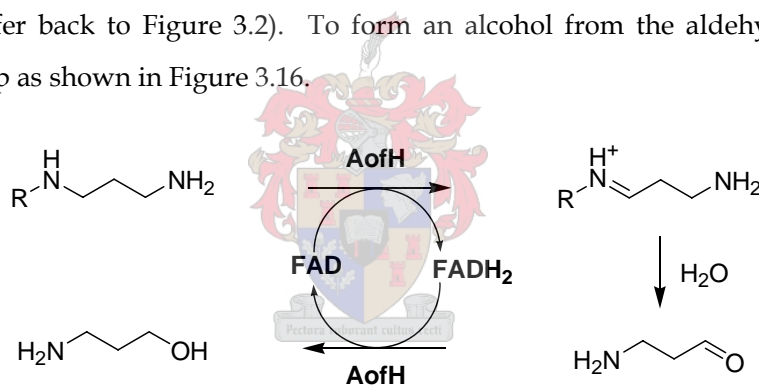


Figure 3.16: Proposed reaction for the formation of 2-aminopropanol from 3-aminopropanal via a PAO reaction.

Before this unusual activity could be investigated further, the dependence of AofH on the cofactor had to be confirmed. Furthermore, we had to identify whether the normal product of FADH₂ oxidation to FAD was formed or not. To test whether FADH₂ is oxidized back to FAD by O₂ via the known route, or if the oxidizing agent is indeed the aldehyde, we assayed for H₂O₂.

3.7.1 Horseradish peroxidase assay

The first assay used to determine the formation of H₂O₂ was a continuous spectrophotometric assay as described by Palcic *et al.* (18) for MAO reactions. This same method was used by McIntire *et al.* to determine the steady-state kinetics of murine PAO

(19). In this assay horseradish peroxidase (HRP) reduces H_2O_2 to water while 4-aminoantipyrine is oxidized. (Refer to Figure 3.17) This reagent condenses with vanillic acid to form a red quinoneimine dye, which has an extinction coefficient of 4654cm^{-1} at pH 7.6. It has also been shown that the absorbance at 498nm increases proportionally to the amount of H_2O_2 reduced (19).

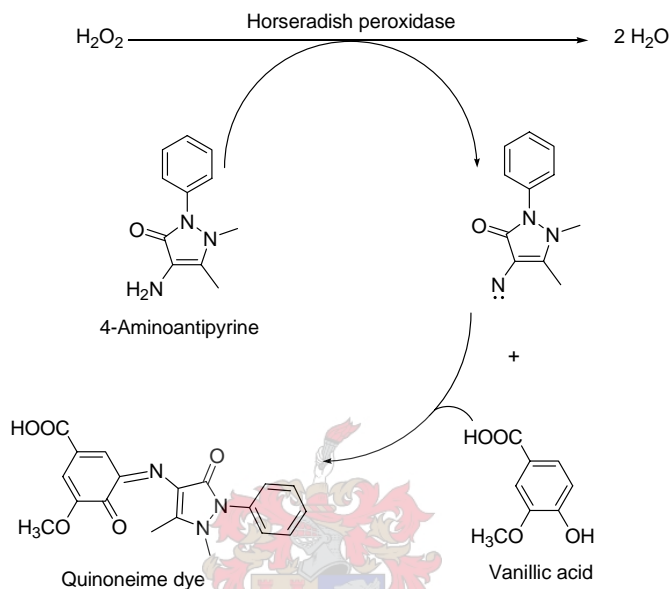


Figure 3.17: H_2O_2 assay. Horseradish peroxidase reduces H_2O_2 to H_2O while at the same time oxidizing 4-aminoantipyrine. The oxidized product binds with vanillic acid to form a quinoneimine dye that has a distinctive red color.

All analyses were done in triplicate and included reactions of both enzymes (Fms1 and MBP-AofH) with 5 different substrates (spm, spd, N^1 -spm, N^8 -spd and benzylamine). Benzylamine is a monoamine oxidase (MAO) substrate and was used in all assays to test for MAO activity (refer back to section 3.6). Only the reactions of Fms1 with N^1 -spm yielded a positive result. This means that Fms1 showed no activity with compounds that are known substrates of the enzyme, indicating that this method was not sensitive enough. The analyses were also time-consuming with an average analysis taking 30min.

To test if the low sensitivity of this method was due to the assay itself or due to the sample preparation, two minor changes were done in further investigations. The first of these involved the addition of FAD to all reaction mixtures to a final concentration of 0.05mM (20). Due to the problems experienced during purification, the protein may have

denatured. To overcome these effects, a second assay was done that made use of the enzymatic crude extract. No activity was found with either of these experiments.

3.7.2 Fluorescent assay

Landry *et al.* reported activity of Fms1 with spm, N^1 -spm and N^8 -spd and have determined the steady-states kinetics of the enzyme with these substrates (2). The HRP assay used so far showed that only spm is a substrate of Fms1. Due to the low sensitivity of the previous assay, we decided to repeat the experiment with a fluorescent assay (2).

In this coupled assay described by Guilbault *et al.* non-fluorescent homovanillic acid is oxidized by H_2O_2 to highly fluorescent 2,2'-dihydroxy-3,3'-dimethoxybiphenyl-5,5'-diacetic acid. (Refer to Figure 3.18) The initial rate of the formation of the fluorescent compound can be related back to the activity of the target enzyme. The formation of the fluorescent compound is measured at $\lambda_{ex}=315nm$ and $\lambda_{em}=425nm$ (21).

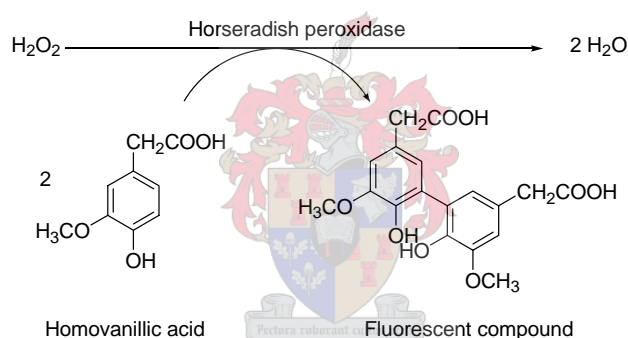


Figure 3.18: Fluorescent assay for H_2O_2 with horseradish peroxidase and homovanillic acid.

The assays were done in triplicate and included enzymatic reactions of Fms1 and Nus-AofH with the same 5 substrates as before. (Refer to Figure 3.19) The reactions of Fms1 with spm (pink lines), N^1 -spm (turquoise lines) and N^8 -spd (purple lines) formed fluorescent compounds as expected. However, the reaction with N^8 -spd was slower than the reactions with spm and N^1 -spm. Spermidine (yellow line) and benzylamine (brown line) are not substrates of Fms1. None of the Nus-AofH reactions yielded positive results. The Nus-AofH reactions were also supplemented with 0.05mM FAD, but no difference in results was observed.

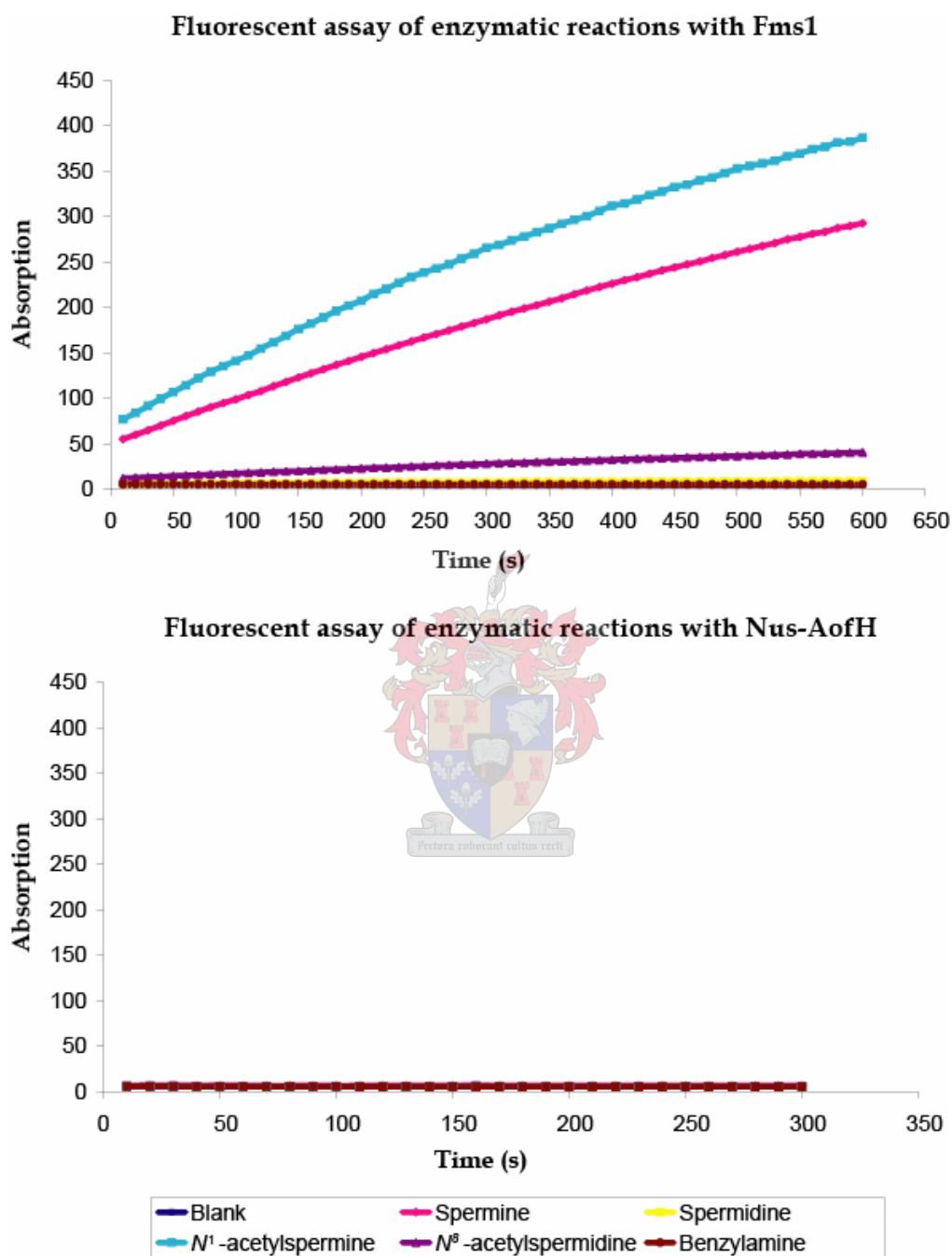


Figure 3.19: Graphs of the fluorescent assays of the Fms1 and Nus-AofH reactions. The graph at top is of the reactions of Fms1 with the different substrates and the graph at the bottom is of AofH with the different substrates.

3.8 FAD Scans

From the H₂O₂ assays it can be concluded that AofH either does not use O₂ to oxidize FADH₂ back to FAD, or that the enzyme is inactive. So far we have tested for the formation of H₂O₂, but have not confirmed the presence of FAD. To accomplish this fluorescent scans of the three purified enzymes were recorded. The extinction coefficient of FAD = 11.3mM.cm⁻¹ and the scans taken with the $\lambda_{\text{ex}} = 370\text{nm}$ and scanned over $\lambda_{\text{em}} = 420 - 680\text{nm}$.

The graphs obtained from the scans (Figure 3.20, top graph) of Fms1 (turquoise line), Nus-AofH (purple line) and MBP-AofH (brown line) were compared to those recorded for three FAD standards of different concentrations of 20 μM (blue line), 10 μM (pink line) and 1 μM (yellow line). Emission peaks were observed for the standards and Fms1, but not for Nus-AofH or MBP-AofH.

Photometric scans were also performed from 300nm to 700nm using these same samples. The signature two peak absorbance of FAD was present in the scans of the 20 μM and the 10 μM standards and of Fms1, but not in the scans of Nus-AofH, MBP-AofH and the 1 μM standard. However, the background absorbance of the two AofH-fusions was higher than the absorbance of the 1 μM FAD standard. Furthermore, the concentrations of Nus-AofH (0.22mg.ml⁻¹) and of MBP-AofH (0.25mg.ml⁻¹) were much lower than that of Fms1 (0.86mg.ml⁻¹). To overcome this problem both AofH fusions were spun down to pellet any debris or denatured protein that may be present in the samples. The supernatant was subsequently concentrated. To determine whether the AofH samples were concentrated enough, the following calculations were done:

$$M_r(\text{Fms1}) = 58.833\text{kDa}$$

$$M_r(\text{MBP-AofH}) = 94.410\text{kDa}$$

$$M_r(\text{Nus-AofH}) = 105.889\text{kDa}$$

$$[\text{Fms1}] = 0.861\text{g.l}^{-1} / 58.833\text{kDa} = 0.0146\text{mM} = 14.6\mu\text{M}$$

$$[\text{MBP-AofH}] = 0.790\text{g.l}^{-1} / 91.140\text{kDa} = 0.0086\text{mM} = 8.6\mu\text{M}$$

$$[\text{Nus-AofH}] = 0.152\text{g.l}^{-1} / 105.889\text{kDa} = 0.0012\text{mM} = 1.2\mu\text{M}$$

FAD binds in a molar ratio of 1:1 to Fms1. For our calculation we made the assumption that AofH binds to FAD in the same molar ratio.

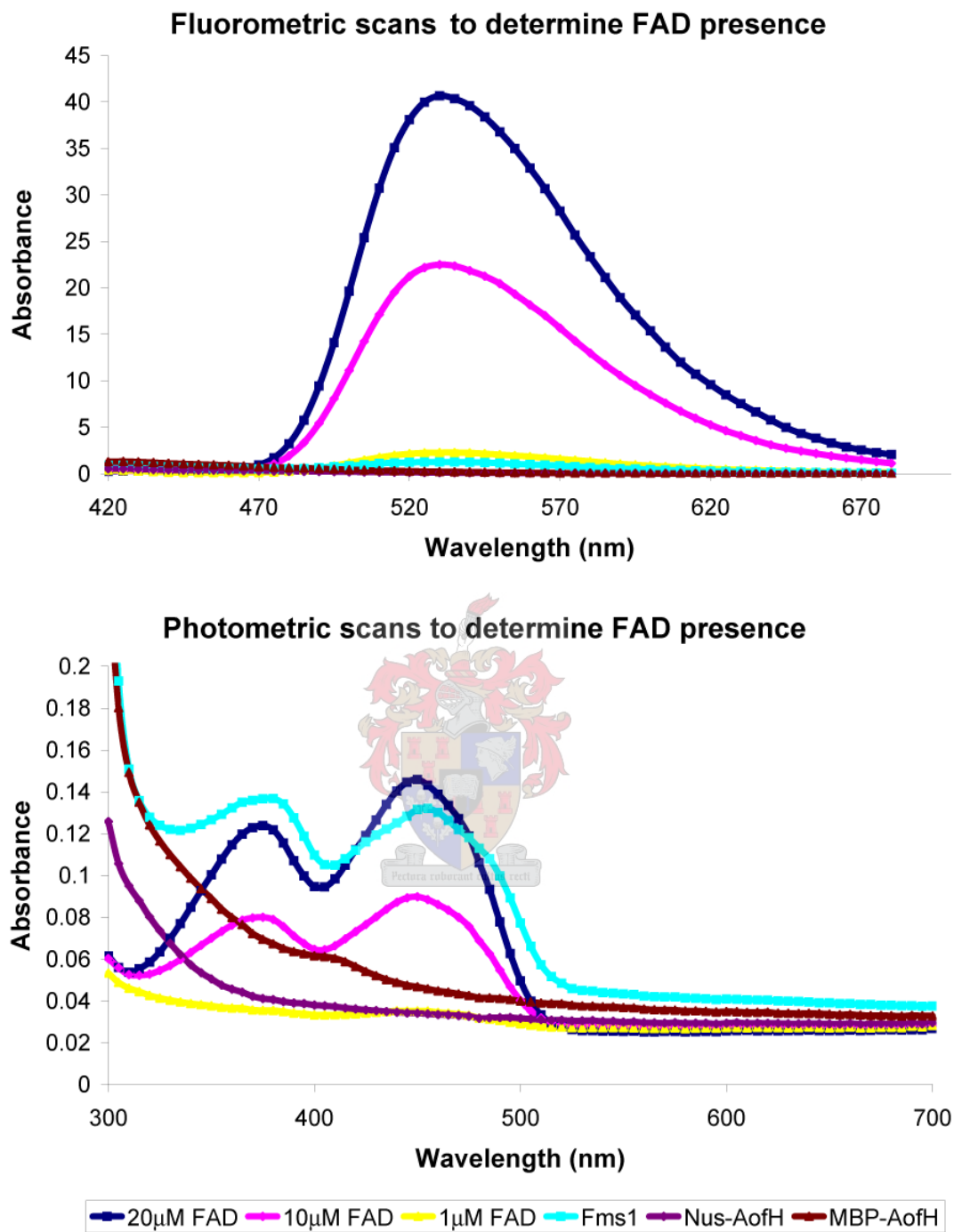


Figure 3.20: FAD scans. The top graph is the fluorescent scans and the bottom graph the photometric scan. In the photometric scan the background absorbance of MBP-AofH is very high and it may appear that the enzyme indeed contains flavin. Further experiments, however, indicated that this was not the case.

Since we found that FAD concentrations of 10 μ M could easily be visualized, the FAD in MBP-AofH should also be visible. However, in the case of Nus-AofH the concentration of protein was obviously too low to be detected. The scans with these proteins were repeated and although the background absorbance was reduced, no FAD peaks could be observed. This led to the conclusion that none of our AofH fusions were purified bound to FAD.

As discussed in section 2.5, denatured His-AofH was also refolded in the presence of FAD. To test whether the refolding was successful, the refolded enzyme was also scanned for FAD content. No FAD was detected in these scans and we concluded that the refolding of AofH was unsuccessful or that it does not bind FAD.

3.9 Conclusion

Different analytical methods were used to determine the products of the AofH enzymatic reactions with the various polyamine substrates. The first set of analyses was performed on TLC. From these we concluded that AofH forms 3-aminopropanol as a product from all the polyamines. This would be a most surprising result, since no other flavin-containing enzyme is known to catalyze a similar reaction. Unfortunately none of the experiments done further could confirm this result; in fact, AofH seemed to be inactive in every additional analysis performed. We finally set out to confirm the presence of the FAD cofactor in the enzyme by variety of methods. These lead us to conclude that the AofH fusions did not contain FAD, and that the observed spots on the TLC analyses of the AofH-catalyzed reactions could not be due to 3-aminopropanol, or that it was formed by some non-enzymatic process.

Further efforts to refold the protein in the presence of FAD had also failed, as detailed in Chapter 2, making it impossible to confirm the activity of AofH by biochemical methods. However, our attempts at confirming the enzyme's activity by genetic methods also proved inconclusive. From the functional complementation studies we were only able to conclude that the Δ *panD* mutants (grown in solution) were in fact able to source β -alanine from other metabolic pathways, making it impossible to determine whether cell lines containing *aofH* could indeed produce a β -alanine precursor at low levels. Taken together, our study shows that the confirmation of the presumed activity of AofH will remain elusive until the enzyme can be purified in its active form, i.e. with FAD bound.

3.10 Experimental

3.10.1 Cloning, overexpression and purification of *Fms1*

Plasmid pJWL94 that comprises of the plasmids pET28a (+)-*FMS1* and Codon⁺ RIL, was a gift from Rolf Sternglanz of State University of New York Stony Brook, USA. The enzyme was expressed from BL21 (DE3) at a 500ml scale in LB media containing 40mg.l⁻¹ kanamycin and 50mg.l⁻¹ chloramphenicol. The expression was induced at OD₆₀₀ = 0.64 with a final concentration of 0.45mM IPTG, 3% ethanol and incubated with vigorous shaking at 18°C overnight. The cells were harvested by centrifugation at 4 500rpm for 30min at 4°C, resuspended in a volume 10× the pellet weight in His-tag binding buffer and lysed with sonication. *Fms1* was purified with affinity chromatography on a 1ml Sigma HIS-Select™ cartridge using the ÄKTAprime-system with His-tag binding buffer (20mM Tris-HCl, 5mM imidazole, 500mM NaCl, pH7.9) and His-tag elution buffer (20mM Tris-HCl, 500mM imidazole, 500mM NaCl, pH7.9). After elution all protein samples were desalted (also on the ÄKTAprime-system) using an Amersham Biosciences 5ml HiTrap™ desalting column and gel filtration buffer (25mM Tris-HCl, 5mM MgCl₂, 5% glycerol, pH 8.0). The protein concentration was determined with the Bradford reagent and BSA standards as 0.86mg.ml⁻¹.

3.10.2 TLC

The experimental procedures were based on the article by Sternglanz *et al.* (2). All enzymatic reactions were carried out in 10mM potassium phosphate buffer, pH 7.2, 200mM NaCl, 0.4mM polyamine and containing ±1.25µg enzyme in a total volume of 50µl. The reactions were incubated at 37°C for 1hour after which they were boiled at 95°C for 5min to denature the enzyme. Polyamines were derivatized by adding 3× the reaction volume of dansylchloride (Dns-Cl) (10mg.ml⁻¹ in acetone) to the reaction mixture. The reaction mixture was saturated with Na₂CO₃ and incubated at 50°C for 30min. 5µl was spotted on 0.2mm thick silica covered plastic TLC plates form Merck. The mixtures were resolved with the eluant 2:3 cyclohexane:ethyl acetate mixture and the spots visualized with UV light at 312nm.

3.10.3 Synthesis of standards

3-aminopropanal was synthesized from 1-amino-3,3-diethoxypropane by hydrolysis of the ethoxy-groups. 1.3mmol 1-amino-3,3-diethoxypropane was stirred in 20ml 0.1M HCl at room temperature for 45 min. Aliquots were derivatized with Dns-Cl and resolved on TLC to assess the reaction. The solvent was removed under reduced pressure and the resulting colorless oil washed with ddH₂O until HCl the odour was absent. The liquid was diluted with ddH₂O and lyophilized overnight. The resulting product was stocked and stored at -20°C.

3.10.4 HPLC

For HPLC analysis a Phenomenex 5µ Luna C18(2) reverse phase column (unless specified otherwise), size 250 × 4.6mm was used with the Waters Alliance 2960 Separation module. All compounds were visualized with a Waters 474 Scanning fluorescent detector. All solvents were HPLC grade (Riedel-de Haën®) and purchased from Sigma-Aldrich. The buffers were filtered through 0.45micron membrane and degassed by sonication.

3.10.4.1 Dansylated products

Mobile phase A was 65% ACN in ddH₂O and B 93% MeOH in ddH₂O. A gradient program from 100%A to 100%B in 28 minutes, a hold step for 2 minutes at 100% B and a gradient back to 100% A over 5 minutes was used at a flow tempo of 1ml.min⁻¹ (3). Chromatography was recorded at excitation 337nm, emission 530nm, gain 10 and attenuance 256.

For the analysis according to the procedure of Cervelli *et al.* (4) a 5µm Gemini C18 110Å reverse phase column, dimensions 250 × 4.6mm, was used. Mobile phase A = 0.5% TFA in ddH₂O and B = 0.5% TFA in ACN. The chromatography was performed at flow rate of 0.1ml.min⁻¹ and a gradient of 0 to 45% B from 0 to 0.1min, 45-80%B from 0.1 to 8min, hold at 80%B from 8 to 11min, 80-90% B from 11 to 12 min. The compounds in 10µl of sample were detected at λ_{ex} = 337nm, λ_{em} = 530nm, gain = 10 and attenuance = 256.

3.10.4.2 NBD-Cl

Stock solutions were prepared by mixing 100µl 20mM polyamine, 100µl 0.1M NaHCO₃ and 400µl 0.5% NBD-Cl in ethanol together and incubating the reaction mixtures for 60min at 55°C in the dark (22). The chromatography was visualized at λ_{ex} = 337nm and λ_{em}=530nm. For the first sets of experiments the mobile phases A = 0.1% TFA in ddH₂O

and B = 0.1% TFA in ACN were used and a number of gradient programs were investigated. The second set of experiments used isocratic elution with 70% A and 30% B where mobile phase A was 93% methanol in ddH₂O and mobile phase B was 0.1% TFA in ACN.

To obtain the chromatographic parameter of the various standard compounds the following program was used: 100% A to 50% A over 30min; back to 100% A from 30 to 35min and hold at 100% A until 40 min at flow rate 1ml.min⁻¹ and the oven temperature at 25°C. The detector was set at $\lambda_{\text{ex}}=430\text{nm}$, $\lambda_{\text{em}}=550\text{nm}$, gain 10 and attenuation 256 for analysis of 10 μl of stock solutions.

The enzymatic reaction mixtures were prepared as described in section 3.10.2 and the derivatization with NBD-Cl as described earlier. For the derivatization with larger excesses of NBD-Cl 100 μl enzymatic reaction (0.4mM polyamine) was added to 98 μl 0.1 M NaHCO₃ and 2 μl 0.25M NBD-Cl (2.5mM) and incubated at 50°C for 60min. 5 μl of the samples were injected onto the column.

3.10.4.3 *o*-Phthaldialdehyde and β -mercaptoethanol

Samples were derivatized by using 100 μl enzymatic mixture/stock solution with 90 μl 0.05M Borate buffer, pH 9.5, 1.5 μl 10mg.ml⁻¹ OPA in EtOH and 1.5 μl 5 μl .ml⁻¹ β -mercaptoethanol in EtOH. After incubation of 1 minute at room temperature, 5 μl of the samples were injected onto the column. Elution was isocratic at 1ml.min⁻¹ flow rate from 100% Buffer A (100mM CH₃COONa) to 100% Buffer B (MeOH + 0.1% TFA) in 30 min at 25°C. Fluorescent detector was set at $\lambda_{\text{ex}}=340\text{nm}$, $\lambda_{\text{em}}=455\text{nm}$, attenuation 256 and gain 10.

3.10.4.4 *Fluram*

For analysis a 5 μm Gemini C18 110Å reverse phase column, 250 × 4.6mm, was used. To obtain separation, an isocratic program was used with 20mM CH₃COONa, pH 5.9 and 30% ACN at 1ml.min⁻¹ flow rate and 25°C. Fluorescence during chromatography was detected at $\lambda_{\text{ex}}=390\text{nm}$, $\lambda_{\text{em}}=475\text{nm}$, gain 10 and attenuation 256. Enzymatic reactions were done as described in section 3.10.2. After the incubation time elapsed, the 50 μl reactions were boiled at 95°C for 5min and 2.5 μl NaOH (2M) added. The protein was precipitated with centrifugation and 50 μl supernatant used further. To the supernatant was added 145 μl 500mM borate buffer, pH10 and 50 μl 0.3mg.ml⁻¹ fluram in ACN (23). Samples of 10 μl were injected onto the column.

To separate the polyamines, different ratios of ACN and CH₃COONH₄; pH 6.0 was tried without success.

3.10.5 ESI-MS and LC-MS analysis

The ESI-MS analysis was done by Dr Andre Venter of the mass spectroscopy unit at the central analytical facility of Stellenbosch University on a Waters API Q-TOF Ultima. For the analysis the following parameters were used: capillary voltage = 3.5kV, cone voltage = 35, RFI = 40, source = 120°C, desolvation temperature = 350°C, desolvation gas = 400l.h⁻¹, cone gas = 50l.h⁻¹ and the source was ESI⁺.

Dr Marietjie Stander did the LC-MS analysis on the same instrument as above at the central analytical facility of Stellenbosch University. The sample were introduced with a Waters Alliance 2690 on a 5µm Gemini C18 110Å reverse phase column, 250 × 4.6mm, by isocratic elution with mobile phase 30%ACN 70% 10mM CH₃COONH₄ at a flow rate 1ml.min⁻¹ with and a 4:2 split to the MS. As for the MS analysis the following parameters were used: capillary voltage = 3.5kV, cone voltage = 35, RFI = 40, source = 100°C, desolvation temperature = 350°C, desolvation gas = 400l.h⁻¹, cone gas = 50l.h⁻¹ and the source was ESI⁻.

3.10.6 Functional complementation studies

3.10.6.1 In *E. coli* DV-strains

Overnight cultures were made of the colonies containing the constructs pYES-EXP49-*aofH*, pYES-EXP49-*panD* and pYES-EXP49-*gus*. These overnight cultures were streaked on minimal media plates (E-salts, 0.2% glycerol, 0.001% thiamine, 0.01% methionine, 100mg.ml⁻¹ ampicillin, 0.2% L-arabinose and 0.2% agar). The metabolites (β-alanine, L-aspartate, pantothenate and spermine) were added to a final concentration of 0.01%. Complementation was also tried from minimal media (same composition as above, just without agar).

3.10.6.2 In JW0127

Complementation was only carried out with the plasmid pYES-EXP49-*aofH*, pYES-EXP49-*panD* and pYES-EXP49-*gus*. All the plate and liquid assays used minimal media, as described above, with added 30mg.ml⁻¹ kanamycin. All liquid assays were on 1ml scale.

3.10.7 Test for monoamine oxidase activity

96-well Corning flat bottom UV-STAR microtiter plates were used for the analysis on the Thermo Varioskan™. Three sets of reactions were done, each in triplicate. The first set contained no enzyme, the second set Fms1 and the third set MBP-AofH. The reaction mixtures consisted of 200µM potassium phosphate buffer, pH 7.2, 10µM benzylamine, and 15µg of enzyme. The reaction was started with the addition of enzyme and the increase of absorption monitored at 250nm and 37°C.

3.10.8 Assays for FAD activity

3.10.8.1 HRP

The reaction mixtures consisted of 0.2M potassium phosphate buffer, pH 7.2, 1mM vanillic acid, 0.5mM 4-aminoantipyrine, 4U.ml⁻¹ of HRP, 0.8µg PAO enzyme and 0.5mM substrate. The reactions were initiated with the addition of the PAO enzyme and the increase in absorbance monitored at 498nm for at least 30min at 25°C. All analyses were done in triplicate on 300µl scale in Corning 96 well microtiter plates on a Thermo Varioskan™ and Skanit software version 2.2.1.

3.10.8.2 Fluorescent assay

For the fluorescent based assay, 300µl of enzymatic reaction mixture was analyzed in black Nunc non-treated 96-well F-bottom multiwell plates from AEC Amersham. The reactions mixtures contained 50mM Tris-HCl pH 9.0, 18U HRP, 1mM homovanillic acid, 0.5mM substrate and 2.34µg enzyme. The reactions were initiated with the addition of the substrate. All analysis was performed on a Thermo Varioskan™ and Skanit software version 2.2.1. Readings were taken at $\lambda_{ex} = 315\text{nm}$ and $\lambda_{em} = 425\text{nm}$ every 1s for 60s for the Fms1 reactions. For the AofH reactions measurements were taken over the same time span, but with larger intervals between each measurement.

3.10.8.3 FAD scans

The Thermo Varioskan™ at 25°C was used for all the scans. Black Corning 96-well microtiter plates were used for the fluorescent scans. $\lambda_{ex} = 370\text{nm}$ and scanned over the range of $\lambda_{em} = 420 - 680\text{nm}$ with a 5nm step size and excitation bandwidth of 12nm.

Corning UV Star 96-well microtiter plates were used for the photometric scans. The samples were scanned from 300nm to 700nm.

3.11 References

- (1) Wilson, K., and Walker, J. (2000) *Practical Biochemistry: Principles and techniques*, 5th edition ed., Cambridge University Press.
- (2) Landry, J., and Sternglanz, R. (2003) *Yeast Fms1 is a FAD-utilizing polyamine oxidase*. *Biochemical and Biophysical Research Communications* **303**, 771-776.
- (3) Phenomenex (2003/4) *HPLC GC SPE catalogue*. p154
- (4) Cervelli, M., Polticelli, F., Federico, R., and Mariottini, P. (2003) *Heterologous Expression and Characterization of Mouse Spermine Oxidase*. *Journal of Biological Chemistry* **278**, 5271-5276.
- (5) Toyooka, T., Watanabe, Y., and Imai, K. (1983) *Reaction of amines of biological importance with 4-fluoro-7-nitrobenzo-2-oxa-1,3-diazole*. *Analytica Chimica Acta* **149**, 305-12.
- (6) Ware, B. R., Klein, J. W., and Zero, K. (1988) *Interaction of a fluorescent spermine derivative with a nucleic acid polyion*. *Langmuir* **4**, 458-63.
- (7) Roth, M. (1971) *Fluorescence reaction for amino acids*. *Analytical Chemistry* **43**, 880-2.
- (8) Cooper, J. D. H., Ogden, G., McIntosh, J., and Turnell, D. C. (1984) *The stability of the o-phthalaldehyde/2-mercaptoethanol derivatives of amino acids: an investigation using high-pressure liquid chromatography with a precolumn derivatization technique*. *Analytical Biochemistry* **142**, 98-102.
- (9) Udenfriend, S., Stein, S., Boehlen, P., Dairman, W., Leimgruber, W., and Weigele, M. (1972) *Fluorescamine. Reagent for assay of amino acids, peptides, proteins, and primary amines in the picomole range*. *Science* **178**, 871-2.
- (10) Snyder, L., and Champness, W. (2003) *Molecular genetics of bacteria*, 2nd edition, ASM press, Washington D.C.
- (11) Vallari, D. S., and Rock, C. O. (1985) *Isolation and characterization of Escherichia coli pantothenate permease (panF) mutants*. *Journal of Bacteriology* **164**, 136-42.

- (12) Vallari, D. S., and Rock, C. O. (1987) *Isolation and characterization of temperature-sensitive pantothenate kinase (coaA) mutants of Escherichia coli*. Journal of Bacteriology **169**, 5795-800.
- (13) Vallari, D. S., and Jackowski, S. (1988) *Biosynthesis and degradation both contribute to the regulation of coenzyme A content in Escherichia coli*. Journal of Bacteriology **170**, 3961-6.
- (14) Colibri - Colibri World-Wide Web Server - <http://ecoli.aist-nara.ac.jp/GBS/search/jsp> (Last accessed: 4 January 2006)
- (15) Liu, B., Sutton, A., and Sternglanz, R. (2005) *A Yeast Polyamine Acetyltransferase*. Journal of Biological Chemistry **280**, 16659-16664.
- (16) Tuberculist -TubercuList World-Wide Web Server - <http://genolist.pasteur.fr/TubercuList/> (Last accessed: 4 January 2006)
- (17) Tabor, C. W., Tabor, H., and Rosenthal, S. M. (1954) *Purification of amine oxidase from beef plasma*. Journal of Biological Chemistry **208**, 645-61.
- (18) Holt, A., Sharman, D. F., Baker, G. B., and Palcic, M. M. (1997) *A continuous spectrophotometric assay for monoamine oxidase and related enzymes in tissue homogenates*. Analytical Biochemistry **244**, 384-392.
- (19) Wu, T., Yankovskaya, V., and McIntire, W. S. (2003) *Cloning, Sequencing, and Heterologous Expression of the Murine Peroxisomal Flavoprotein, N¹-Acetylated Polyamine Oxidase*. Journal of Biological Chemistry **278**, 20514-20525.
- (20) Witt, S., Singh, M., and Kalisz, H. M. (1998) *Structural and kinetic properties of nonglycosylated recombinant Penicillium amagasakiense glucose oxidase expressed in Escherichia coli*. Applied and Environmental Microbiology **64**, 1405-1411.
- (21) Guilbault, G. G., Brignac, P. J., Jr., and Juneau, M. (1968) *New substrates for the fluorometric determination of oxidative enzymes*. Analytical chemistry **40**, 1256-63.
- (22) Strauss, E. (2003) PhD thesis p. 163, Cornell University, USA
- (23) Chopra, S., Pai, H., and Ranganathan, A. (2002) *Expression, purification, and biochemical characterization of Mycobacterium tuberculosis aspartate decarboxylase, PanD*. Protein Expression and Purification **25**, 533-540.

Chapter 4

L-Aspartate- α -Decarboxylase:

Overview and development of possible inhibitors

4.1 Introduction

L-Aspartate- α -decarboxylase (PanD) decarboxylates L-aspartate to form β -alanine and CO₂. As was mentioned in chapter 1 this enzyme forms part of the small class of pyruvoyl-dependent enzymes that includes the histidine, arginine, S-adenosylmethionine (SAM) and phosphatidylserine decarboxylases, and proline reductase. Due to our failure to show the formation of β -alanine precursors from the oxidation of the polyamines, we shifted our focus to PanD since we expected that this enzyme, and not AofH, may be the main source of β -alanine production in Mtb.

The L-aspartate- α -decarboxylases from different organisms share a high degree of sequence conservancy as can be seen in Figure 4.1. Among the strictly conserved residues are Lys⁹, His¹¹, Thr¹⁶, Tyr²², Gly²⁴, Ser²⁵, Asp²⁹, Asn⁵¹, Arg⁵⁴, Thr⁵⁷, Tyr⁵⁸, Gly⁷², Ala⁷³, Ala⁷⁴, Asp⁸², Ile⁸⁵ and Asn¹¹¹ (numbering based on the sequence of PanD purified from *H. pylori*) (1). Twelve of these residues are located around the active site although they are not all on the same chain. The Lys⁹, His¹¹ and Arg⁵⁴ residues that form part of the active site are located on an adjacent chain of the homotetramer (1, 2).

The crystal structure of *E. coli* PanD was solved at 2.2Å resolution (3). This structure consists of a homotetramer with pseudo four-fold rotational symmetry (refer to Figure 4.2, structure b). Each strain comprises of a 6-stranded β -barrel capped by small α -helices at both ends. (Refer to Figure 4.2, structure a) Of the four chains in the tetramer only three contain the active pyruvoyl site. The fourth has the ester intermediate functionality (3, 4).

The crystal structure for *H. pylori* PanD has also been solved at 2.0Å resolution for the apo structure and 1.55Å for the iso-asparagine bound complex. Iso-asparagine is a structural analogue of L-aspartate and was used to study the binding interactions in the active site (Figure 4.2, boxed) (1).

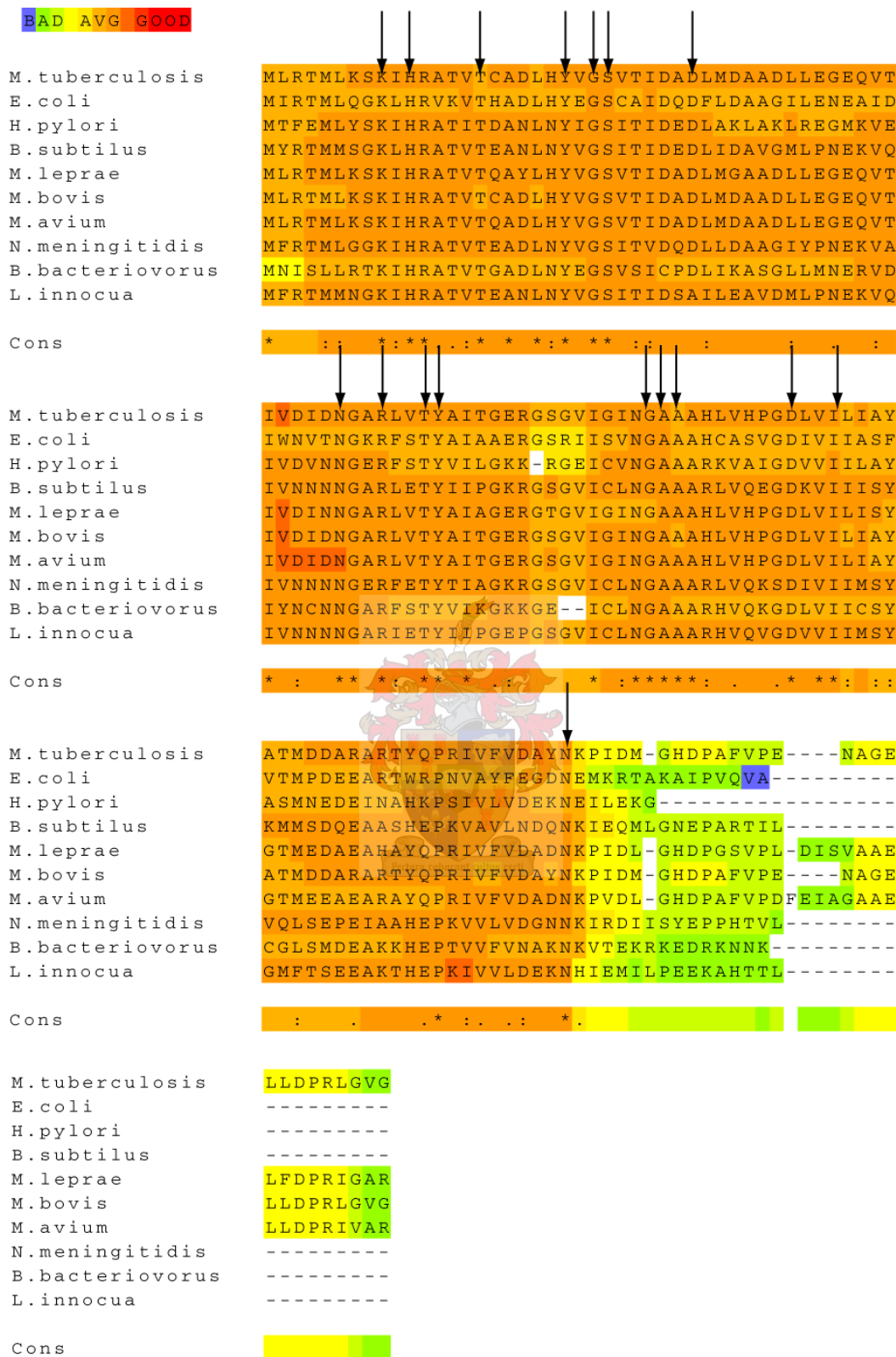


Figure 4.1: Sequence alignment of PanD's from different species constructed on T-coffee (5). The highly conserved residues mentioned in the text are indicated with arrows.

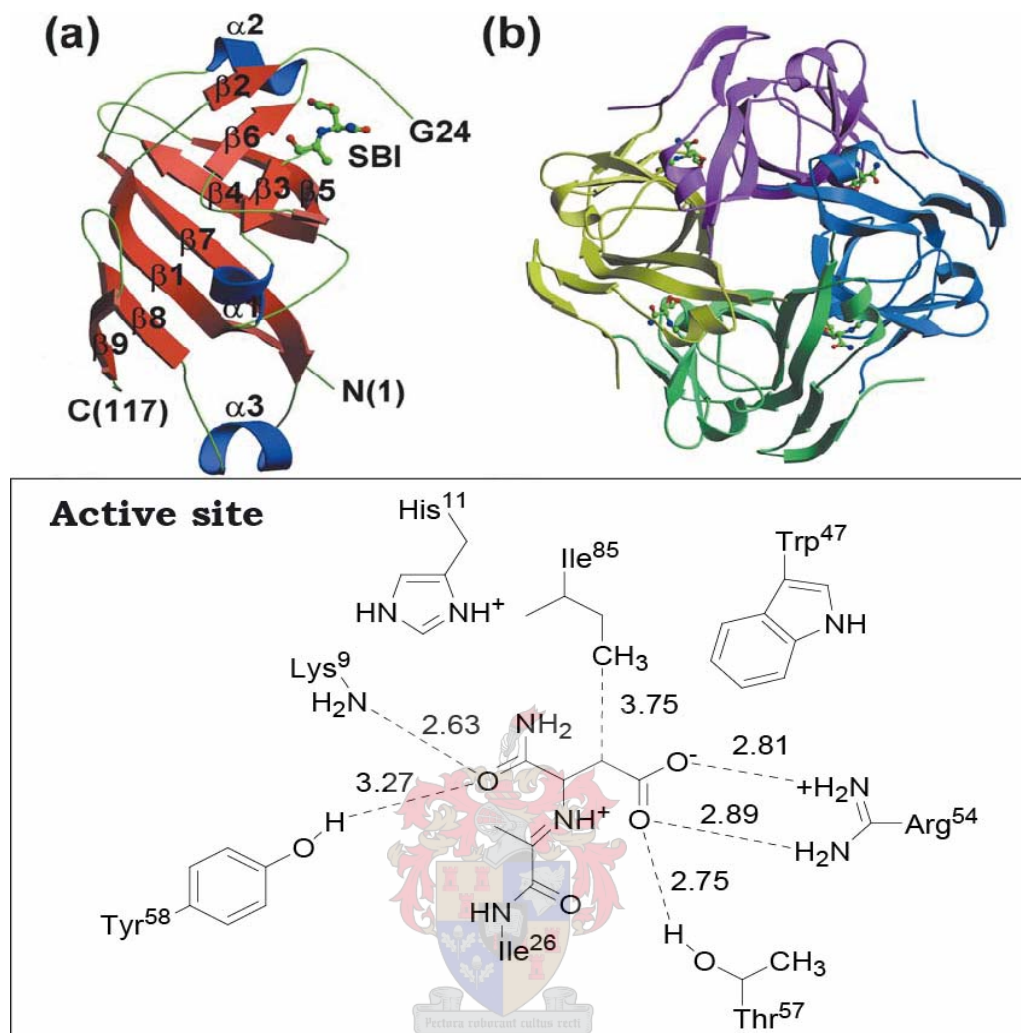


Figure 4.2: The crystal structure (top 2 pictures) and schematic representation of the active site (in block at bottom) of *H. pylori* PanD. Picture (a) represents the monomer (in ribbon presentation) with the pyruvoyl group covalently bound to iso-asparagine (ball and stick presentation). Picture (b) is the protein tetramer. The dashed lines in the active site representation indicate the distances between the active site residues and the bound isoasparagine groups in Å. (Figure reprinted with permission of Elsevier from the article of Byung II Lee and Se Won Suh. (2001) *Crystal Structure of the Schiff Base Intermediate Prior to Decarboxylation in the Catalytic Cycle of Aspartate- α -Decarboxylase*. Journal of Molecular Biology 340 (1), 1-7 © 2001 (1).)

The most important covalent interaction in the active site is the formation of the iminium ion (Schiff base). As far as the non-covalent interactions are concerned, a salt bridge forms between Arg⁵⁴ and the β -carboxylate of L-aspartate. This leads to the selectivity toward β -amino acids. Other interactions include hydrophobic packing interactions with Trp⁴⁷ and hydrophilic with Thr⁵⁷. These interactions may be the reason why α - and β -branched compounds don't bind, but β -hydroxy compounds do. Lys⁹ and His¹¹ stabilized

the α -carboxylate functionality on the opposite side of Arg⁵⁴. The selectivity of these residues seems to be weaker, since a degree of chain extension is possible for the substrates in this area (6).

Based on our knowledge of sequence homology between the different PanD's and on the active site, we set out to design an inhibitor for Mtb PanD.

4.2 Inhibitors

There are two approaches for the rational design of inhibitors for PanD. The first is to inhibit the self-processing cleavage that leads to the formation of the pyruvoyl group. The second is to develop a substrate-based inhibitor that would inhibit the decarboxylation reaction (1).

4.2.1 Inhibition of pyruvoyl formation

Mtb PanD is translated into an inactive pro-enzyme called the π -protein. The activation of the enzyme is temperature dependent and occurs with the formation of the pyruvoyl groups. The residues Gly²⁴ and Ser²⁵ are involved in this modification. As is shown in Figure 4.3 the process starts with nucleophilic attack of the hydroxyl oxygen of Ser²⁵ on the carbonyl group in Gly²⁴ (4.1). This N-O acyl shift *via* an oxazolidine intermediate leads to the formation of an ester intermediate (4.3). The alpha proton in relation to the Ser carbonyl group is abstracted and the resulting charge is stabilized through resonance. β -elimination of the ester containing chain leads to the formation of the PanD β -chain of 2.74kDa (4.4). The longer α -chain (4.5) of 13.22kDa now ends with dehydroalanine. Rearrangement to the imine and subsequent hydrolysis forms a carbonyl group. This gives rise to the two adjacent carbonyl groups of the pyruvoyl group (4.6) (2, 7).

The cleavage of the PanD to form the pyruvoyl groups was found to be temperature dependent. Optimum cleavage occurs at 37°C (physiological temperature) and the rate of cleavage decreases with increase of temperature. Complete cleavage of the Mtb enzyme is obtained after 24 hours. This corresponds to the doubling time of the mycobacterium (7).

As far as the inhibition of the formation of the pyruvoyl group is concerned, studies have been done to mutate the residues involved in protein maturation *in vitro* (8). However, these effects have not been studied *in vivo* and furthermore no small molecule has yet been identified that can prevent the post translational process from happening. As a

result, we decided to focus on the design of a small molecule that is a structural analogue of L-aspartate and can act as a mechanism-based inhibitor.

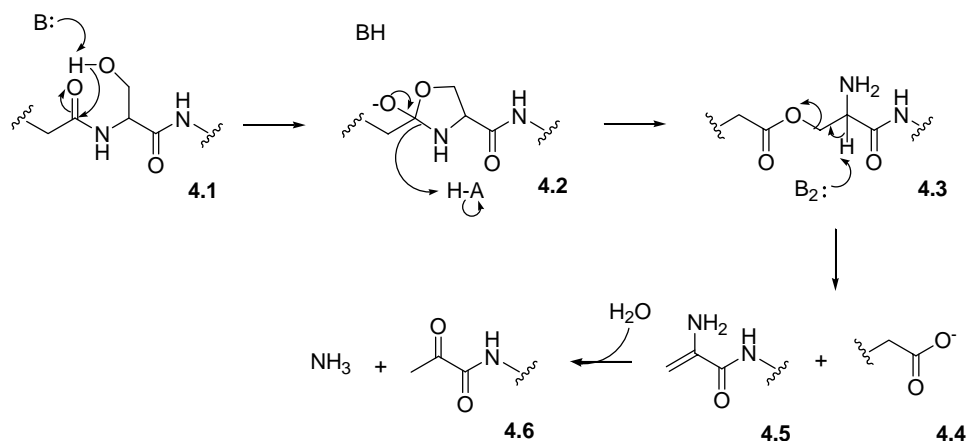


Figure 4.3: Formation of the pyruvoyl group

4.2.2 Structural- and mechanism- based inhibitors

A mechanism-based inhibitor is an inactive compound that has structural similarity to the substrate or product of the target enzyme. These compounds are converted by the action of the target enzymes to intermediates that are reactive and can normally deactivate the same enzyme. One of the problems with creating a mechanism-based inhibitor for PanD is that this enzyme has a similar reaction mechanism to the enzymes that use the cofactor pyridoxal 5'-phosphate (PLP). Even so, this would not normally be a problem since enzymes are very specific for their substrates and the inhibition of one group of enzymes would not necessarily affect the function of another group. In this case, however, the PLP dependent aspartate aminotransferase also binds aspartate. Some of the other reactions that the PLP-dependent enzymes catalyse include racemization, transamination, retro-aldol cleavage, decarboxylation (9) and α,β - and β,γ -eliminations (10) and further examples of these enzymes include arginine decarboxylase, cysteine synthetase, serine hydroxymethyltransferase, alanine racemase and 3,4-dihydroxyphenylalanine (11). Various ways to inhibit the PLP-dependent enzymes have already been described and include inhibition by structural analogues (9, 12), and metal ions (10). The transaminase enzymes are also inhibited by aminoxyacetate, semicarbazide, cyanide and isoniazid (13).

As in the case of the pyruvoyl group, the PLP cofactor reacts with the amine functionality on the target molecule to form a Schiff base (refer to Figure 4.4) where it acts as an electron sink for the charge generated during the enzymatic reaction. In mechanism-based inhibition the PLP enzymes convert the inhibitor into an electrophile. However, for the inhibition of the pyruvoyl group we focused on the design of an inhibitor that would convert the pyruvoyl group into a nucleophile, which would then attack a nearby electrophile to form a covalent bond. This method of deactivation would distinguish our PanD inhibitor from other PLP inhibitors, offering some selectivity.

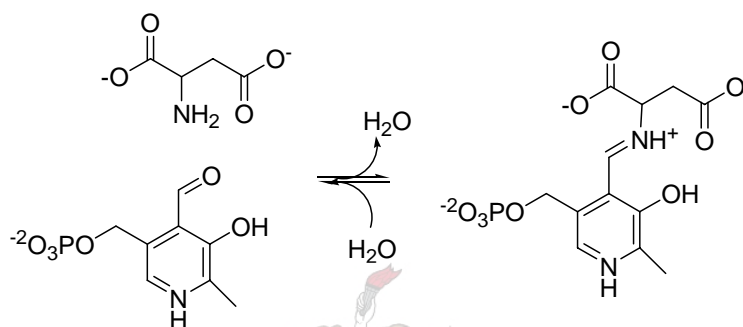


Figure 4.4: Binding of the PLP cofactor to the substrate. The formation of the Schiff base is a mechanistic characteristic that these enzymes share with the pyruvoyl group of enzymes (compare to Figure 1.4)

In our studies we focused on the design of a mechanistic inhibitor that is a structural analogue of the natural substrate of PanD, L-aspartate. To do this however the inhibitors that have already been identified for PanD first have to be reviewed.

4.3 Overview of inhibitors for *E. coli* PanD

Shive and Mascow already identified the first inhibitor of PanD in 1946, although at that time it was not recognized as such. This, however, led to the discovery of the function of L-aspartate in pantothenate biosynthesis. Their experiments with β -hydroxyaspartate caused inhibition of cellular growth in test cultures. This inhibition was lifted by addition of asparagines, pantothenate and aspartate. Inhibition also occurred when the cultures were treated with cysteic acid, a structural analogue of aspartate (2). Soon thereafter *E. coli* PanD was purified to near homogeneity, and it was confirmed that the decarboxylase is inhibited by D-serine, β -hydroxy-D,L-aspartate and L-cysteic acid (14).

Webb *et al.* (6) performed a binding screen with *E. coli* PanD in which they tested 55 compounds that bear the primary amine functionality. The covalent adducts that formed were identified with MALDI-TOF spectroscopy after the enzyme was incubated with the possible substrates in the presence of NaCNBH₃. From these analyses they reached the following conclusions about which structures will not bind in the active site (L-aspartate is used as reference for discussions):

1. Extension in the linker between the α -carbon and β -carboxylate is unfavourable. Example of molecule: L-glutamate.
2. Extension in the chain between the α -carbon and the α -amino group is unfavourable. Example of molecule: 2-aminomethylsuccinate.
3. Increase in chain length between the α -carbon and α -carboxylate is tolerated, for example β -glutamate. These compounds cannot act as substrates, but they are promising competitive inhibitors.
4. Both α - and β -branching are unfavourable except in the case of β -hydroxyaspartate and *D*-serine. Example of molecules for which binding is unfavourable: α - and β -methyl aspartate.

Although these experiments were not done with Mtb PanD, the active site is presumed to have a great deal of similarity to the active site of the *E. coli* enzyme, (refer to Figure 4.1). We could therefore use these principles in the design of an inhibitor.

4.4 Design of an inhibitor

In the design on an inhibitor we focused on compounds that are substrate analogues of L-aspartate, since they are the most likely to bind to the enzyme. We decided to synthesize an inhibitor by adding a potential good leaving group in the β -position of L-aspartate. This would act as an efficient way of deactivating the enzyme. Based on the work done on *E. coli* inhibitors substitution in the β -position of L-aspartate with a methyl group is unfavourable. However, β -hydroxyaspartate and *D*-serine do bind to the enzyme. Webb *et al.* (6) postulated that this discrepancy in their analysis might be due to hydrophilic interactions in the active site with Thr⁵⁷ (refer to active site, Figure 4.2 box). The inhibitors investigated and considered for this study are shown in Figure 4.5. Even though β -hydroxyaspartate (4.7) binds to the enzyme, it is a known competitive inhibitor

of PanD (2). We set out to synthesize β -fluoroaspartate (4.8) and test it as a possible inhibitor. The F-atom is small, so steric interference in an active centre designed to fit an H-atom would be kept to a minimum. Fluorine is also a good leaving group and due to its high electronegativity, the hydrophilic interaction in the active site should not prevent binding as in the case of the methyl substituents.

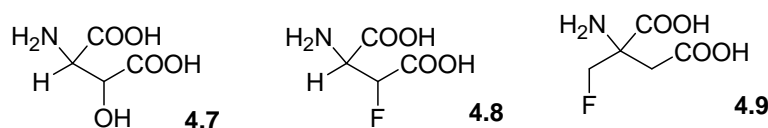


Figure 4.5: Possible inhibitors of PanD. β -hydroxyaspartate (4.7) is a known inhibitor and we investigated fluorine-substituted analogs, β -fluoroaspartate (4.8) and α -fluoromethylaspartate (4.9).

Another possible inhibitor we wanted to investigate was α -fluoromethylaspartate (4.9). However, α -branching is unfavourable according to Webb's analysis. Moreover, α -fluoromethylaspartate is unstable and prone to cyclization. The postulated deactivation mechanism of β -fluoroaspartate with PanD is given in Figure 4.6.

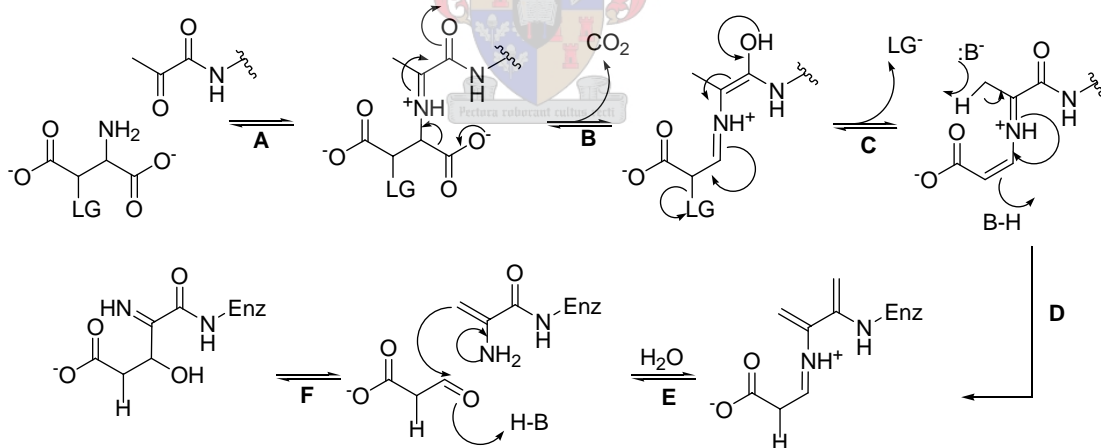


Figure 4.6: Proposed mechanism of action of a mechanism based inhibitor of PanD. The structural analogue of L-aspartate contains a leaving group that is eliminated during the enzymatic process to form a terminal double bond. This can attack the glyoxylate carbonyl group to form a covalent bond.

As shown in the figure, the decarboxylation of the substrate analogue still occurs (step B). The first difference is in the step where the substrate would have picked up an H⁺.

Instead of this happening, the leaving group would rather be eliminated (step C). In the following step abstraction of the H^+ on the methyl group of the pyruvoyl group would lead to the substrate protonation (step D). This complex can be hydrolyzed from the pyruvoyl group to form glyoxylate instead of β -alanine (step E). The terminal double bond that formed from what used to be the pyruvoyl group can now act as a nucleophile and attack the aldehyde functionality of the glyoxylate (step F) and a covalent bond forms.

4.4.1 Synthesis of an inhibitor

4.4.1.1 Overview

The synthesis scheme of β -fluoroaspartate (**4.8**) is shown in Figure 4.7. We based the synthesis of β -fluoroaspartate on the synthesis of β -hydroxyaspartate. Although β -hydroxyaspartate is commercially available, it is expensive with 250mg costing R2 437.38 (Sigma-Aldrich).

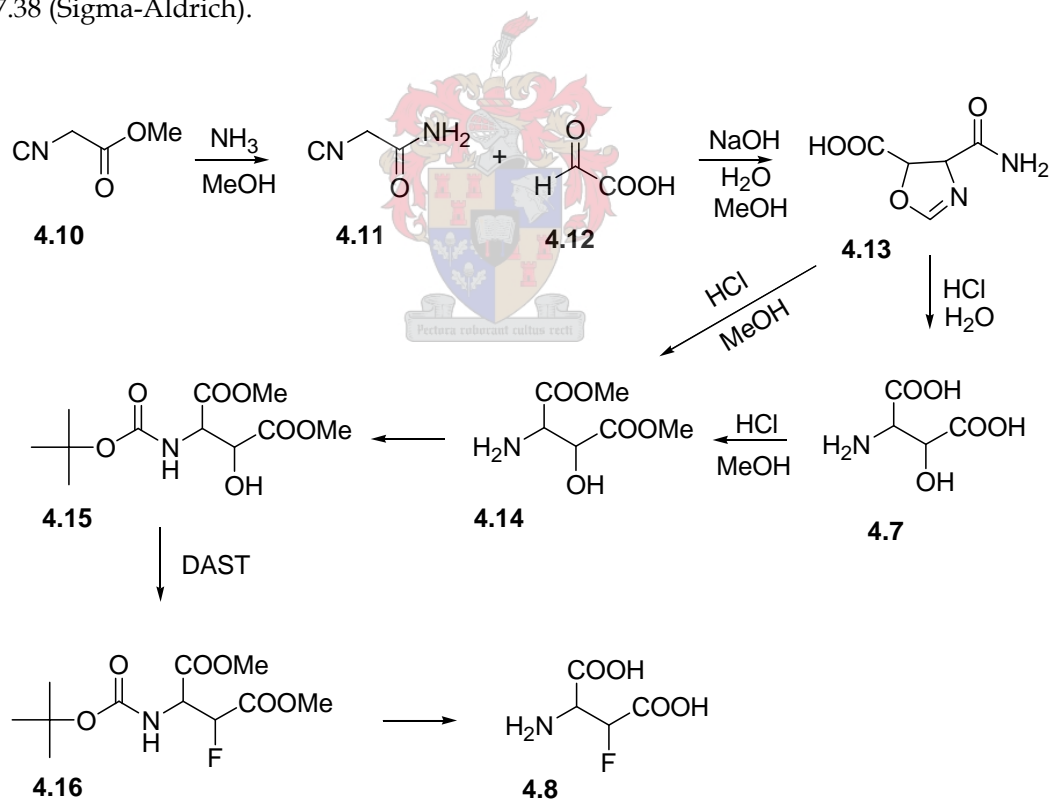


Figure 4.7: Proposed synthesis of β -fluoroaspartate

We decided to pursue the synthesis of this precursor based on the published procedure of Ozaki *et al.* (15). This method consists of the condensation of methylisocyanoacetate (**4.11**) and glyoxilic acid (**4.12**) to form an oxazoline ring (**4.13**). The ring is hydrolyzed by aqueous HCl to form β -hydroxyaspartate (**4.7**). The product is purified with ion exchange chromatography by using an acidic Amberlite® IR-120(plus) column, eluting the product with 5% NH₄OH solution and recrystallization from H₂O. To obtain β -fluoroaspartate, protected β -hydroxyaspartate is required. In the postulated synthesis the carboxylic acid groups would be protected by formation of the methyl esters and the amine functionality with di-*t*-butyl dicarbonate (BOC group). The β -hydroxy-group could then be exchanged by reaction with diethylamino sulphurtrifluoride (DAST) and deprotected to give β -fluoroaspartate.

4.4.1.2 Attempts at the synthesis

α -Isocyanoacetamide (**4.11**) was synthesized by stirring methylisocyanoacetate (**4.10**) in a solution of NH₃ in MeOH (16). The formation of **4.11**, a black sticky substance, was confirmed by ¹H-NMR. (DMSO-*d*⁶), 4.3ppm (2 × H's). β -Hydroxyaspartate (**4.7**) was prepared via intermediate **4.13** according to the procedure of Ozaki *et al.* as described above. Purification was attempted with the correct equivalent of Amberlite (1g binds 4.4meq) and repeated four times. Efficient binding and purification did not occur.

Since the purification of β -hydroxyaspartate was troublesome, we decided to isolate and purify the oxazoline ring (**4.13**) before attempting hydrolysis, in a second synthesis. The purification of **4.13** was attempted by recrystallization from MeOH. This proved to be unsuccessful and the efforts to isolate **4.13** were abandoned and the oxazoline ring was hydrolyzed with aqueous HCl and lyophilized. The solvent was removed *in vacuo* and the powder refluxed in a solution of anhydrous HCl in MeOH to form crude **4.14** (17). To synthesize **4.15**, crude **4.14** derivatized with di-*tert*-butyl dicarbonate. The product was extracted from the reaction mixture with CHCl₃, dried and the solvent removed *in vacuo*. However, the product extracted was a brown sticky substance that could not be resolved with TLC.

The synthesis was repeated to form the oxazoline ring (**4.13**) for a third time in which we attempted to synthesize the protected β -hydroxyaspartate methyl ester (**4.14**) directly by refluxing **4.13** with dry HCl in MeOH overnight. The solvent was removed *in vacuo* and

the product purified on a silica column and the fractions obtained analyzed with $^1\text{H-NMR}$. According to these spectra, none of the samples contained the product.

4.4.1.3 Conclusion on synthesis

The synthesis of β -fluoroaspartate was more difficult than anticipated. The biggest problem is the failure to purify β -hydroxyaspartate (4.7) from the reaction mixture. To side step this purification step direct protection of 4.7 was investigated by refluxing with dry HCl and derivatization of the primary amine with a BOC-group. Unfortunately the less polar product that formed did not prove easier to purify. An additional problem that hampered progress on the synthesis of the inhibitor is the low yield of the hydrolysis steps, which afforded very little product in our hands. This combination of factors led to a third unsuccessful attempt to synthesize the inhibitor. Instead, we decided to focus our attention on the development of qualitative and quantitative assays to test for possible inhibitors.

4.5 Testing of substrates and inhibitors

4.5.1 Overview of existing assay methods

The existing assay methods for PanD were all designed to determine the steady-state kinetics of the enzyme. Assays to determine the steady-state kinetics of Mtb PanD activity was done by Chopra *et al.* (7) and for *E. coli* PanD by Ramjee *et al.* (4) and Williamson *et al.* (14). Chopra (7) and Ramjee (4) both used stop assays based on the derivatization of L-aspartate and β -alanine with fluorescamine (fluram). Aliquots of the enzymatic reaction were taken at given time intervals, the enzymatic reaction quenched, derivatized with fluram and the components separated and quantified with HPLC (7). Williamson and Brown (14) assayed PanD activity by measuring the release of $^{14}\text{CO}_2$. They trapped the gas with hyamine and measured the radioactivity with a scintillation counter. Another method used was to measure the formation of ^{14}C - β -alanine from either $[\text{U-}^{14}\text{C}]$ -aspartate or $[\text{4-}^{14}\text{C}]$ -aspartate with separation by chromatography and subsequent scintillation counting (14).

We set out to develop assay methods that did not involve radioactive compounds. Firstly we wanted a qualitative method to test whether certain compounds are substrates of PanD or not. For this reverse phase HPLC was used. Secondly a quantitative method is

required to compare different substrates and inhibitors with each other. To fulfil this requirement a coupled enzymatic assay was used.

4.5.2 Testing with HPLC

With the HPLC method we wanted to identify whether or not certain compounds are substrates of PanD. To accomplish this, enzymatic reactions were analysed of Mtb PanD with different substrates. After derivatization with fluram these compounds were analyzed with HPLC on a C18 column. The obtained results were analysed by comparison to the retention times of stock solutions of the presumed substrate/inhibitor and the postulated products to determine whether the enzymatic reactions occurred or not. The inhibitors investigated are shown in Figure 4.8 along with the postulated products.

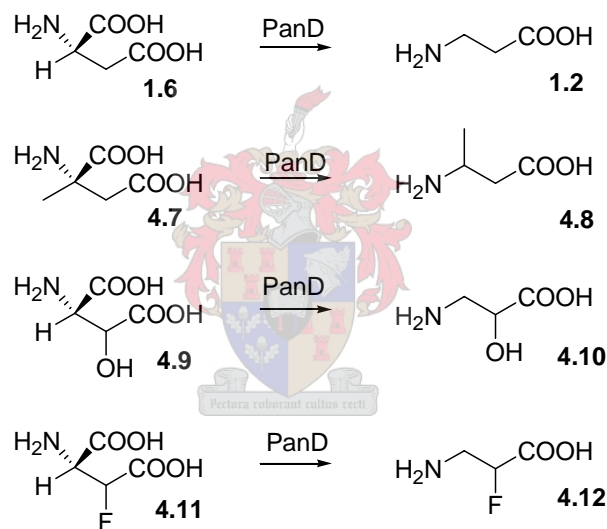


Figure 4.8: The inhibitors investigated and the theoretical products that would form if they were decarboxylated.

In our initial HPLC analysis reaction mixtures were derivatized with OPA and β -mercaptoethanol. Although analysis could be done in this manner, we found that the aspartate derivative was not very stable under these derivatization conditions. Literature confirmed that the diacidic amino acids aspartate and glutamate are unstable and therefore show loss in fluorescence when derivatized with OPA (19). Furthermore our studies of the AofH reaction with fluram (section 3.3.2.2) proved successful, both

pertaining to the stability of the derivatized compounds and reproducibility of the analysis. As a result, we decided to continue the studies with the fluram derivatives.

With the HPLC analysis we expected to see product peaks in the chromatogram of the enzymatic reaction with L-aspartate, but not for the enzymatic reactions with α -methyl-D,L-aspartate (4.17) and β -hydroxyaspartate (4.7). The chromatograms of the PanD with L-aspartate (1.6) clearly showed the formation of β -alanine (1.2) (Figure 4.9, top). No product peak were present for the reaction of PanD with α -methyl-D,L-aspartate (4.17) (Figure 4.9, bottom) as was expected, since it is known that this compound does not bind to PanD (6). Interestingly, the chromatograms of β -hydroxyaspartate (4.7) showed the formation of isoserine (4.19) (Figure 4.9, middle). From these results we conclude that L-aspartate and β -hydroxyaspartate are substrates of PanD, while α -methylaspartate is not. To compare the effectiveness of the decarboxylation reaction of the two substrates, the steady-state kinetics have to be determined.

4.5.3 Developing assays for steady-state kinetics

In the reaction of PanD with L-aspartate, the two products, CO₂ and β -alanine, could both be assayed (refer to Figure 4.10).

CO₂ can be assayed by labelling with ¹⁴C and measuring the release of radioactive CO₂ (14). A coupled enzymatic assay of CO₂, based on the enzymes phosphoenolpyruvate carboxylase (PEPC) and malate dehydrogenase has also been described. This assay coupled the production of CO₂ to the decrease of NADH in the assay mixture. Unfortunately L-aspartate is an allosteric inhibitor of PEPC, and thus this assay cannot be used to assay PanD (2).

The second product, β -alanine, has previously been assayed by derivatization with fluram and quantification on the HPLC (4, 7) as well as by radioactive labelling with ¹⁴C (14). Alternatively, the production of β -alanine can be measured by a coupled enzymatic reaction based on the activity of the β -alanine-utilizing enzyme PanC. However, such an assay requires an optimized assay of PanC.

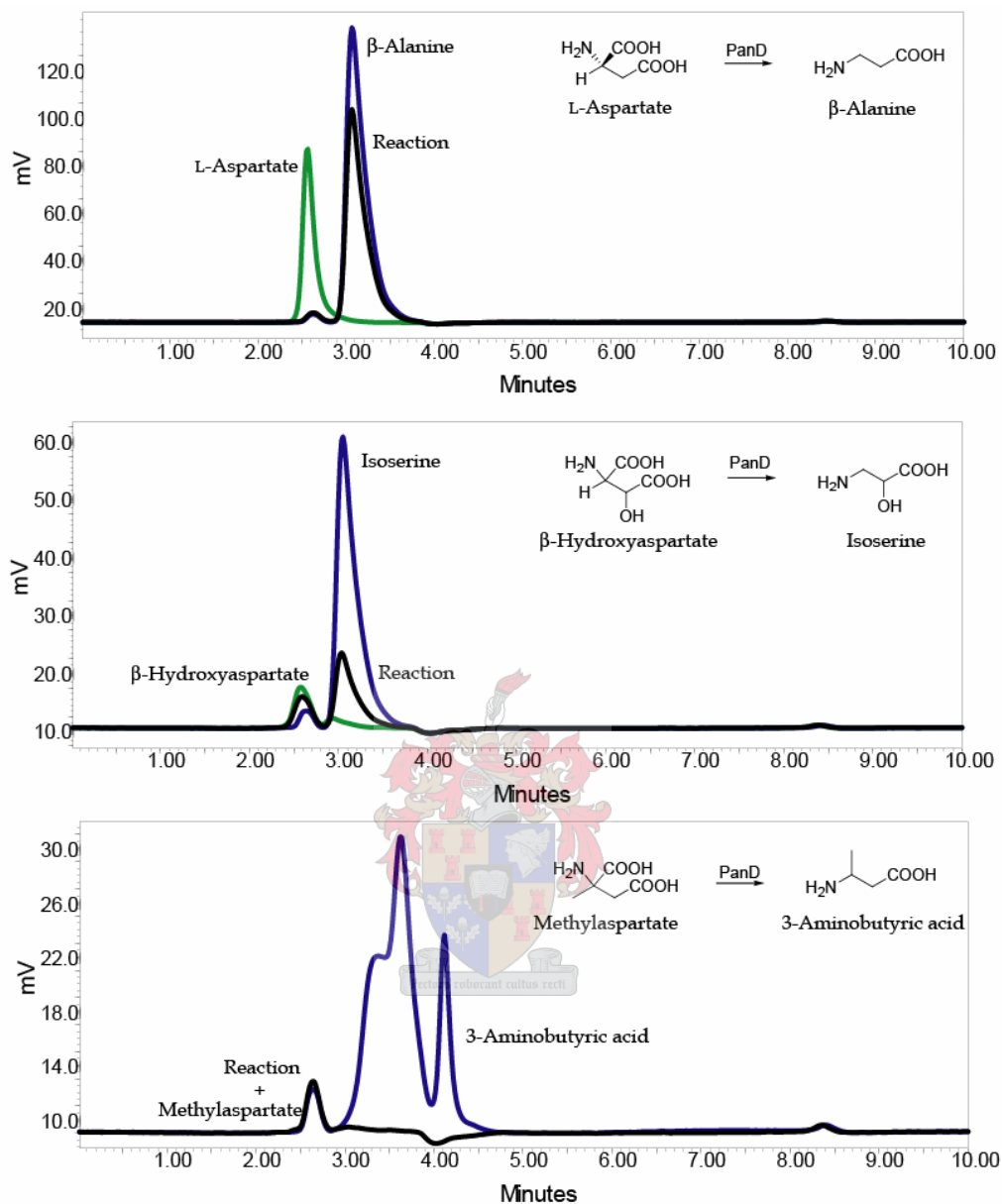


Figure 4.9: Chromatograms from HPLC analysis of the substrates, their postulated products and the enzymatic of the substrates with PanD as fluram derivatives. All analyses were done on a C18 column with and isocratically eluted with 20mM CH_3COONa and 30% ACN at $1\text{ml}\cdot\text{min}^{-1}$ flow rate. The substrate peaks are all green, the product peaks blue and the analysis of the reactions are shown in black. In the bottom graph the chromatograms of the α -methyl-D,L-aspartate stock and of the reaction are identical, therefore only one spectrum is observed.

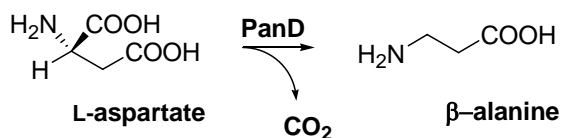


Figure 4.10: The enzymatic reaction of PanD with L-aspartate to form β -alanine and CO_2 .

4.5.3.1 Assays for PanC activity

E. coli PanC was used in all the assays. As can be seen in Figure 4.11, PanC catalyses the condensation of β -alanine and pantoic acid in the presence of ATP. The three products that form, namely AMP, pantothenic acid and pyrophosphate (PPi), can be used to assay for PanC activity.

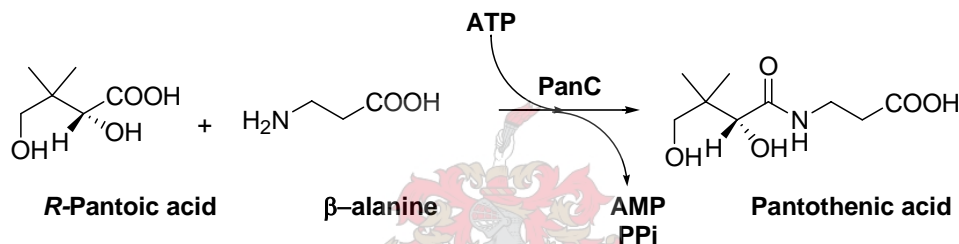


Figure 4.11: The enzymatic reaction of PanC with R-pantoic acid and β -alanine to form pantothenic acid. In this reaction ATP is used and AMP and PPi formed.

4.5.3.2 Assay with AMP

The first assay (Figure 4.12, A) we investigated makes use of a coupled enzymatic reaction where the AMP produced from the PanC reaction is converted to ADP by the enzyme adenylate kinase (Adk, also known as myokinase) in the presence of ATP. This ADP is used by pyruvate kinase (PK) to reduce phosphoenolpyruvate (PEP, **4.21**) to pyruvate (**4.22**). ATP is regenerated and is recycled back into the Adk reaction. The pyruvate (**4.22**) is further reduced to lactate (**4.23**) by lactate dehydrogenase (LDH) in the presence of NADH. For every molecule of pantothenate (**1.1**) formed in the PanC reaction, one molecule of NADH is oxidized to NAD^+ . The kinetic parameters can thus be determined by measuring the decrease in NADH at 340nm (17). Kinetic analysis of the PanC reaction with this method was time consuming with an average run time of 30 minutes. High concentrations of enzyme ($\pm 150\mu\text{g}$ per $300\mu\text{l}$ reaction) were also required. We therefore explored other possibilities for the coupled assays.

4.5.3.3 Assay using pantothenic acid

The second method we tried was an assay that utilized pantothenic acid. (Figure 4.12, **B**) The PanC reaction was coupled with the reaction of pantothenate kinase (CoaA). CoaA phosphorylates pantothenic acid (**1.1**) with the consumption of ATP to form ADP. This ADP molecule is recycled into the PK and LDH reactions as described above. This method was not an improvement on the previous assay as far as duration of the assay and amount of enzyme required was concerned.

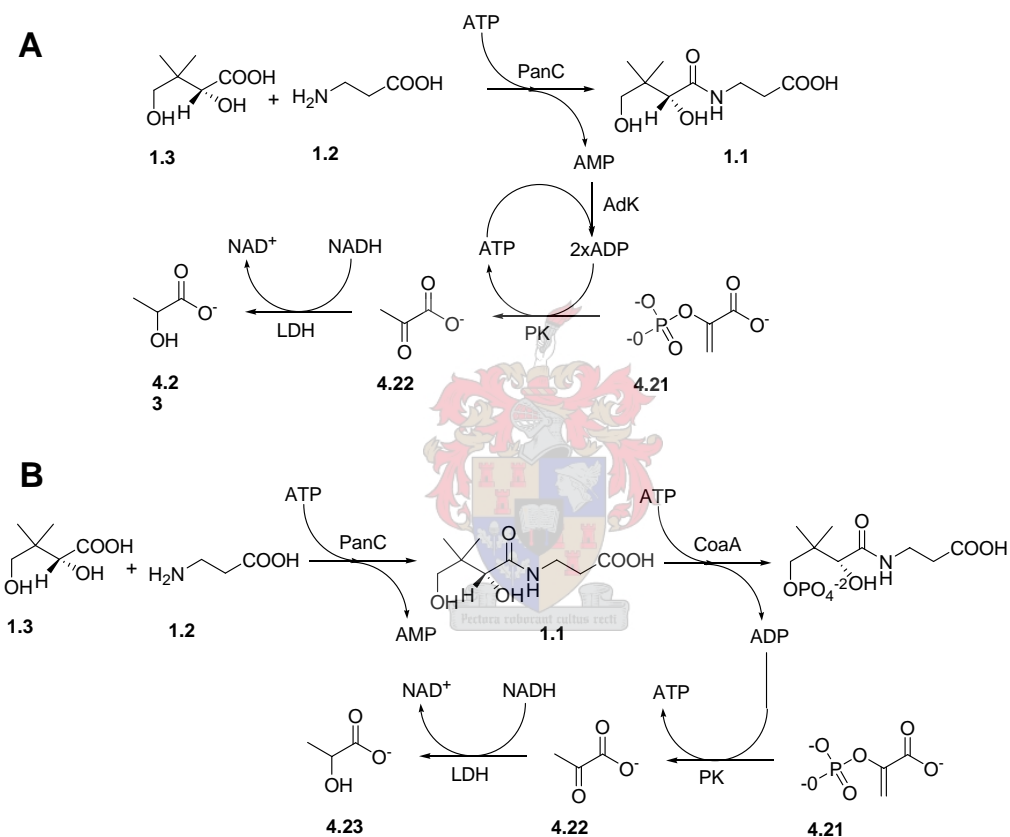


Figure 4.12: Coupled assay to determine the kinetic parameters of PanC. All the assays measured the decrease of NADH at 340nm.

4.5.3.4 Assay using pyrophosphate

The third approach was to assay the PPi that formed. This was done by using a Sigma[®] Enzymatic Determination of Pyrophosphate kit that contains a complete enzymatic method to assay the production of PPi with a coupled assay to NADH. In the condensation reaction of β -alanine (**1.2**) and pantoic acid (**1.3**) in the presence of PanC and ATP, one molecule each of AMP and PPi are released per molecule of pantothenate

formed. In the assay fructose-6-phosphate kinase catalyses the reaction of PPi with D-fructose-6-phosphate to form D-fructose-1,6-diphosphate. This molecule is degraded by the enzyme aldolase to form D-glyceraldehyde-3-phosphate (GAP) and dihydroxyacetone phosphate (DHAP). GAP is also converted to DHAP by triosephosphate isomerase. DHAP are reduced to glycerol-3-phosphate by glycerophosphate dehydrogenase in the presence of NADH (20). For every one molecule of PPi consumed, two molecules of NADH are oxidized to NAD⁺. The decrease of NADH is followed at 340nm.

The kinetic parameters for PanC with β -alanine using this assay was determined as $V_{\max} = 0.04 \pm 0.002 \text{ nmol} \cdot \text{s}^{-1}$, $K_M = 121 \pm 26 \mu\text{M}$, $k_{\text{cat}} = 0.018 \text{ s}^{-1} \pm 0.001$ and $k_{\text{cat}}/K_M = 0.15 \pm 0.039$. The Michaelis-Menten curve fit is given in Figure 4.13 (top) and the literature values for the different PanCs and the assays used to determine them are given in Table 4.1. Our kinetics parameters correspond well with the values obtained in literature.

Table 4.1: Steady state kinetic parameters for PanC with β -alanine according to literature and the assays used (2).

Organism	K_M (μM)	k_{cat} (s^{-1})	k_{cat}/K_M	Assay
<i>Mycobacterium tuberculosis</i>	800 ± 0.1		4.3×10^3	Coupled enzymatic assay (21) with Adk, PK and LDH
<i>Escherichia coli</i>	950			Coupled enzymatic assay (2) with Adk, PK and LDH
<i>Escherichia coli</i>	56			¹⁴ C labeled β -alanine (2)
<i>Escherichia coli</i>	62.6			¹⁴ C labeled β -alanine (2)
<i>Escherichia coli</i>	530 ± 70			Microbiological assay (2)
<i>Escherichia coli</i>	121 ± 26	0.018 ± 0.001	0.15 ± 0.039	Our assay with PPi kit

4.5.3.5 Steady-state kinetics for PanD

The kinetic parameters for the Mtb PanD reaction with L-aspartate were determined by using the coupled enzymatic reactions of PanC and PanD and assaying with the PPi kit. Two sets of reactions were done to test the influence of the amount of PanC on the enzymatic reactions. In the first set $\pm 5 \mu\text{g}$ Mtb PanD and $\pm 150 \mu\text{g}$ PanC (all enzymatic

concentrations were determined with the Bradford reagent) was used per 300 μ l reaction and in the second set 5 μ g Mtb PanD and 137 μ g PanC.

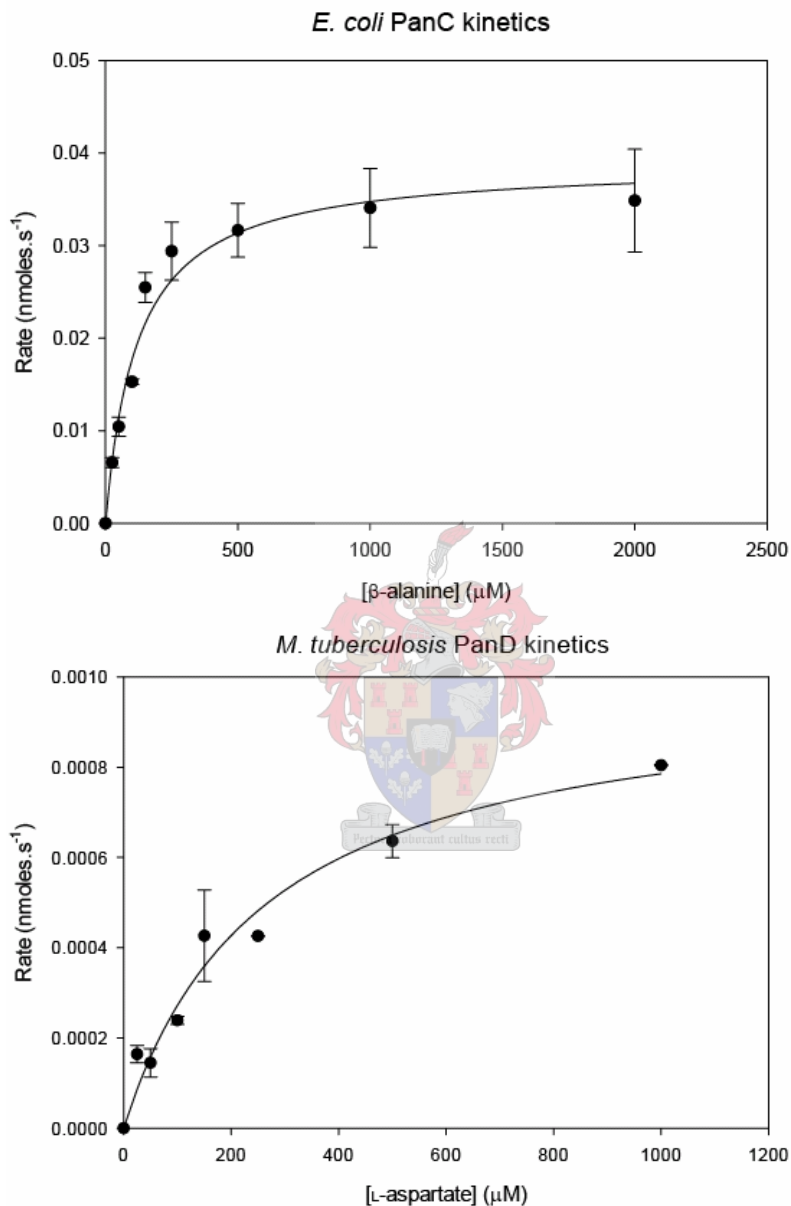


Figure 4.13: The steady state kinetics of PanC with β -alanine (top) and PanD with varied L-aspartate (bottom). Each point represents the average of three readings and the bars the standard error. Solid lines represent the best-fit of the data to the Michaelis-Menten equation.

Only slight differences were noticed between these two sets of results. The kinetic parameters for Mtb PanD were determined as $V_{\max} = 1.3 \pm 0.7$ pmol.s⁻¹, $K_M = 210 \pm 32$ μ M, $k_{\text{cat}} = 0.0013 \pm 0.00007$ s⁻¹ and $k_{\text{cat}}/K_M = 0.0061 \pm 0.002$. The Michaelis-Menten curve fit is

given in Figure 4.13 (bottom) and the literature values and assay methods from which they were obtained are given in Table 4.2. These results validated our coupled enzymatic method as the kinetic parameters we obtained for PanD compare well to the literature values.

Table 4.2: Steady state kinetic parameters for PanD according to literature and the assays used (2).

Organism	K_M (μM)	k_{cat} (s^{-1})	Specific activity	Assay
<i>Mycobacterium tuberculosis</i>	219.6	0.65	2 100 nmol/min/mg	HPLC quantification of fluram derivatives(7)
<i>Escherichia coli</i>	160	0.66		Formation of ^{14}C labeled products(14)
<i>Escherichia coli</i>	151 \pm 16	0.57		HPLC quantification of fluram derivatives(4)
<i>Mycobacterium tuberculosis</i>	210 \pm 32	0.002		Our coupled enzymatic assay (section 4.5.3.2)

4.6 Conclusion

We focused on the design of an inhibitor that is specific for the pyruvoyl-dependent PanD enzyme, as well as developing methods to assay such potential inhibitors. The synthesis of β -fluoroaspartate as a PanD inhibitor was more cumbersome than anticipated and must be revisited. Both qualitative and quantitative analytical techniques were designed to compare the reactions of PanD with substrate analogues of L-aspartate to each other. Reverse phase HPLC was employed to determine whether certain compounds are substrates of PanD, while a coupled enzymatic assay was developed to determine the steady-state kinetics. Various assay methods were investigated to find an easy, quick and efficient enzyme coupled reaction for the steady-state kinetics and to study the inhibitory effects of different compounds on PanD. Our assay of choice relied on the enzyme PanC, which uses the β -alanine produced by PanD to form pantothenate. One of the side products of this reaction is pyrophosphate. We assayed for PPI by using an assay kit that contains a complete enzymatic mixture to assay for the production of PPI by coupling its production to the utilization of NADH. Our analysis of different compounds showed that as expected α -methyl-D,L-aspartate is not a substrate of PanD, but that β -hydroxyaspartate is. While the inhibitory effects of these molecules on PanD in the presence of L-aspartate have not yet been studied, this interesting result suggests that

substrates similar to β -hydroxyaspartate may be good mechanism-based inhibitors of PanD. It also lends support to our hypothesis that β -fluoroaspartate is a possible mechanism-based inhibitor of PanD.

4.7 Experimental

4.7.1 DNA amplification, cloning, expression and purification

The *panD*-gene sequence was amplified from genomic DNA from Mtb strain H37Rv with the forward primer 5'-ACATTGGAGAAACATATGTTACGGACGATGC-3' and reverse primer 5'-TCGCCAGCAGCACTCGAGTCCCACACCGAG-3'. The forward primer introduced an NdeI-site and the reverse primer an XhoI-site, both underlined in the primer sequences. The stop codon was also removed. Amplification was done in AMP-buffer, 0.4mM dNTP mix, 1mM forward primer, 1mM reverse primer, 2ng genomic DNA, 1.25U *pfu* and ddH₂O to the final volume of 25 μ l with varied MgSO₄ concentrations. The PCR program had an initial step of 3 min at 94°C followed by 30s at 94°C, 30s at 55°C and 1min at 72°C for 30 cycles. This was followed by incubation at 72°C for 10min and finally a hold step 4°C. Analysis of the reaction mixtures was done by electrophoresis on a 1% agarose gel and the bands visualized by staining with SYBR® gold and viewed on a Darkreader. Product bands at 420bp were obtained at 2.5, 3 and 3.5 μ M MgSO₄ and were purified from the gel.

The *panD* PCR product was digested with NdeI and XhoI and purified as described in section 2.7.2. Ligation of 60 fmoles of digested *panD* with the same amount of digested pENTR4NT was done according to method 1 described in section 2.7.3.1 and transformed into DH5 α . The construct was confirmed with screening on 1% agarose gel in comparison to undigested pENTR4NT and by digestion with NdeI and XhoI to regenerate the insert. The regenerated insert was purified from the gel with the GFX PCR DNA and gel band purification kit and was used to ligate into digested pET28a(+). 31 fmoles of each was ligated using method 1 again. To check that the correct construct formed screening on a 1% agarose gel in comparison to undigested pET28a(+) and digestion check with NdeI and XhoI were done. The plasmid was also sequenced. pET28a-*panD* was transformed into BL21(DE3) and expressed from 500ml LB containing 30mg.l⁻¹ kanamycin. The inoculated media was incubated at 37°C, 200rpm shaking till OD₆₀₀=0.6 was reached after which it was induced with a final concentration of 0.5mM IPTG at 30°C overnight. Cells

were harvested by centrifugation at 4500rpm for 30min at 4°C. The pellet was resuspended in a volume of 10× the pellet weight of binding buffer and cooled down to below 10°C. Lyses of the cells occurred by sonication and the cell debris was collected by centrifugation at 15 000rpm for 30min at 4°C and the supernatant filtered with an 0.45micron filter and purified with affinity chromatography on a 1ml HiTrap Chelating HP columns the ÄKTAprime-system. After desalting the concentration was determined with the Bradford reagent and BSA standards as 1.29mg.ml⁻¹. Purity of the enzyme was confirmed by running a 15% SDS PAGE gel.

4.7.2 Synthesis of β -fluoroaspartate (4.11)

All chemicals were purchased from Sigma-Aldrich and were of highest purity.

Methylisocyanoacetate (4.15) (547.6mg, 5.53mmol) was stirred in 7.5ml NH₃-solution (2M in MeOH) for 24 hours. The solvent was removed *in vacuo* to yield an orange precipitate. This was dissolved in another portion of NH₃-solution, stirred for another 24hours and the solvent removed again to yield a lighter orange precipitate. The formation of α -isocyanoacetamide was confirmed with ¹H-NMR (DMSO-d₆), 4.3ppm (2 × H's).

4.7.2.1 Synthesis of oxazoline ring (4.13)

α -Isocyanoacetamide (4.16) (\approx 5,5mmol) was dissolved as is in 2.5ml MeOH and glyoxilic acid monohydrate (4.17)(556mg, 5.5mmol) added to it. This mixture was added slowly to a stirring solution of NaOH (220mg, 5.5mmol) in 1.25ml ddH₂O over a 30min period at temperature \leq 15°C (H₂O bath with ice). After everything was added the mixture was stirred for a further 30 min at 15°C followed by 4.75h at room temperature. The solvent was removed *in vacuo* and black sticky substance formed. This was dissolved in ddH₂O and lyophilized overnight to yield the sodium salt as a greenish powder.

4.7.2.2 Ring opening with aqueous HCl

For ring opening with aqueous HCl acid 3ml 3M HCl were added to the powder and refluxed for 2h at 70-80°C. The solvent was removed *in vacuo* with the rotary evaporator and lyophilized overnight. A reddish brown substance was obtained. Formation of β -hydroxyaspartate was confirmed on TLC (eluant: 50% butanol, 30% ddH₂O and 20% CH₃COOH; stain: 1.5% ninhydrin) in comparison with a commercial sample of β -hydroxyaspartate. To purify 4.9 an acidic Amberlite column was used with the elution buffer 5% NH₄OH, pH 11.0.

4.7.2.3 Ring opening with dry HCl

For ring opening with dry HCl the sodium salt (800mg, 5mmol) was dissolved 5ml MeOH. The slurry was added to a mixture of 20ml MeOH and CH₃COCl (500 μ l, 7mmol) and refluxed for overnight (17). The solvent was removed *in vacuo* to give a yellow brownish powder. Purification was done on a silica column with the eluant 5% MeOH, 1% triethylamine in CH₂Cl₂.

4.7.2.4 Protection with BOC-group to form 4.15.

For protection with the BOC-group, 2.2mmol of the **4.14** was dissolved in 2.4ml CHCl₃. To this mixture was added (in this sequence) NaHCO₃ (328mg, 3.9mol), NaCl (777mg, 13.4mmol) and di-*tert*-butyl dicarbonate (851mg, 3.9mmol). The reaction mixture was refluxed for 90min, extracted 4x 25ml CHCl₃ and the product dried overnight on Na₂SO₄. The drying agent was filtered off and the solvent removed *in vacuo* (18).

4.7.3 HPLC

All analyses were done on a Waters Alliance 2960 system with 5 μ m Gemini C18 110Å reverse phase column, dimensions 250 \times 4.6mm. All solvents were HPLC grade (Riedel-de Haën®) and purchased from Sigma-Aldrich. The buffers were filtered through 0.45micron membrane and degassed by sonication. Fluorescence was detected with a Water 474 scanning fluorescent detector at λ_{ex} =390nm, λ_{em} =475nm, gain 10 and attenuation 256. Enzymatic reactions were done in 50mM potassium phosphate buffer, pH 7.0, 1mM EDTA with 4mM substrate and incubated at 37°C for 1h. After the incubation time elapsed, the 50 μ l reactions were boiled at 95°C for 5min and 2.5 μ l 2M NaOH added. The protein was removed by centrifugation and 50 μ l of the supernatant used in further applications. To the supernatant was added 145 μ l 500mM borate buffer, pH10 and 50 μ l 0.3mg.ml⁻¹ fluram in ACN and left at room temperature for a minute to derivatize (7). Samples of 10 μ l were injected and isocratically eluted with 20mM CH₃COONa and 30% ACN at 1ml.min⁻¹ flow rate.

4.7.4 Steady-state kinetics

All reactions were done in triplicate on 300 μ l scale in Corning flat bottom microtiter plates. The decrease of NADH was measured at 340nm over a period of 30 minutes using a Thermo Varioskan™ UV-spectrometer with Skanit software version 2.2.1.

4.7.4.1 Preparation of *D*-pantoic acid (1.3)

To pantolactone (1mmol) was added 1M NaOH (1.1mmol) and ddH₂O to give a final concentration of 100mM. The solution was boiled at 95°C for 1h.

4.7.4.2 Coupled assay with myokinase, pyruvate kinase and lactose dehydrogenase

The assay mixture consisted of 50mM Tris.HCl, pH 7.6, 10mM MgCl₂, 20mM KCl, 5mM β -alanine, 5mM *D*-pantoic acid, 10mM ATP, 2.5mM NADH, 10mM PEP, 7.5U PK, 7.5U LDH, 9U Adk and ddH₂O. Reactions were initiated with the addition of 65 μ g PanC. The decrease of NADH was followed at 340nm for 30min.

The reactions were repeated according to the protocol used by Zheng *et al.* (21) with assay mixture composition of 100mM Hepes, pH 7.8, 10mM MgCl₂, 10mM ATP, 5mM β -alanine, 5mM *D*-pantoic acid, 1mM PEP, 0.2mM NADH, 5.4U PK, 5.4U LDH, 5.4U Adk and ddH₂O. The reaction was done in the same way as above.

4.7.4.3 Assay coupled to CoaA

The assay mixture contained 100mM Hepes, pH 7.8, 10mM MgCl₂, 1mM PEP, 5mM β -alanine, 5mM *D*-pantoic acid, 5.4U PK, 5.4U LDH, 3 μ g CoaA and ddH₂O. The reaction mixture was incubated at 25°C for 5min before the reaction was initiated with the addition of 65 μ g PanC. The decrease of NADH was followed at 340nm for 30min.

4.7.4.4 Assay with the Sigma Pyrophosphate kit.

For an assay reaction 120 μ l of reagent supplied in the kit is used per 300 μ l assay reaction. The assay mixture contained 10mM Hepes, pH 7.8, 10mM MgCl₂, 10mM ATP, 5mM β -alanine, 5mM *D*-pantoic acid, PPI reagent and ddH₂O. The master mix was incubated at 25°C before initiation of the enzymatic reaction with the addition of PanC. The decrease of NADH was followed at 340nm for 5min.

For the determination of the kinetic parameters of PanC in relation to β -alanine, 65 μ g PanC was used per 300 μ l reaction. PanC was added to the master mix and the reactions were initiated with the addition of β -alanine. Concentrations of β -alanine were varied as follows: 0, 0.01, 0.025, 0.05, 0.10, 0.15, 0.25, 0.50, 1.00 and 2.00mM.

4.7.4.5 Coupled *Mtb* PanD and PanC reaction

The assays were done with the same enzymatic kit as in previous section. The assay mixtures contained 10mM Hepes, pH 7.8, 10mM MgCl₂, 10mM ATP, 5mM *D*-pantoic acid,

PPi reagent, 150 μ g PanC or 137 μ g PanC per reaction, 5 μ g Mtb PanD and ddH₂O. The assay mixture was incubated at 30°C for 5 minutes before initiation of the reaction with the addition of L-aspartate. The concentration of L-aspartate used was 0, 0.025, 0.05, 0.10, 0.15, 0.25, 0.50 and 1.00mM.

4.8 References

- (1) Lee, B. I., and Suh, S. W. (2004) *Crystal Structure of the Schiff Base Intermediate Prior to Decarboxylation in the Catalytic Cycle of Aspartate α -Decarboxylase*. *Journal of Molecular Biology* **340**, 1-7.
- (2) Webb, M. E., Smith, A. G., and Abell, C. (2004) *Biosynthesis of pantothenate*. *Natural Product Reports* **21**, 695-721.
- (3) Albert, A., Dhanaraj, V., Genschel, U., Khan, G., Ramjee, M. K., Pulido, R., Sibanda, B. L., von Delft, F., Witty, M., Blundell, T. L., Smith, A. G., and Abell, C. (1998) *Crystal structure of aspartate decarboxylase at 2.2 Å resolution provides evidence for an ester in protein self-processing*. *Nature Structural Biology* **5**, 289-93.
- (4) Ramjee, M. K., Genschel, U., Abell, C., and Smith, A. G. (1997) *Escherichia coli L-aspartate- α -decarboxylase: preprotein processing and observation of reaction intermediates by electrospray mass spectrometry*. *Biochemical Journal* **323**, 661-669.
- (5) Notredame, C., Higgins, D., and Heringa, J. (2000) *T-Coffee: A novel method for multiple sequence alignments*. *Journal of Molecular Biology* **302**, 205-217.
- (6) Webb, M. E., Stephens, E., Smith, A. G., and Abell, C. (2003) *Rapid screening by MALDI-TOF mass spectrometry to probe binding specificity at enzyme active sites*. *Chemical Communications*, 2416-2417.
- (7) Chopra, S., Pai, H., and Ranganathan, A. (2002) *Expression, purification, and biochemical characterization of Mycobacterium tuberculosis aspartate decarboxylase, PanD*. *Protein Expression and Purification* **25**, 533-540.
- (8) Schmitzberger, F., Kilkenny, M. L., Loble, C. M. C., Webb, M. E., Vinkovic, M., Matak-Vinkovic, D., Witty, M., Chirgadze, D. Y., Smith, A. G., Abell, C., and Blundell, T. L. (2003) *Structural constraints on protein self-processing in L-aspartate- α -decarboxylase*. *EMBO Journal* **22**, 6193-6204.

- (9) Balbo, P. B., Patel, C. N., Sell, K. G., Adcock, R. S., Neelakantan, S., Crooks, P. A., and Oliveira, M. A. (2003) *Spectrophotometric and Steady-State Kinetic Analysis of the Biosynthetic Arginine Decarboxylase of Yersinia pestis Utilizing Arginine Analogues as Inhibitors and Alternative Substrates*. *Biochemistry* **42**, 15189-15196.
- (10) Zabinski, R. F., and Toney, M. D. (2001) *Metal Ion Inhibition of Nonenzymatic Pyridoxal Phosphate Catalyzed Decarboxylation and Transamination*. *Journal of the American Chemical Society* **123**, 193-198.
- (11) Bugg, T. D. H. (2004) *Introduction to enzyme and coenzyme chemistry*, 2nd ed., Blackwell publishing.
- (12) Shin, J.-S., and Kim, B.-G. (2001) *Substrate inhibition mode of ω -transaminase from Vibrio fluvialis JS17 is dependent on the chirality of the substrate*. *Biotechnology and Bioengineering* **77**, 832-837.
- (13) Hirase, K., and Molin, W. T. (2001) *Effect of Inhibitors of Pyridoxal-58-Phosphate-Dependent Enzymes on Cysteine Synthase in Echinochloa crus-galli L*. *Pesticide Biochemistry and Physiology* **70**, 180-188.
- (14) Williamson, J. M., and Brown, G. M. (1979) *Purification and properties of L-aspartate- α -decarboxylase, an enzyme that catalyzes the formation of β -alanine in Escherichia coli*. *Journal of Biological Chemistry* **254**, 8074-82.
- (15) Ozaki, Y., Maeda, S., Miyoshi, M., and Matsumoto, K. (1979) *An improved stereoselective synthesis of threo-beta-hydroxyamino acids*. *Synthesis*, 216-217.
- (16) Matsumoto, K., Suzuki, M., Yoneda, N., and Miyoshi, M. (1977) *Synthesis of amino acids and related compounds*. 16. Alkylation of α -isocyanoacetamides; synthesis of 1,4,4-trisubstituted 5-oxo-4,5-dihydroimidazoles. *Synthesis*, 249-50.
- (17) Strauss, E., and Begley, T. P. (2002) *The antibiotic activity of N-pentylpantothenamide results from its conversion to ethyldeithia-coenzyme A, a coenzyme A antimetabolite*. *Journal of Biological Chemistry* **277**, 48205-48209.
- (18) Tarbell, D. S., Yamamoto, Y., and Pope, B. M. (1972) *New Method to Prepare N-t-Butoxycarbonyl Derivatives and the Corresponding Sulfur Analogs from di-t-Butyl Bicarbonate or di-t-Butyl Dithiol Dicarbonates and Amino Acids*. *Proceedings of the Natural Academy of Sciences* **69**, 730-732.

- (19) Cooper, J. D. H., Ogden, G., McIntosh, J., and Turnell, D. C. (1984) *The stability of the o-phthalaldehyde/2-mercaptoethanol derivatives of amino acids: an investigation using high-pressure liquid chromatography with a precolumn derivatization technique.* Analytical Biochemistry **142**, 98-102.
- (20) Sigma. (1999) Product information: *Enzymatic determination of pyrophosphate, product number P7275* -<http://www.sigmaaldrich.com/sigma/bulletin/p7275bul.pdf> (Last accessed: 4 January 2006)
- (21) Zheng, R., and Blanchard, J. S. (2001) Steady-State and Pre-Steady-State Kinetic Analysis of Mycobacterium tuberculosis Pantothenate Synthetase. Biochemistry **40**, 12904-12912.



Conclusion and future directions:

5.1 Solubility of AofH

Overexpression of Mtb proteins from the *E. coli* expression systems are known to often give low yields and solubility problems (1). One of the factors that contribute to this problem is the difference in G-C content between the DNA of the organisms. The G-C content of *E. coli* DNA are about 50% while it is 65-70% of the Mtb proteins (1). To overcome the insolubility problems we investigated the expression of native AofH fused to different fusion tags (His, GST, His-GST, Nus and MBP). Solubility was obtained with all the tags except with the His-tag. AofH fusions with the Lumio™-tag were also created for use in fluorescent-based screening in further application. Methods that increase the solubility of the expressed protein and translation efficiency were also employed. These include the co-expression of the AofH fusions with the His-Lumio™- and His-GST-tags with the scarce codon tRNAs and the chaperone proteins as contained in the Takara chaperone plasmid sets. Only the co-expression of His-Lumio™ -AofH with the chaperone protein trigger factor (Tig) gave soluble expression.

From this we can conclude that soluble expression of AofH from the *E. coli* system is successful when the enzyme is fused to the various fusion tags. Other ways to overcome the solubility problem may be expression of AofH in a eukaryotic expression system. The use of such expression systems has not been well documented in literature (1). We have identified two yeast systems that may be suitable for the task. The first system is expression in *S. cerevisiae*, which has already been mentioned in Chapter 2, section 2.4.1. Our initial experiments with this system were unsuccessful, but this can be ascribed to the use of the wrong detection methods. The second system that can be used is the *Pichia pastoris* expression system.

5.2 AofH activity

Different analytical methods were used to determine the products of the AofH enzymatic reactions with the various polyamine substrates. The first set of analyses was performed

by TLC; from these we deduced that AofH forms 3-aminopropanol as a product from all the polyamines. This was an unexpected result, since no other flavin-containing enzyme is known to catalyze a similar reaction. Unfortunately we could not confirm this result; in fact, AofH seemed to be inactive in every additional analysis performed. We finally set out to confirm the presence of the FAD cofactor in the enzyme by variety of methods. These lead us to conclude that the AofH fusions did not contain FAD, and that the observed spots on the TLC analysis of the AofH-catalyzed reactions could not be due to 3-aminopropanol, or that it was formed by some non-enzymatic process. Further efforts to refold the protein in the presence of FAD also failed, as detailed in Chapter 2. Taken together, our study shows that the confirmation of the presumed activity of AofH will remain elusive until the enzyme can be purified in its active form, i.e. with bound FAD. The expression of AofH from another expression system may help to achieve this goal.

The functional complementation studies, to determine the enzyme's activity by genetic methods, also proved inconclusive. We found that whether transformed with pBAD-EXP49-*gus* (the negative control) or pBAD-EXP49-*aofH* Δ *panD* mutants showed similar rates of growth (in solution) in minimal media. This is an unexpected result, since previous reports indicated that PanD is the sole source of β -alanine in *E. coli*. This result indicates that the Δ *panD* mutants were able to source β -alanine from other metabolic pathways, complicating the determination of whether cell lines containing AofH could indeed produce a β -alanine precursor at low levels. Future studies in this area will have to make use of a β -alanine auxotroph that is not *E. coli* based, preferable a β -alanine auxotroph strain of *S. cerevisiae* (BY4742) or of *Mtb* itself.

5.3 Synthesis of PanD inhibitors

The synthesis of the inhibitor β -fluoroaspartate was more complicated than originally anticipated. Most of the problems experienced were purification-based, while the yield of the different synthetic steps was also low. Although this synthesis is still viable, it may be simpler to source the β -hydroxyaspartate precursor commercially and continue the synthesis from this step forward. However, such a step may be prohibitively expensive.

5.4 Assay methods

We successfully developed qualitative and quantitative assays to identify inhibitors/substrates of PanD. Qualitative analyses of PanD enzymatic reactions can be performed by reverse phase HPLC to identify whether certain compounds are substrates of the enzyme.

As far as the quantitative method is concerned, we assayed for PanD by coupling the formation the β -alanine product to the reaction catalyzed by PanC, and subsequently to the the formation of pyrophosphate (PPi). This assay works well and at a sufficient rate for our analysis. The steady-state kinetics of PanD was determined with this method and compares well to literature values. The effects of inhibitors on the PanD reaction with L-aspartate still have to be studied.

5.5 Conclusion

The work done by Sasetti *et al.* (2) indicated that PanD, the enzyme involved in the decarboxylation of L-aspartate to β -alanine, is not essential in Mtb. This implies that an alternative source of β -alanine must exist for the survival of the mycobacterium. After careful evaluation of all the possible routes for β -alanine production we postulated that the most likely alternative is the oxidation of the polyamines by a polyamine oxidase. Mtb AofH was identified as a likely PAO candidate based on sequence homology to the FAD-dependent *Saccharomyces cerevisiae* polyamine oxidase Fms1. Due to various obstacles in the soluble expression and purification of AofH in its active form we were not able determine the activity of AofH or whether it has a role in pantothenate biosynthesis.

Furthermore the results obtained from the functional complementation studies lead us to question the validity of the essentiality studies done by Sasseti *et al.* (2) In their study the essentiality of genes were determined by transposon site hybridization (TraSH). Although TraSH gives good indications of the essentiality of genes, the results obtained still needs to be verified independently which in this case would be by the creation of a Δ panD mutant. Although Sambandamurthy *et al.* made the double deletion mutant Δ panCpanD, the essentiality of PanD has not been verified (3).

We continued our studies of β -alanine biosynthesis by attempting the design a mechanism-based inhibitor, β -fluoroaspartate, for the PanD enzyme. The synthesis of this

compound was more cumbersome than anticipated and has to be revisited. Both qualitative and quantitative analytical techniques were designed to compare the reactions of PanD with substrate analogues of L-aspartate to each other. Our results show that β -substituted aspartate analogues may be good potential inhibitors of Mtb's PanD protein.

5.6 References

- (1) Bellinzoni, M., Riccardi, B. (2003) *Techniques and Applications: The heterologous expression of Mycobacterium tuberculosis genes is an uphill road*. *TRENDS in Microbiology* **11**, 351-358.
- (2) Sassetti, C. M., Boyd, D. H., and Rubin, E. J. (2003) *Genes required for mycobacterial growth defined by high density mutagenesis*. *Molecular Microbiology* **48**, 77-84.
- (3) Sambandamurthy Vasan, K., Wang, X., Chen, B., Russell Robert, G., Derrick, S., Collins Frank, M., Morris Sheldon, L., and Jacobs William, R., Jr. (2002) *A pantothenate auxotroph of Mycobacterium tuberculosis is highly attenuated and protects mice against tuberculosis*. *Nature Medicine* **8**, 1171-4.

